TECHNISCHE UNIVERSITÄT MÜNCHEN
FAKULTÄT FÜR MEDIZIN

Identification of the molecular mechanisms promoting neuroendocrine tumor formation

Ninelia Minaskan Karabid

Vollständiger Abdruck der von der Fakultät für Medizin der Technischen Universität München zur Erlangung des akademischen Grades eines Doktors der Naturwissenschaften genehmigten Dissertation.

Vorsitzende: Prof. Dr. Gabriele Multhoff

Prüfer der Dissertation:

1. Prof. Dr. Michael John Atkinson
2. Prof. Dr. Nina Henriette Uhlenhaut

Die Dissertation wurde am 30.01.2019 bei der Technischen Universität München eingereicht und durch die Fakultät für Medizin am 11.02.2020 angenommen.

Statutory Declaration:

I hereby declare that this thesis has been written independently, without any unauthorized use of services of a third party. No sources or aids have been used in the preparation of this thesis other than those indicated in the thesis itself. All materials, which have been quoted either literally or by content from other sources, have been marked explicitly.

Munich, 30.01.2019

Ninelia Minaskan Karabid

Eidesstattliche Erklärung:

Ich erkläre hiermit, dass Ich die vorliegende Arbeit selbstständig und ohne unzulässige Hilfe Dritter verfasst habe. Ich habe keine anderen als die angegebenen Hilfsmittel und Quellen verwendet. Insbesondere habe ich wörtlich oder sinngemäß aus anderen Werken übernommene Inhalte als solche kenntlich gemacht.

München, 30.01.2019

Ninelia Minaskan Karabid

Zusammenfassung

Hypophysenadenome (PA`s) sind häufig auftretende, intrakraniale Tumore. Etwa ein Drittel dieser Tumore bilden die nicht-funktionelle Hypophysenadenome (NFPA`s), die in 80% der Fälle aus gonadotropen Zellen bestehen. Da sie keine aktiven Hormone sezernieren, werden sie häufig relativ spät, im Makroadenoma-Stadium, diagnostiziert. Dadurch ist eine komplette chirurgische Entfernung oft erschwert und Rezidive können entstehen. Diese Adenome sprechen selten auf klassische medikamentöse Behandlungen an.

Im Rahmen dieser Arbeit konnten wir zeigen, dass die Expression von Angiopoietin-1 (Ang-1) und Angiopoietin-2 (Ang-2) in Hypophysenadenomen des MENX-Rattenmodels dysreguliert ist. Im Speziellen fanden wir, dass die Menge an Ang-2 sowohl in Ratten- als auch humanen NPFA auf mRNA- und Proteinebene erhöht war. Ang-2 wurde von primären Hypophysentumorkulturen aus Ratte und Mensch ins Zellkulturmedium sekretiert. Eine erhöhte Konzentration an ANG-2 konnte nachfolgend auch in Plasmaproben von NFPA-Patienten nachgewiesen werden.

Außerdem wurde es gezeigt, dass Ang-2 als aktivierender Ligand für den Rezeptor Tie-2 fungieren kann. Durch Stimulation mit rekombinantem ANG-2 Protein, konnten wir eine extrazelluläre Stimulierung des Rezeptors in GH3 Hypophysenzellkulturen nachweisen, welche wiederum im Stande war intrinsische Signalkaskaden zu aktivieren. Dieser aktive Ang-2/Tie-2 Signalweg zeigte proliferative und anti-apoptotische Wirkungen in NFPA Zellen.

Diese Studie zeigte, dass anti-angiogene Behandlung von Hypophysentumoren im MENX-Rattenmodel mit AMG386 die Proliferation in PA`s inhibierte und gleichzeitig Apoptose aktivierte.

Diese Arbeit schlägt vor, dass die Blockierung von Ang-2/Tie-2 Signalweg eine potentielle Therapiemöglichkeit für NFPA-Patienten darstellen könnte.

Abstract

Non-functioning pituitary adenomas (NFPAs) count for 30-40% of all pituitary tumors. These adenomas belong mainly to the gonadotroph type (80%). Lack of signs and symptoms of hormone hypersecretion allows these tumors to grow asymptomatic till macroadenoma stage and infiltrate cavernous sinus. Therefore, a complete surgical removal of tumor is not always possible and the tumors tend to recur. Currently, radiotherapy is the main post-operative option for NFPA patients but it is not curative.

Studies of MENX rat pituitary adenomas (PAs) confirmed overexpression of *Angiopoietin-2* (*Ang-2*), a growth factor which acts on Tie-2 (tyrosine kinase receptor). This receptor is originally expressed and well-studied in endothelial cells (ECs). Recent studies reported Tie-2 expression in tumor cells as well.

We detected Ang-2/ANG-2 in supernatant of rat and human primary PA cultures/established cell lines and plasma of NFPA patients indicating that this ligand is secreted by PA cells into culture medium or circulating blood. Moreover, we demonstrated a functional Ang-2/Tie-2 pathway for the first time in NFPAs having an impact on cell viability and apoptosis. Blocking of this pathway in PA cells reduced cell viability and enhanced apoptosis in these cells *in vitro*.

in vivo treatment of MENX rats with anti-angiogenic drug AMG386 suppressed cell proliferation and induced apoptosis after 2 weeks, which suggests that blocking of this pathway might be a potential therapy option for NFPA patients.

Abbreviations

ANG/Ang	Angiopoietin
°C	degree Celsius
%	percent
α	anti
µ	micro- (10^{-6})
ACTH	adrenocorticotropic hormone
Akt	serine/threonine-specific protein kinase
ADH	antidiuretic hormone
APS	ammonium persulfate
ATP	adenosine triphosphate
bp	base pair
BCA	bicinchoninic acid
Bidest.	bidestillatus
BSA	bovine serum albumin
Cdk	cyclin-dependent kinase
Ctrl.	control
cDNA	complementary deoxyribonucleic acid
DMEM	Dulbecco's Modified Eagle's Medium
DMSO	dimethyl sulfoxide
DNA	deoxyribonucleic acid
Dok-R	docking protein R
dNTP	deoxyribonucleotide
DPBS	Dulbecco`s Phosphate Buffered saline
DTT	dithiothreitol
E	embryonic day
EC	endothelial cell
E. coli	Escherichia coli
ECL	enzymatic chemiluminescence
EDTA	ethylenediamine-tetraacetic acid
eNOS	endothelium nitric oxide synthase
Erk	extracellular signal-regulated kinase
EtBr	ethidium bromide

F	female
Fak	focal adhesion kinase
FBS	fetal bovine serum
FITC	fluorescein thioisocyanate
FS cells	folliculostellate cells
FSH	follicle-stimulating hormone
FSHβ	follicle-stimulating hormone β-subunit
g	gravitational constant
GFP	green fluorescent protein
GH	growth hormone
GHRH	growth hormone-releasing hormone
GnRH	gonadotropin-releasing hormone
h	hour
HRP	horseradish peroxidase
HS	horse serum
HUVEC	human umbilical vein endothelial cells
i.e.	id est
IF	immunofluorescence
IP	immunoprecipitation
k	kilo- (10^3)
kbp	kilo-base pair
kDa	kilo Dalton
l	litre
LB	lysogeny broth (Luria-Bertani medium)
LH	luteinizing hormone
LHβ	luteinizing hormone β-subunit
M	male/molar concentration
m	metre/milli- (10^{-3})
MEN	multiple endocrine neoplasia
MENX	multiple endocrine neoplasia-like syndrome
min	minute(s)
MMP	matrix metalloproteinases
mo	months
n	nano- (10^{-9})

NFPA	nonfunctioning pituitary adenoma
NC	nitrocellulose membrane
OD	optical density
p	pico- (10^{-12})/plasmid
P	probability
PBS	phosphate buffered saline
PC	pheochromocytoma
PDGF	platelet-derived growth factor
PCR	polymerase chain reaction
PFA	paraformaldehyde (polyoxymethylene)
pH	minus the decimal logarithm of the hydrogen ion activity in a solution
PI3K	phosphatidylinositol 3-kinase
PRL	prolactin
pTie-2	phospho Tie-2
Rb	Retinoblastoma protein
RIPA	radioimmunoprecipitation assay
RNA	ribonucleic acid
RT	room temperature
SDS	sodium dodecyl sulfate
SDS-PAGE	sodium dodecyl sulfate poly-acrylamide gel electrophoresis
SF-1	steroidogenic factor 1
scRNA	scrambled RNA
siRNA	small interfering RNA
TBE	Tris/boric acid/EDTA
TBP	TATA-Box Binding Protein
TBS-T	Tris buffered saline with Tween 20
TEMED	*N,N,N',N'*-tetramethylethane-1,2-diamine
TGF	transforming growth factor
Tie	tyrosine kinase with immunoglobulin-like and EGF-like domains
TNF-α	tumor necrosis factor alpha
TRH	thyrotropin-releasing hormone
Tris	2-amino-2-hydroxymethyl-propane-1,3-diol
TSH	thyroid-stimulating hormone
UV	ultraviolet

v/v	volume per volume
VEGF/Vegf	Vascular Endothelial Growth Factor
vol	volume
WGA	Wheat Germ Agglutinin
w/v	weight per volume
WPB	Weibel-Palade body

All gene names are indicated in italics, human genes in capital letters, e.g. *ANG-2*, genes from other species in lowercase with capital first letters, e.g. *Ang-2*. All proteins, regardless of species, are written in regular font. Chemical elements and compounds are abbreviated.

Table of Content

1 Introduction

1.1 Pituitary gland

The pituitary gland plays a central role in the regulation of the neuroendocrine system. This organ is located at the base of the brain, in the sella turcica of the sphenoid bone near the optic chiasm. The pituitary stalk connects the pituitary to the hypothalamus through which pass the neural and vascular connections (Amar and Weiss 2003). The pituitary secretes hormones regulating growth and development, metabolism, as well as reproductive and nervous system functions. The hypothalamus regulates hormone production in the pituitary gland by producing releasing and inhibitory hormones. These hormones reach directly the anterior pituitary via hypothalamic-hypophyseal portal veins, bind to their specific receptor and modulate hormone production and release in anterior pituitary (Kelberman *et al.* 2009). The human pituitary consists of three parts that differ anatomically and functionally, the anterior pituitary (adenohypophysis), the intermediate lobe (pars intermedia) and the posterior pituitary (neurohypophysis). The anterior lobe is the largest part of the gland, and consists of five hormone-producing cell types, somatotropes, lactotropes, corticotropes, gonadotropes and thyrotropes. Somatotropes, the most common cell type in the anterior pituitary, produce growth hormone (GH) under the influence of hypothalamic Growth Hormone-Releasing Hormone (GHRH). Thyrotropes, the least common pituitary cell type, secrete TSH (Thyroid Stimulating Hormone), also called thyrotropin. Gonadotropes secrete the gonadotropins, FSH (Follicle Stimulating hormone) and LH (Luteinizing Hormone). Lactotropes secrete prolactin. Corticotropes secrete ACTH. Beside these five cell types in the anterior lobe, there is also one more cell type, the folliculostellate cells which are non-hormone producing cells, surrounding endocrine cells and producing growth factors (Asa and Ezzat 2002, Inoue *et al.* 1999). The intermediate lobe has the same embryological origin as the anterior lobe (oral ectoderm). It is located between the anterior and posterior pituitary, and produces melanocyte-stimulating hormone (α- and β-MSH) and synthesizes and releases specific peptide products of the pro-opiomelanocortin (POMC) gene, like in the anterior pituitary, but the hydrolytic end product of this precursor protein is not identical in these two lobes (corticotropin, β-LPH and small

amounts of β-endorphin in anterior pituitary and CLIP, γ-lipotropin, and β-endorphin in intermediate lobe).

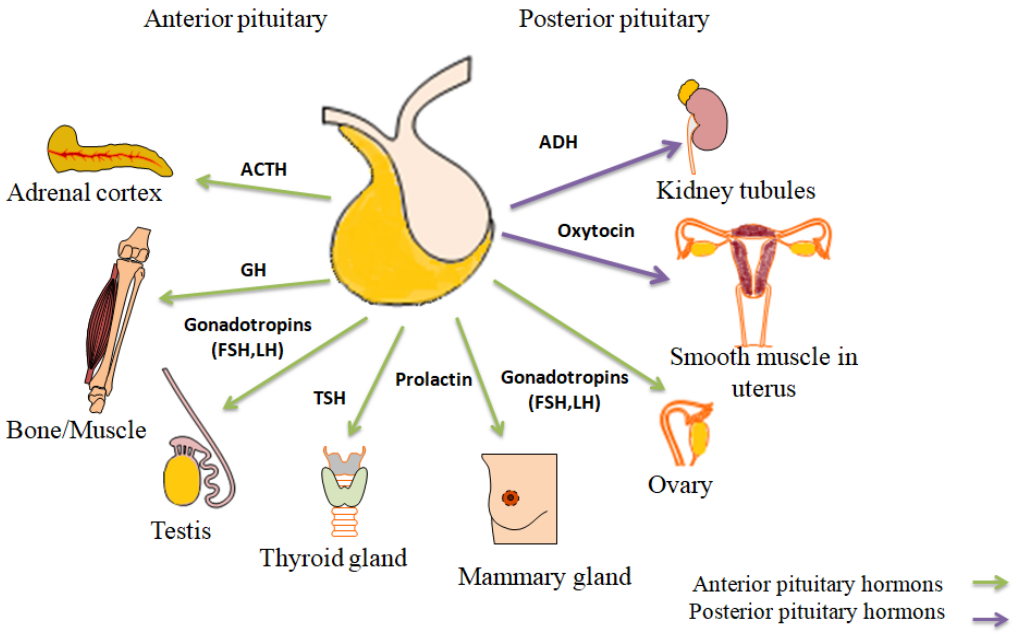

Figure 1: The pituitary gland, its hormones and their target organs.

The posterior lobe originates from the infundibulum during embryonal development and consists of neuroglial cells (pituicytes), as well as the nerve fibers and terminals of cells originating from hypothalamic nuclei. These secrete anti-diuretic hormone and oxytocin, which are synthesized in separate cells in the supraoptic and paraventricular nuclei of the hypothalamus. Following their synthesis, these peptide hormones are transported down the axons and stored in secretory granules in nerve terminals in the posterior pituitary (Amar and Weiss 2003, Ooi *et al.* 2004).

1.2 Pituitary adenomas

Pituitary adenomas (PAs) constitute 15% of intracranial tumors (Asa and Ezzat 1998). Most of them have a sporadic origin but familial cases are also reported (5%) (Daly *et al.* 2009). PAs are usually benign neoplasms; however, excessive hormone production or a mass effect can cause clinical symptoms (Asa and Ezzat 2002).

Pituitary adenomas are classified according to their size by MRI into microadenomas (>1cm), macroadenomas (≥1 cm) or giant adenomas (>4 cm) (Trouillas *et al.* 2013).

Clinically, according to their hormonal activity, PAs are classified into two groups: functioning and non-functioning PAs. Based on pathological immunoreactivity for the hormones of anterior pituitary and linage-specific pituitary transcription factors, functioning adenomas are divided into different subtypes: lactotroph, somatotroph and thyrotroph which express PIT1 (pituitary specific transcription factor 1), corticotroph expresses TPIT (pituitary cell restricted factor) and gonadotroph expresses SF1 (splicing transcription factor 1). Additionally, there are too more subtypes which are plurihormonal adenomas expressing PIT1 and null cell adenomas. The last subtype is completely negative for hormones as well as adenohypophyseal transcription factors (Lloyd *et al.* 2017, Nishioka and Inoshita 2018, Mete and Lopes 2017, Inoshita and Nishioka 2018).

Functioning adenomas cause problems by producing an excess of hormone in a deregulated manner, independent of feedback signals (Table 1). Transsphenoidal surgery, medical treatments and radiation are the options to treat functional pituitary adenomas (Oki 2014).

Table 1: Classification of anterior pituitary adenomas (Kovacs 2001, Asa and Ezzat 2002).

Adenoma type	Lactotroph	Somatotroph	Mammo-somatotroph	Corticotroph	Thyrotroph	Gonadotroph
produced hormone	PRL	GH	PRL/GH	ACTH	TSH	FSH/LH
Clinical syndrome	Prolactinoma Galactorrhea Amenorrhea Infertility Hypogonadism	Agromegaly Gigantism Soft tissue swelling Cardiac Hypertrophy Hypertension Hyperglycemia Sleep apnea	Acromegaly somatotroph gigantism with hyperprolac-tinaemia	Cushing's disease Nelson's syndrome Hypercortisolism Central obesity Striae Hyperglycemia Osteoporosis Hirsutism	TSH-cell – Adenoma Thyroid goiter Hyperthyroxi-nemia	Non-functioning – Adenoma Central effects Hypogonadism Hypergonadism (rare) Clinically silent
incidence	35%	10-15%	5%	10-15%	2%	35%

Because of the lack of symptoms caused by hormone hypersecretion, non-functioning pituitary adenomas (NFPAs) are usually diagnosed late, at the macroadenoma stage infiltrating cavernous sinuses. Therefore, a complete surgical removal of NFPAs is not always achieved and the tumor tends to recur. Visual field defects and headaches are the common symptoms which lead to the diagnosis of NFPAs (Greenman and Melmed 1996, Brochier *et al.* 2010, Micko *et al.* 2015).

Morphologically NFPAs are heterogeneous and so, classified into several histological subtypes using different methods including immunohistochemistry to confirm hormone expression electron microscopy, in situ hybridization, reverse hemolytic plaque assay as well

as assessing expressed transcription factors enabling to distinguish them from null cell adenomas (Mete and Asa 2012, Mete and Lopes 2017).

The most common NFPAs are gonadotroph adenomas (80%) that do not secrete gonadotropins, but exhibit nuclear expression of the Sf-1 transcription factor, which regulates the expression of *LHβ* and *FSHβ* genes, despite the absence or very low amount of secreted LH or FSH hormones (Asa *et al.* 1996). Most of them are benign, slowly growing tumor presenting in older age (Manojlovic-Gacic *et al.* 2018). They also express variable amounts of α-subunit of gonadotropin hormones (α-GSU) (Al-Brahim and Asa 2006).

In parallel to determination of tumor subtypes, assessment of proliferative markers (mitotic count, Ki-67 index, and p53 positivity) and other clinical parameters such as tumor invasion, are highly recommended to predict malignant potential of tumors (Nishioka and Inoshita 2018, Mete and Lopes 2017, Lloyd *et al.* 2017, Chiloiro *et al.* 2014). The main treatment of NFPAs is transsphenoidal surgery that reduces tumor mass effects (Chanson *et al.* 2015). Nevertheless, the tumor resection is often incomplete because the tumors are already large at the time of diagnosis and may recur (Ebersold *et al.* 1986). Postoperative radiotherapy is an option to prevent tumor recurrence, but the risk of side effects (visual disturbances, hypopituitarism, neurological dysfunction and secondary brain tumors) should not be disregarded (Colao *et al.* 1998, Greenman *et al.* 2003, Hansen and Molitch 1998). Since dopamine and somatostatin receptors are expressed in NFPAs, treatment with dopamine agonists or somatostatin analogues has been considered for these patients, but the results, except in some cases, were disappointing (Bevan *et al.* 1992, de Bruin *et al.* 1992, Pereira and Biermasz 2012). So, there is a great need of new therapeutic approaches for recurrent NFPAs.

1.3 Multiple endocrine neoplasia (MEN)

1.3.1 MEN1 and MEN2

Multiple endocrine neoplasia (MEN) syndromes are a set of autosomal dominant genetic disorders in humans, characterized by the occurrence of tumors in two or more endocrine glands (Wermer 1954). Two major MEN syndromes are described: MEN type1 (MEN1) and MEN type 2 (MEN2) (Steiner *et al.* 1968). MEN1 and MEN2 are caused by germline mutation of the *MEN1* and *RET* genes, respectively. *MEN1* is a tumor suppressor gene located on chromosome 11q13 encoding the menin protein (Thakker *et al.* 1989, Guru *et al.* 1998, Mulligan *et al.* 1993). Menin is localized in the nucleus and is involved in transcriptional

regulation, DNA replication and cell cycle control (Guru *et al.* 1998). Loss-of-function mutations of *MEN1* are accompanied by multiple parathyroid adenomas, pancreatic islet cell neoplasia and anterior pituitary adenomas in affected people. MEN1 patients develop pituitary adenomas (18- 80%) with increasing age (usually after the age of 40) (Carroll 2013).

The MEN2 syndrome occurs as a result of missense gain-of-function mutations in the *RET* (REarranged in Transfection) proto-oncogene, encoding a receptor tyrosine kinase expressed in neural-crest-derived cells. *RET* maps to chromosome 10q11.2 (Mulligan *et al.* 1993). Patients affected by MEN2 develop medullary thyroid carcinoma (MTC) with complete penetrance. Depending on the additional presence of pheochromocytoma, hyperparathyroidism, and the presence or absence of characteristic physical features, MEN2 is divided into the following subtypes: MEN2 type A (MEN2A), MEN2 type B (MEN2B or MEN3) and familial medullary thyroid carcinoma (FMTC) (Raue *et al.* 1994).

MEN2A, the most common variant, occurs in 20-50% of MEN2 cases and is defined by MTC and unilateral or bilateral pheochromocytoma or by MTC and primary hyperparathyroidism in 5-20% of cases. MEN2B (5-10% of all MEN2 cases) is a more aggressive syndrome than MEN2A and presents with MTC, pheochromocytoma, marphanoid habitus and mucosal and digestive ganglioneuromatosis. MEN2B patients do not usually develop parathyroid tumors (Marini *et al.* 2006). FMTC is a rare variant of MEN2 that is diagnosed in families when four or more cases of MTC without pheochromocytoma or parathyroid adenoma/hyperplasia occur (Raue *et al.* 1994).

1.3.2 MENX and MEN4

A MEN-like syndrome was discovered in a Sprague Dawley rat colony. Affected animals spontaneously develop multifocal anterior pituitary adenoma, bilateral pheochromocytoma, paraganglioma, thyroid C-cell hyperplasia, parathyroid hyperplasia and pancreatic islet hyperplasia. Additionally, bilateral cataracts were observed in affected animals in the first few weeks of life. This tumor spectrum is very similar to both MEN1 and MEN2 in humans, therefore the rat syndrome was named MENX. Despite the phenotype similarities, no mutation of *MEN1* or *RET* was found in the affected animals (Fritz *et al.* 2002).

Further studies led to the discovery of a recessive germline loss-of-function mutation in the cyclin-dependent kinase inhibitor gene *Cdkn1b*, encoding for $p27^{Kip1}$(p27). p27 is a member of the KIP/CIP family of cyclin-dependent kinase inhibitors (CDKIs) and is a cell cycle

inhibitor that regulates the transition from G1 to S phase. The transit from G1 to S phase is regulated by the activity of the cyclin E/CDK2 complex. This complex phosphorylates and thereby inactivates the retinoblastoma protein (Rb), causing its disassociation from transcription factors of the E2F family. The released E2F is thus active and drives the transcription of genes required for entry into the S phase (Figure 2). In the cytoplasm of proliferating cells, p27 is predominantly bound to cyclin D/CDK4-6, whereas in the nucleus of the G1-arrested cells, p27 is found in complexes with cyclin E/CDK2 thus keeping them inactive. Cyclin D/CDK4-6 can sequester p27 from the cyclin E/CDK2 complex and promote the progression into S phase (Chu *et al.* 2008).

In MENX rats, the causative mutation is a tandem duplication of eight nucleotides in *Cdkn1b* exon 2, which results in a frameshift and encodes 23 amino acid longer p27. This alteration reduces the amount of p27 protein due to its rapid degradation. The mRNA expression level was not changed in tissues of MENX rats compared to wild-type rats (Molatore *et al.* 2010). Heterozygous mutant MENX rats develop the same disorders as reported for homozygous ($p27^{-/-}$) animals with slower progression (Molatore *et al.* 2018).

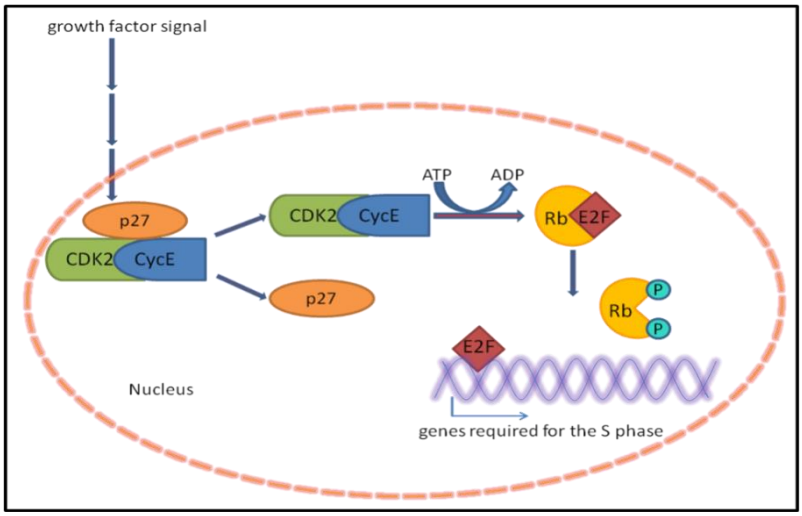

Figure 2: Regulation of G1/S progression and the function of the Rb Protein. Upon mitogenic signals, p27 is released from CDK2/CycE complex. This activated complex phosphorylates Rb, which then disassociates from E2F. E2F in turn can activate gene transcription.

About 10% of patients with a MEN1-like phenotype had no detectable mutation in the *MEN1* gene (Namihira *et al.* 1999, Alrezk *et al.* 2017). The discovery of the *Cdkn1b* mutation in rats led to the search for mutations in the human homologue *CDKN1B* in patients with unclassified endocrine disorders. These studies discovered a germline *CDKN1B* mutation in a

patient, presenting with a MEN1-like phenotype (Pellegata *et al.* 2006). Subsequently, other mutations in *CDKN1B* have been identified in patients with multiple endocrine tumors. This new MEN syndrome was named MEN4 (Agarwal *et al.* 2009, Georgitsi *et al.* 2007).

Table 2: Overview of multiple endocrine neoplasia syndromes.

Syndrome	Mutated gene	Manifestations
MEN1	*MEN1*	Primary hyperparathyroidism (usually four-gland hyperplasia), anterior pituitary adenomas, tumors of endocrine pancreas and duodenum, foregut carcinoids
MEN 2A	RET proto-oncogene	Medullary thyroid cancer, pheochromocytoma, primary hyperparathyroidism (usually single adenoma), cutaneous lichen amyloidosis, Hirschsprung disease
MEN 2B	RET proto-oncogene	Medullary thyroid cancer, pheochromocytoma, marfanoid body habitus, facial features resulting from mucosal neuromas, ganglioneruomatosis of the gastrointestinal tract
FMC	RET proto-oncogene	Medullary thyroid cancer in at least four family members, with documented absence of other endocrinopathies
MEN4	*CDKN1B*	Primary hyperparathyroidism, GH-secreting pituitary tumor, small-cell neuroendocrine cervical carcinoma, ACTH-secreting pituitary adenoma (Cushing's disease), papillary thyroid carcinoma, microadenoma in the pituitary gland
MENX	*Cdkn1b*	Multifocal pituitary adenoma, bilateral pheochromocytoma, multifocal thyroid C-cell hyperplasia, parathyroid hyperplasia, extra-adrenal pheochromocytoma (paragangliomas) and pancreatic islet cells hyperplasia

To date, 15 MEN4 patients have been reported with heterozygous mutation of *CDKN1B* which indicates that MEN4, unlike MENX, is an autosomal dominant syndrome. Primary hyperparathyroidism is the most common feature of MEN4 and pituitary adenoma is the second most common tumor type, but due to the limited number of MEN4 patients the tumor spectrum is not clearly defined (Table 2) (Lee and Pellegata 2013).

1.4 Pituitary adenoma in MENX rats

MENX-affected rats develop multifocal pituitary hyperplasia with complete penetrance at around 4 months of age, which progresses to larger adenomas infiltrating the gland by the age of 8-12 months (Pellegata *et al.* 2006).

The non-invasive pituitary tumors occurring in MENX-affected rats belong to the gonadotroph lineage and express the transcription factor steroidogenic factor 1 (SF1), a

marker of gonadotroph cells. Rat adenomas show variable expression of the specific gonadotropin β-subunits (FSHβ and LHβ) and pronounced immunohistochemical staining (IHC) for the common α-GSU of the heterodimeric gonadotropins compared to normal tissue. The expression of FSHβ and LHβ reduces with the tumor progression. These lesions also exhibit mitotic activity and express high levels of Ki67. A few neoplastic cells express growth hormone (GH) or prolactin (PL) with atypical nuclei (Marinoni *et al.* 2013).

1.5 Angiogenesis

Blood vessels penetrate every organ and tissue where they deliver oxygen and nutrients to the cells, and transport metabolic waste products away from the cells. The regulation of blood vessel growth is important for normal biological processes such as reproduction, development repair and wound-healing. In addition to these beneficial characteristics, increased blood vessels and subsequently enhanced blood flow can fuel inflammatory and malignant diseases and facilitate metastasis of malignant tumors (Carmeliet 2003, Folkman 1995).

During embryogenesis, the primary vascular plexus forms by differentiation of mesoderm-derived endothelial precursor cells (angioblasts), which subsequently differentiate into endothelial cells (ECs), which in turn form fine capillaries. This process is known as vasculogenesis. After generation of more ECs from angioblasts, new capillaries can form by sprouting or by splitting of pre-existing vessels in a complex process termed angiogenesis. (Risau 1997, Cleaver and Krieg 1998). Moreover, circulating endothelial precursor cells are also able to differentiate into EC, to be integrated into vessel walls expanding their diameter or to be recruited in vessel sprouts.

Distinct factors like ephrin/Eph/Notch signaling and VEGF specify arterial or venous differentiation at this stage (Adams and Alitalo 2007).

Subsequently, arteries and veins form from primary capillaries becoming covered by pericytes and vascular smooth muscle cells (vSMCs), which provide stability and resistance against pulsatile blood flow (Pepper 1997). The walls of capillaries and fine vessels are covered by pericytes, whereas the walls of arteries and veins are associated with mono- or several layers of smooth muscle cells. Pericytes are cells of mesenchymal origin, and are capable of differentiating into other types of mesenchymal cells like smooth muscle cells, fibroblasts, and osteoblasts. The combination of vSMCs and pericytes covering blood vessels is called mural cells (Gerhardt and Betsholtz 2003).

In adults, formation and growth of new vessels are under strict control in both time and space. The presence of an angiogenic signal (hypoxia, inflammation and factors released by tumor cells) leads to the upregulation of angiogenesis regulators such as endothelium nitric oxide synthase (eNOS), vascular endothelial growth factor (VEGF), Angiopoietin-2 (Ang-2), fibroblast growth factor (FGF) and chemokines, which in turn activate quiescent ECs (Papetti and Herman 2002). Both, the VEGF and the angiopoietins (Angiopoietin-1 and -2) play complementary and coordinated roles in vascular development (Maisonpierre *et al.* 1997).

1.6 VEGF and VEGF receptors

VEGF is probably the best characterized angiogenic factor. *VEGF-A* (also referred to as *VEGF*) belongs to a gene family that includes placental growth factor (*PLGF*), *VEGF-B*, *VEGF-C* and *VEGF-D* (Ferrara and Davis-Smyth 1997). The *VEGF* gene, which is located on the short arm of chromosome 6, is composed of eight exons. The first 26 amino acids in VEGF constitute the signaling peptide showing that VEGF is a secreted protein. Alternative splicing of the *VEGF* produces six different isoforms composed of 121, 145, 165, 183, 189 and 206 amino acids, but despite of identical biological activities only VEGF121 and VEGF165 are secreted into the extracellular environment (Park *et al.* 1993). VEGF-A and its receptor, vascular endothelial growth factor receptor 2 (VEGFR-2) also known as Flkl/ KDR, play an important role in angioblast migration, differentiation into mature EC and initiation of vascular formation and promote angiogenesis in health and disease (Carmeliet *et al.* 1996).
VEGF can stimulate the endothelial cells to produce both plasminogen activators (uPA and tPA) and plasminogen activator inhibitor-1 (PAI-1), which suggests that VEGF may induce balance in proteolytic processes (Pepper *et al.* 1991, Ferrara *et al.* 2003). Moreover, VEGF is able to increase the expression of uPA receptor (uPAR) (Mandriota *et al.* 1995) and increase interstitial collagenase in human umbilical vein endothelial cells (HUVECs) (Unemori *et al.* 1992). These processes are essential for the remodeling of extracellular matrix components and initiation of EC migration. Mouse embryos, deletion of the *VEGF-A* is lethal, resulting in vascular defects and cardiovascular abnormalities (Carmeliet *et al.* 1996). Furthermore, VEGF affects an important number of angiogenic processes including wound healing, ovulation, maintenance of blood pressure, menstruation and pregnancy. The expression of VEGF can be increased by epidermal growth factor (EGF), transforming growth factors (TGFα and TGFβ), insulin-like growth factor 1 (IGF-1), fibroblast growth factors (FGF),

platelet derived growth factors (PDGF), etc. which indicates the possibility of autocrine or paracrine regulation of VEGF expression in the case of secretion of any of the above mentioned factors by cells (Ferrara and Davis-Smyth 1997). Hypoxia is one of the important factors, which induces VEGF expression through the binding of hypoxia-inducible factor-1 (HIF-1) to *cis* elements of VEGF promoter, and increases VEGF gene transcription and mRNA stability (Takagi *et al.* 1996).

1.7 Angiopoietins and Tie receptors

1.7.1 Angiopoietins

Angiopoietins are a family of secreted growth factors that bind endothelial specific receptors, Tie-1 and Tie-2 (**t**yrosine kinase with **i**mmunoglobulin and **e**pidermal growth factor homology domains), acting primarily on the vasculature to control blood vessel development and stability. The four identified angiopoietins are Angiopoietin-1, Angiopoietin-2, Angiopoietin-3, and Angiopoietin-4 (Ang1-4). Ang-3 is the mouse ortholog of human Ang-4 (Davis *et al.* 1996, Valenzuela *et al.* 1999, Maisonpierre *et al.* 1997). Ang-1 and -2 are the best characterized members of the angiopoietin family. All angiopoietin proteins are composed of: 1) an amino-terminal super clustering domain; 2) a coiled-coil domain, which is responsible for oligomerization of angiopoietin monomers enabling receptor activation (monomers can also bind Tie-2 receptor but not activate it); 3) a linker peptide; and 4) a carboxy-terminal fibrinogen-like domain necessary for receptor binding (Davis *et al.* 1996, Procopio *et al.* 1999).

1.7.1.1 Angiopoietin-1

Ang-1 is a 70kDa glycoprotein located on chromosome 8q22 and the first identified ligand that binds with high affinity to the Tie-2 receptor. Four different *Ang-1* splice variants have been reported: 1.5kb (full length Ang-1), 1.3kb, 0.9kb and 0.7kb. All of them encode proteins that bind Tie-2, but only the first two splice variants induce receptor autophosphorylation (Huang *et al.* 2000). Secreted human Ang-1 was found as heterogeneous multimers made up of basic trimeric, tetrameric, or pentameric oligomers (Kim *et al.* 2005, Procopio *et al.* 1999), but, to be able to activate Tie-2, it needs to be at least a tetramer (Davis *et al.* 2003).

1.7.1.2 Angiopoietin-2

Ang-2, the second identified ligand of Tie-2 receptors, shares about 60% sequence homology with Ang-1 (Maisonpierre *et al.* 1997). Ang-2 is mainly expressed in EC and stored in Weibel-Palade bodies (storage granules of endothelial cells). Upon stimulation by cytokines, Ang-2 is rapidly released from Weibel-Palade bodies (Fiedler *et al.* 2004). Additionally, tumor cells and retinal neurons express also Ang-2 (Ahmad *et al.* 2001, Koga *et al.* 2001, Hackett *et al.* 2000). The gene encoding Ang-2 is located on chromosome 8q23 (Cheung *et al.* 1998). There are two known splice variants of *Ang-2*. The first one, *Ang-2B,* was identified in chickens, which encodes a variant with a truncated amino-terminal domain. The second variant was *Ang-2(433),* which lacks parts of the coiled-coil domain and is therefore unable to stimulate Tie-2 (Mezquita *et al.* 1999, Kim *et al.* 2000d). Ang-2 was found almost always as dimer and less frequently as multimeric and oligomeric forms (Kim *et al.* 2005).

1.7.2 Tie receptors

Tie receptors comprise a family of receptor tyrosine kinases with a molecular weight of approximately 140kDa and are expressed by vascular and lymphatic endothelial cells. So far, two members of this family have been characterized, Tie-1 and Tie-2. Each has an extracellular domain consisting of two immunoglobulin (Ig)-like domains at the N-terminus, followed by three EGF (epidermal growth factor)-like cysteine rich repeats, three fibronectin type III domains, a transmembrane domain and an intracellular domain consisting of two kinase domains which can bind different molecules after autophosphorylation (Dumont *et al.* 1992, Partanen *et al.* 1992, Schnurch and Risau 1993). Tie receptors exhibit 76% amino acid sequence identity in the cytoplasmic region but only 33% and 37% in the extracellular part and transmembrane domain, respectively (Schnurch and Risau 1993). Tie-1 is expressed by EC, whereas Tie2 is expressed by endothelial cells, hematopoietic and endothelial precursor cells and tumor cells (Dumont *et al.* 1992, Sato *et al.* 1995, Helfrich *et al.* 2009). Tie-1 is known as orphan receptor and its signaling compared to Tie-2 is not well understood. COMP-Ang-1 (chimeric protein), native Ang1, and Ang4 are able to induce Tie-1 phosphorylation in primary and immortalized ECs. COMP-Ang-1 induced a weak phosphorylation of Tie-1 in HEK293 cells overexpressing Tie-1 and the phosphorylation was enhanced, if Tie-2 was co-expressed. Moreover, Tie-1 and Tie-2 form heterodimers, if co-expressed (Saharinen *et al.* 2005). However, another group reported that in Tie-2-silenced ECs, Ang-1 was not able to

activate Tie-1. Furthermore, phosphorylation of Tie-1 could be induced, if Ang-1 was absent, and HUVECs were transfected with a constitutively active form of Tie-2. Additionally, kinase activity of Tie-2 was essential for Tie-1 activation by Ang-1 in Hek293, but kinase activity of Tie-1 was not necessary for the phosphorylation of this receptor after stimulation with Ang-1, If Tie-2 was present in Hek293 (Yuan *et al.* 2007). Therefore, the activation mechanism of Tie-1 remains unclear.

Ang-1/Tie-2 interaction results in vascular remodeling, maturation and stabilization by promoting interactions between EC and surrounding mural cells (Dumont *et al.* 1994, Sato *et al.* 1995), whereas Ang-2 binding to this receptor induces vessel sprouting and regression (Holash *et al.* 1999).

1.7.3 The importance of Angiopoietins and Tie receptor during embryogenesis

Studies of mice deficient for *Tie-1* or *Tie-2* showed the importance of both receptors for the formation of the microvasculature during late organogenesis and for the maintenance of blood vessels in adult (Puri *et al.* 1999).

In embryos lacking *Tie-1*, vessels lost their structural integrity causing severe edema and hemorrhage leading to death between E13.5 and birth. Defects in the integrity of the microvasculature suggest that Tie-1 is required for survival and proliferation of microvascular endothelial cells and subsequently for the angiogenic growth of capillaries but this receptor is not essential for angioblast differentiation during vasculogenesis (Puri *et al.* 1995, Puri *et al.* 1999).

Tie-2 $^{-/-}$ embryos die between day E10.5 and E12.5 because of disturbed capillary maturation and stabilization. Vasculogenesis was not impaired in these embryos, but the development and maturation of primary capillary plexus was not progressed. Moreover, a reduced head and heart size, fewer endothelial cells (ECs) and poor association of endocardium with myocardium were observed because of Tie-2 absence suggesting that the Tie-2 system plays a role in vessel remodeling, and in maturation and stabilization of the cardiovascular system (Dumont *et al.* 1994, Sato *et al.* 1995).

Double-knockout embryos for *Tie-1* and *Tie-2* show a phenotype similar to *Tie-2* null embryos but with more severe defects. They die at E10.5 because of cardiovascular defects, but up to this time point, vasculogenesis proceeded normally indicating that Tie receptors are

not essential for the initial vessel formation but are necessary for the formation of microvasculature during late organogenesis (Puri *et al.* 1999).

Interestingly *Ang-1* $^{-/-}$ mice exhibit a phenotype similar to *Tie-2* deficient embryos with defects in heart development, decreased complexity and branching of the vascular network. Furthermore, a poor association between EC and mural cells with the extracellular matrix is also observed. These mice die between E11.5 and E12.5. The similarity in phenotypes suggests that Ang-1 stimulates Tie-2, and mediates vascular remodeling and stabilization of cell-cell and cell-matrix interactions via the recruitment of perivascular support cells (Suri *et al.* 1996).

In contrast, transgenic mice with localized overexpression of Ang-1 in their skin show an increase in vessel number, diameter and in the number of EC with normal cell-cell contacts with mural cells, which suggests that Ang-1 is an agonist of Tie-2 and required for vessel maturation and EC survival and proliferation (Suri *et al.* 1998).

In addition, *Ang-2* deficient mice appear normal at birth, but they develop chylous ascites due to defects in lymphatic system and edema within a few days after birth, which often results in morbidity within two weeks or, depending on the genetic background of mice strain, some of them even reach adulthood but with persistent disorganized lymphatic vascular system and poor smooth muscle cell coverage in large vessels (Gale *et al.* 2002, Dellinger *et al.* 2008, Shimoda *et al.* 2007). Moreover, hyaloid vasculature in the eye's lens of wild type mice regresses after birth, but in Ang-2-deficient mice this does not happen (Hackett *et al.* 2002, Gale *et al.* 2002). If *Ang-2* was replaced with *Ang-1* in mice, the lymphatic phenotype was rescued, but the hyaloid vessels persisted after birth and retinal vessels failed to grow normally to the retinal periphery. Therefore, Ang-2 is necessary for vascular regression and remodeling (Gale *et al.* 2002).

On the contrary, transgenic mice overexpressing *Ang-2* die at E9.5-10.5 and have a phenotype similar to that of in *Ang-1* or *Tie2*- null mice leading to the hypothesis that Ang-2 blocks the stimulatory effects of Ang-1 and acts as a natural antagonist of Ang-1. Additionally, when Ang-1 and Ang-2 were added exogenously together to the ECs the level of phosphorylated Tie-2 was decreased compared with the stimulation of Tie-2 with Ang-1 alone, which supports the hypothesis that Ang-2 acts as an antagonist of Ang-1 (Maisonpierre *et al.* 1997).

1.7.4 Angiopoietin /Tie-2 signaling in EC

Ang-1 and -2 can both bind to Tie-2 receptor but for years, it was believed that only Ang-1 can activate the Tie-2 receptor whereas, Ang-2 was described as a receptor antagonist (Davis *et al.* 1996, Maisonpierre *et al.* 1997). Recently, it has been reported that Ang-2 can also activate Tie-2 in a concentration- and context-dependent manner. However, the role of Ang-2 in Tie-2 activation remains controversial. Ang-2 acts as a dose-dependent antagonist of Tie-2 in the presence of Ang-1, but as a receptor agonist if Ang-1 is absent (Yuan *et al.* 2009).

Recombinant human ANG-2 (rhANG-2) binds with lower affinity to Tie-2 in HUVECs compared to rhANG-1 and is able to activate PI3K/Akt pathway in these cells promoting HUVECs survival, migration, and tube formation (Yuan *et al.* 2009, Kim *et al.* 2000c).

Tie-2 is rapidly internalized after the binding of Ang-1, while Ang-2 functions as a weak activator of Tie-2, leading to reduced rate of Tie-2 internalization and degradation. Interestingly, both ligands are released from the cell surface into the culture medium after Tie-2 activation and are not internalized with the receptor (Bogdanovic *et al.* 2006).

After ligand binding, Tie-2 receptor auto-phosphorylates itself at tyrosine residues within the intracellular kinase domain located at the C-terminus (Figure 3).

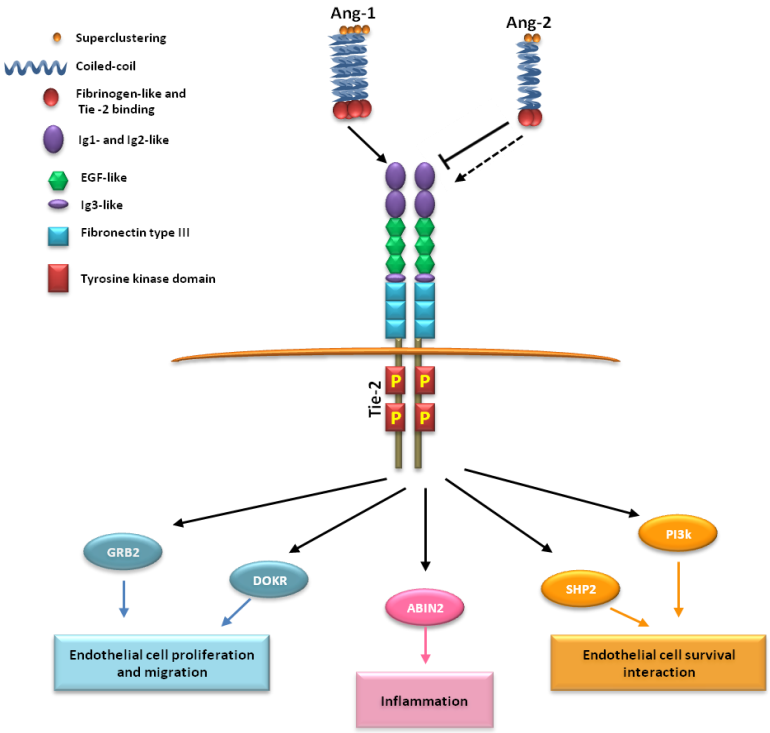

Figure 3: A schematic representation of Angiopoietin/Tie2 signaling and subsequent biological effects of Tie-2 activation by either Ang-1 or -2.

Activated Tie-2 receptor (human Tie-2: phosphorylated on tyr1101) stimulates the activation of the p85 regulatory subunit of phosphoinositide 3-kinase (PI3K) and Grb2 (Kontos *et al.* 1998). Grb2 is an adaptor protein that has been linked to activation of Ras/Raf and mitogen activated protein kinase (MAPK) cell growth signaling pathway (Huang *et al.* 1995, Sturk and Dumont 2010). The PI3K pathway activates Akt, which in turn phosphorylates and inhibits FKHR-1 (also called FOXO1), a transcription factor which induces Ang-2 expression in EC (Daly *et al.* 2004). Moreover, activated PI3K promotes Ang-1-induced EC cell migration and sprouting (Kim *et al.* 2000b, Kim *et al.* 2000a). Furthermore, Akt upregulates survivin, an apoptosis inhibitor thereby, supporting cell survival (Papapetropoulos *et al.* 2000).

Once Akt is activated, it is also able to induce EC survival via phosphorylation of eNOS (Chen and Meyrick 2004). Activation of Akt stimulates the phosphorylation and consequently the inhibition of proapoptotic proteins like BAD and procaspase-9 (Cardone *et al.* 1998).

There are also other adapter molecules, which interact with phosphorylated Tie-2 via their SH2 domain inducing growth factor binding partner 7 (Grb7), Grb14 and SH2 domain-containing tyrosine phosphatase 2 (Shp2) (Huang *et al.* 1995, Sturk and Dumont 2010).

Activated Tie-2 (Tyr1107) also associates with Dok-R, which in turn establishes binding sites for Nck and p21-activated kinase (PAK). The Dok-R-PAK pathway is involved in the Ang1-induced-migratory effect of EC (Jones and Dumont 1998).

SHP2 interacts with activated Tie-2 receptor (Tyr1112), which leads to the activation of MAPK pathway having an impact on cell migration (Huang *et al.* 1995, Kontos *et al.* 1998).

Additionally, Ang-1 is also able to activate the Ras-Raf-MEK-ERK1/2 pathway supporting migration of EC (Kim *et al.* 2002). Ang-1 through activation of the Ras-Raf-Mek-Erk1/2 pathway triggers sphingosine kinase-1 (SK-1), resulting in reduced vascular permeability by decreasing PECAM-1 phosphorylation and re-localizing VE-cadherin to endothelial cell-cell contacts (Li *et al.* 2008).

A further signaling event, which is related to Tie-2 activation includes the interaction of ABIN-2 (A20-binding inhibitor of NFκB-2) with this receptor, which suppresses NFκB-mediated inflammatory gene expression, including intercellular adhesion molecule 1 (ICAM1), vascular cell adhesion molecule 1 (VCAM1), and E-selectin (Kim *et al.* 2001, Jeon *et al.* 2003). Moreover, ABIN-2 inhibits apoptosis caused by serum deprivation in EC and promotes cell survival (Tadros *et al.* 2003).

Binding of Ang-1 to Tie-2 may have different signaling outcomes depending on receptor localization. In confluent HUVECs, Tie-2 is localized in cell-cell junctions and a strong Akt signaling is induced due to ligand receptor binding (quiescent endothelium), which leads to EC survival, and vascular stabilization by pericytes recruitment via release of pericytes recruitment factors such as TGF-β1 and platelet-derived growth factor-B (PDGF-B) from ECs (Hellstrom *et al.* 1999, Nishishita and Lin 2004). By contrast, Erk signaling is strongly induced when the cells are growing sparse and Tie-2 is localized at cell-substratum contacts leading to cell migration (activated endothelium) (Saharinen *et al.* 2008).

Tie-2 is also able to interact with integrin α5β1. This interaction is regulated and enhanced by fibronectin. Tie-2/α5β1 cross-talk at low concentration of Ang-1 promotes EC motility (Cascone *et al.* 2005).

in vitro studies indicated that rhANG-2 phosphorylates Tyr1101/1112 in HUVECs, and is also able to activate PI3K and Erk1/2 signaling pathways effecting cell survival and apoptosis (Harfouche and Hussain 2006b). Tyrosine residues 1102 and 1108 of Tie-2 are also important for activation of downstream signaling pathways and both are phosphorylated in HUVECs after stimulation with higher concentrations of rhANG-2 compared to concentrations used for stimulation of Tie-2 with rhANG-1 (Bogdanovic *et al.* 2006). These findings suggest that Ang-2 acts as a partial agonist of Tie-2 receptor.

1.8 Angiopoietins and VEGF

Upon angiogenic signals like VEGF or hypoxia, Ang-2 is released from Weibel-Palade bodies (Fiedler *et al.* 2004) resulting in increased ratio of Ang-2/Ang-1, which leads to blocking of Ang-1 stabilizing action due to binding of Ang-2 to Tie-2 receptor (Maisonpierre *et al*., 1997). *in vivo* studies indicate that in the presence of endogenous VEGF, Ang-2/Tie-2 binding increases capillary diameter, remodels the basal lamina, promotes proliferation and migration of ECs, and stimulates sprouting of new blood vessels (Figure 4).

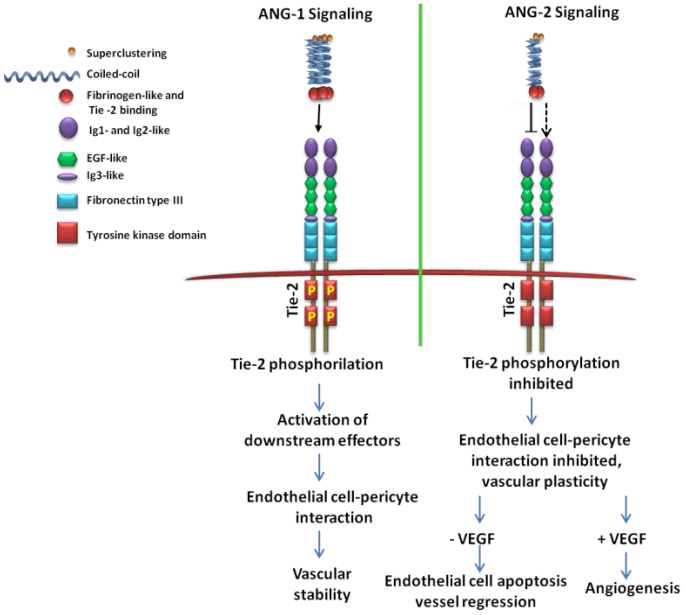

Figure 4: Agonistic and antagonistic effect of Ang-1 and -2 binding to Tie-2 receptor in presence and absence of VEGF.

If VEGF is inhibited, the binding of Ang-2 to the Tie-2 receptor promotes EC death and vessel regression. This observation indicates the impact of VEGF on anti- or pro-angiogenic features of Ang-2/Tie-2 binding (Lobov *et al.* 2002).

1.9 Angiopoietins and cancer

Solid microtumors (< 2mm diameter) start growing around existing vessels and initially do not need to induce angiogenesis to survive. With tumor progression the balance between angiogenic inhibitors and inducers shifts toward an angiogenic phenotype (angiogenic switch). As a result of cross talk between tumor cells and surrounded ECs in a glioblastoma model, the later one becomes activated and Ang-2 expression increases (Holash *et al.* 1999). Since VEGF is still absent, Ang-2 promotes disassociation of mural cells from ECs, which results in vessel regression and induction of hypoxia leading to VEGF expression and secretion by tumor cells (Hammes *et al.* 2004, Holash *et al.* 1999). The combination of VEGF and Ang-2 facilitates vessel remodeling (activating EC migration) and induces tumor angiogenesis, although the new vascular network is highly disorganized, and the vessels possess poor mural cell coverage (Maisonpierre *et al.* 1997, Holash *et al.* 1999). Newly formed vessels continue to overexpress Ang-2. Notably, by *in situ* hybridization, Ang-2

mRNA was found in ECs of tumor vessels but not in ECs of adjacent healthy tissues, and it is one of the earliest markers of tumor-induced neovascularization (Carmeliet *et al.* 1996, Zagzag *et al.* 1999).

Interestingly, not only EC or hematopoietic progenitor cells but also some tumor cells, like colon cancer, melanoma and bladder carcinoma have the ability to express Ang-2, which is correlated with poor prognosis (Ahmad *et al.* 2001, Oka *et al.* 2005, Takanami 2004). Elevated Ang-2 amounts can also be detected in the circulating blood of patients suffering some tumor types such as lung cancer and melanoma (Park *et al.* 2007, Helfrich *et al.* 2009).

The role of Ang-1 in tumor progression is controversial. The systemic overexpression of Ang-1 in nude mice bearing tumor xenotransplants results in increased metastasis to the lungs (Holopainen *et al.* 2009). Inoculation of breast cancer cell lines overexpressing Ang-1 in mammary fat pads of nude mice exhibit reduced tumor growth rate, if compared to the tumors originated from injection of control vector or parental cells (Hayes *et al.* 2000).

These observations suggest that Ang-1 function depends on tumor cell type and the concentration of Ang-2.

1.10 Pituitary adenoma and its angiogenic characteristics

The pituitary tissue is a highly vascularized gland, but unlike other solid tumors, pituitary adenomas possess lower microvascular density (MVD) compared to normal glands (Jugenburg *et al.* 1995). Furthermore, the expression of VEGF, and its corresponding receptors, is detected in highly vascularized anterior pituitary. Paradoxically evidence for a neovascularization due to high expression of VEGF/VEGFR is not observed (Onofri *et al.* 2006).

Previous studies investigating MVD and VEGF expression in pituitary adenomas were performed with different methods leading to controversial results. Therefore, it is not clear which pituitary adenoma subtype associates with the highest MVD or with the highest level of VEGF expression. In one study, the highest MVD was reported for prolactin-secreting adenomas, whereas the lowest MVD was found in GH-secreting adenomas, but the differences in MVD between the various adenoma subtypes were not significant (Jugenburg *et al.* 1995). In another work, the lowest MVD was described for ACTH-secreting adenomas and microprolactinomas (Turner *et al.* 2000b). Regarding VEGF expression, it has been

reported that this protein is elevated in ACTH- and GH- producing adenomas (Lloyd *et al.* 1999). In contrast, another study demonstrated that NFPAs express significantly higher VEGF mRNA and protein compared to normal pituitary (McCabe *et al.* 2002).

VEGF receptors are rarely co-expressed in pituitary adenomas. In some cases, no expression of the receptor is observed. In pituitary adenomas, VEGFR-1 is localized in tumor cells whereas VEGFR-2 and neuropilin-1 are detected in pituitary adenoma-associated ECs. Functional studies suggest that VEGF expression in pituitary adenomas may play a role in the maintenance of the vascular system and stimulation of pituitary adenoma cell proliferation (Onofri *et al.* 2006).

1.11 Anti-angiogenic drugs

Establishment of a blood vessel plexus is an important prerequisite for the growth of solid tumors providing them with nutrients and oxygen and facilitating invasion and metastasis. Therefore, angiogenesis promoting factors, involved receptors and signaling pathways are attractive targets to develop anti-angiogenic drugs.

VEGF is one of the important pro-angiogenic factors, where lost even as single allele can cause developmental abnormalities and early embryonic lethality due to impaired angiogenesis in mice. Moreover, the ability of *Vegf* $^{-/-}$ embryonic stem cells to form tumors is significantly reduced in nude mice (Ferrara *et al.* 1996). Additionally, treatment of nude mice injected with human tumor cell lines, with monoclonal anti VEGF antibodies inhibits tumor growth (Kim *et al.* 1993). These observations led to the generation of the first anti-angiogenic antibodies targeting VEGF and its receptor (VEGFR).

Bevacizumab (Avastin) is the first approved anti-angiogenic humanized monoclonal antibody targeting VEGF, which was administrated with standard chemotherapy to treat colorectal cancer (Hurwitz *et al.* 2004), non-small cell lung cancer (Lauro *et al.* 2014, Kosty *et al.* 2011), renal cell cancer (Harshman and Srinivas 2010) and pituitary carcinoma (Ortiz *et al.* 2012) with promising results.

Meanwhile, antibodies against VEGFR or multikinase small molecule inhibitors have been developed and approved or are being tested in clinical trials (Prewett *et al.* 1999, Palmer 2008).

Discovery of the Ang/Tie system as the second important regulatory system associated with angiogenesis (Partanen *et al.* 1992) awakened the interest to target also this system. After primary vascular plexus is formed by VEGF-mediated signaling, Tie-2 and its ligands undertake an important role in vascular remodeling and maturation (Maisonpierre *et al.* 1997). During Tumor development, the expression of Ang-2 is increased leading to detachment of mural cells from EC and vessel regression, which in turn causes hypoxia and VEGF upregulation, followed by initiation of angiogenesis (Holash *et al.* 1999).

Therefore, several agents have been developed to inhibit Ang/Tie axis (Gerald *et al.* 2013). Among them AMG386 (trebananib) has successfully achieved phase three trials. This agent (previously named 2xCon4[C]) is a recombinant Fc-peptide fusion protein (peptibody) that selectively binds to Ang-1 and -2 and neutralizes their interaction with Tie-2 receptor. In preclinical experiments, AMG386 was able to inhibit tumor EC proliferation without having any effect on tumor cells proliferation (Oliner *et al.* 2004). In several studies AMG386 was administrated in combination with standard chemotherapies (Dales *et al.* 2004, Liontos *et al.* 2014, Herbst *et al.* 2009). It was well tolerated and showed evidence of antitumor activity in adult patients with advanced solid tumors. Long term studies were done to treat epithelial ovarian cancer using a combination of AMG386 and paclitaxel. The study results indicated that AMG386 significantly prolonged progression-free survival of patients in the phase 3 TRINOVA-1 study but overall survival of patients was not significantly longer in the intent-to-treat population (Monk *et al.* 2014, Monk *et al.* 2016). However, there is no study about treatment of adenomas and less aggressive tumors with AMG386.

Beside inhibition of Ang-2/Tie-2 interaction, it is conceivable that small molecules against Tie-2 kinase domain (Tie-2 kinase inhibitor; TKI) could also be promising candidates as anti-angiogenic agents. TKI is able to decrease tumor growth by inducing tumor cell apoptosis in angiosarcomas (Hasenstein *et al.* 2012). One such drug is available through Abcam (named TKI) and it acts as a reversible and selective ATP-binding site binding molecule, targeting Tie2 kinase and inhibits activation of downstream signaling pathways although Tie-2 is activated (Semones *et al.* 2007).

Since TKI could also bind with lower affinity to VEGFR2/3 and PDGFR1b, AMG386 is a more specific inhibitor of Ang-2/Tie-2-mediated signaling.

1.12 The aim of this thesis

MENX-affected rats develop multifocal pituitary gonadotroph adenomas with complete penetrance. Gene expression array analysis has identified a considerable number of genes deregulated in rat pituitary tumors compared to normal pituitary tissues. Some of the deregulated transcripts are associated with angiogenesis, including *Ang-1*, *Ang-2* and *Vegf*. Specifically, *Ang-2* was upregulated whereas *Ang-1* was downregulated in RPAs. We chose *Ang-1* and *-2*, which have not been so far extensively analyzed in human pituitary adenomas when compared to *Vegf.*

The aim of our study was to elucidate the functional role of angiopoietins in pituitary tumorigenesis and to evaluate their therapeutic potential.

We tried to understand the advantages of increased Ang-2 in the PAs of MENX rat and their human counterparts. This project focused on following points:

1) Validation of preliminary studies of mRNA expression changes of *Ang-1* and *Ang-2* in pituitary adenomas (PAs) in MENX-affected rats and in the corresponding human gonadotroph adenomas, followed by characterization of the expression of Ang-1 and Ang-2 at protein level in gonadotroph PA of rats and humans.

2) Investigation of the role of increased Ang-2 expression in PA tumorigenesis.

3) Assessment of ANG-2 levels in circulating blood of PA patients, correlation between ANG-2 expression and clinical parameters.

4) *In vivo* and *in vitro* studies to evaluate the efficacy of drugs targeting angiopoietin signaling in PAs.

We hypothesized that elevated Ang-2 levels in PAs, where blood vessels already exist, might promote tumor growth.

2 Material and Methods

2.1 Materials

2.1.1 Equipment

Table 3: List of used equipment.

Centrifuge Biofuge pico	Heraeus Instruments, Osterode (Germany)
Rotor: 3325B 1.5 ml	Thermo Fisher Sci. Waltham (MA, USA)
Centrifuge Fisherbrand Mini	Fisher Scientific, Schwerte (Germany)
Rotors 0.2 ml, 1.5 ml	Fisher Scientific, Schwerte (Germany)
Centrifuge Mikro 200R	Andreas Hettich, Tuttlingen (Germany)
Rotor: 2424-B 1.5 ml	Andreas Hettich, Tuttlingen (Germany)
Centrifuge Rotanta 460R	Andreas Hettich, Tuttlingen (Germany)
Rotor: 5624 15 ml, 50 ml	Andreas Hettich, Tuttlingen (Germany)
Cell counting chamber, Neubauer	Brand, Wertheim (Germany)
Dispenser Multipette® plus	Eppendorf, Hamburg (Germany)
Electrophoresis Cell GT MINI-SUB®	Bio-Rad Laboratories, Munich (Germany)
Electrophoresis Mini-Cell XCell *SureLock™* Novex	Invitrogen, Darmstadt (Germany)
Electrophoresis Transfer Cell Mini Trans-Blot®	Bio-Rad Laboratories, Munich (Germany)
Freezing container NALGENETM Cryo 1°C	Thermo Fisher Sci., Roskilde (Denmark)
Gel documentation system	Vilber Lourmat, Eberhardzell (Germany)
Heating block Thermomixer® comfort 1.5 ml	Eppendorf, Hamburg (Germany)
Heating block Thermomixer® 5436	Eppendorf, Hamburg (Germany)
Hood Uniflow UVUB 1800	UniEquip, Planegg (Germany)
Incubator innova CO_2 170S	New Brunswick Sci. Edison (NJ, USA)
Incubator shaker Model G25	New Brunswick Sci., Edison (NJ, USA)
Liquid Nitrogen Freezer	Tec lab, Taunusstein (Germany)
Luna™ automated cell counter	Logos Biosystems, Annandale (USA)
Microscope Apotome	Carl Zeiss, Jena (Germany)
Microscope Axio Imager Z1	Carl Zeiss, Jena (Germany)

Microscope EVOS XL	AMG, Bothell (Germany)
Microscope Primo Star	Carl Zeiss, Jena (Germany)
Microscope Olympus BX43F	Olympus, Tokio, Japan
Microtom	Thermo Fisher Sci., Waltham (MA, USA)
Mili-Q Direct 8	Merc/ Millipore, Darmstadt (Germany)
4D-Nucleofector™ System (Core and X unit)	Lonza, Basel (Switzerland)
PCR cycler Real-Time 7300	Applied Biosystems, Carlsbad (CA, USA)
PCR cycler TPersonal Thermocycler	Biometra, Goettingen (Germany)
pH meter inoLab® Level 1	WTW, Weilheim (Germany)
Power supply PowerPac 300	Bio-Rad Laboratories, Munich (Germany)
Power supply PowerPac Basic	Bio-Rad Laboratories, Munich (Germany)
Pressure cooking pot Tender Cooker	Nordic Ware, Minneapolis (MN, USA)
Scales Sartorius basic	Sartorius, Göttingen (Germany)
Scales Sartorius universal	Sartorius, Göttingen (Germany)
Spectrophometer NanoDrop® ND-1000	Thermo Fisher Sci., Waltham (MA, USA)
Vacuum Concentrator plus	Eppendorf, Hamburg (Germany)
Varioskan™ LUX Multimode Microplate Reader	Thermo Fisher Sci., Waltham (MA, USA)
Ventana Discovery XT	Roche, Basel (CH)
Vortexer VF2	IKA®-Werke, Staufen (Germany)
Water bath shaker SW21	Julabo Labortechnik, Seelbach (Germany)

2.1.2 Consumable materials

Table 4: List of consumable materials.

Amicon Ultra-0.5 Centrifugal Filter Unit with Ultracel-30 membrane	Merc/ Millipore, Darmstadt (Germany)
Blotting paper grade 3m/N 65 g/m2	Muntkell & Filtrak, Bärenstein (Germany)
Cell strainer Falcon™ 70 µm, nylon	BD Biosciences, Bedford (MA, USA)
Combitips® for Multipette® 10 ml	Eppendorf, Hamburg (Germany)
Cover slips various sizes	Carl Roth, Karlsruhe (Germany)
Cryogenic vials sterile 2 ml freestanding	BD Biosciences, Franklin Lakes (NJ, USA)

Gel cassettes 1.5 mm	Invitrogen, Grand Island (NY, USA)
Glass slides SuperFrost® 76x26 mm	Carl Roth, Karlsruhe (Germany)
MagnaRack™ Magnetic Separation Rack	Thermo Fisher Sci., Waltham (MA, USA)
MicroAmp™ Clear Adhesive Film	Applied Biosys., Foster City (CA, USA)
Microplate, 96 well,	Nunc, Roskilde (Denmark)
neoCulture Cell scraper	Sarstedt, Nümbrecht (Germany)
NC Membrane, Amersham Protran Premium 0.45	GE Healthcare, Munich (Germany)
Parafilm®	Carl Roth, Karlsruhe (Germany)
PCR plate (0.2 ml) Thermo-Fast® 96-well	Abgene/Thermo Sci., Rockford (IL, USA)
PCR tube strips 0.2 ml	Eppendorf, Hamburg (Germany)
Petri dishes 100 x 15 56.7 cm^2 Nunclon™ Δ	Nunc, Roskilde (Denmark)
Photographic film Amersham HyperfilmTM-ECL	GE Healthcare, Little Chalfont (England)
Pipettes, Pasteur glass 3.2 ml	Carl Roth, Karlsruhe (Germany)
Pipettes, serological CELLSTAR® 5 ml	Greiner BioOne, Frickenhausen (Germany)
Pipettes, serological CELLSTAR® 10 ml	Greiner BioOne, Frickenhausen (Germany)
Pipettes, serological CELLSTAR® 25 ml	Greiner BioOne, Frickenhausen (Germany)
Pipette tips Graduated Filter Tips TipOne® 0.1-10 µl	Starlab, Ahrensburg (Germany)
Pipette tips Graduated Filter Tips TipOne® 1-20 µl	Starlab, Ahrensburg (Germany)
Pipette tips Graduated Filter Tips TipOne® 1-100 µl	Starlab, Ahrensburg (Germany)
Pipette tips Graduated Filter Tips TipOne® 1-200µl	Starlab, Ahrensburg (Germany)
Pipette tips Graduated Filter Tips TipOne® 100-1000 µl	Starlab, Ahrensburg (Germany)
Reaction tubes 1.5 ml	Eppendorf, Hamburg (Germany)
Reaction tubes 2 ml	Eppendorf, Hamburg (Germany)
Reaction tubes FalconTM Blue Max 15 ml	BD Biosciences, Franklin Lakes (NJ, USA)

Reaction tubes FalconTM Blue Max 50 ml	BD Biosciences, Franklin Lakes (NJ, USA)
Reaction tubes, RNase-free 1.5 ml	Zymo Research, Orange (CA, USA)
Scalpel Cutfix	Carl Roth, Karlsruhe (germany)
Slide-A-Lyzer™ Dialysis Cassettes	Thermo Fisher Sci., Waltham (MA, USA)
Syringe, single-use 50 ml	B. Braun, Melsungen (Germany)
Tissue culture flasks 25 cm^2, filter cap	Greiner BioOne, Frickenhausen (Germany)
Tissue culture flasks 75 cm^2, filter cap	Greiner BioOne, Frickenhausen (Germany)
Tissue culture plates 6 well	BD Biosciences, Franklin Lakes (NJ, USA)
Tissue culture plates 24 well MULTIWELL™ flat	BD, Franklin Lakes (NJ, USA)
Tissue culture plates 48 well MULTIWELL™ flat	BD, Franklin Lakes (NJ, USA)
Whatman Paper	GE Healthcare, Munich (Germany)
White 96-well Plates, Solid Bottom	Greiner BioOne, Frickenhausen (Germany)

2.1.3 Chemicals and reagents

Table 5: List of chemicals and reagents.

Agarose LE (gel electrophoresis)	Biozym, Hessisch Oldendorf (Germany)
Ampicillin sodium salt	Sigma-Aldrich, Steinheim (Germany)
Ampuwa® water	Fresenius KABI, Bad Homburg (Germany)
Antibody diluent Dako REAL	Dako, Hamburg (Germany)
Antibody diluent buffer	DCS Innovative Diagn. Sys., Hamburg (Germany)
APS	Sigma-Aldrich, Steinheim (Germany)
β-mercaptoethanol	Sigma-Aldrich, Steinheim (Germany)
Bis-acrylamide ProtoGel 30% (w/v)	National diagnostics, Atlanta (GA, USA)
Blotting grade Blocker Non-Fat Dry Milk	Bio-Rad Lab., Munich (Germany)
Bovin Serum Albumin	Sigma-Aldrich, Steinheim (Germany)
Chemiluminescent substrate Super Signal® West Pico	Pierce / Thermo Sci., Rockford (IL, USA)
Citrate buffer 10X PH6.0	VWR International GmbH, Darmstadt (Germany)
Cresol red	AppliChem, Darmstadt (Germany)
Collagenase type IV	Worthington Biochemical Corporation
DAPI	Sigma-Aldrich, Steinheim (Germany)

DNA loading dye 6x	Thermo Fisher Sci., Waltham (MA, USA)
1kb and 100bp-DNA-Gene Ruler-Markers	Thermo Fisher Sci., Waltham (MA, USA)
dNTP Mix 10 mM each	Fermentas, St. Leon-Rot (Germany)
DPBS	Gibco/Invitrogen, Grand Island (NY, USA)
DTSSP crosslinker	VWR International GmbH, Darmstadt (Germany)
DTT 0.1 M	Invitrogen, Grand Island (NY, USA)
Duolink® in situ PLA probe kit anti-goat	Olink Bioscience, Uppsala (Sweden)
Duolink® in situ PLA probe kit anti-goat	Olink Bioscience, Uppsala (Sweden)
EDTA 0,5M pH 8,0	Life Technologies, Carlsbad (USA)
Endothelial cell growth medium	Sigma-Aldrich, Steinheim (Germany)
Ethanol	Merck, Darmstadt (Germany)
Ethidium bromide	Sigma-Aldrich, Steinheim (Germany)
F-12K Nutrient Mixture, Kaighn's Modification (1X)m liquid	Gibco/Invitrogen, Grand Island (NY, USA)
Fetal bovine serum (FBS)	Gibco/Invitrogen, Grand Island (NY, USA)
First strand buffer 5x	Invitrogen, Grand Island (NY, USA)
Fungizone™	Gibco/Invitrogen, Grand Island (NY, USA)
Glycin	Sigma-Aldrich, Steinheim (Germany)
HEPES	Sigma-Aldrich, Steinheim (Germany)
Glycin	Sigma-Aldrich, Steinheim (Germany)
HBSS 1x without $CaCl_2$/$MgCl_2$	Gibco/Invitrogen, Grand Island (NY, USA)
Hexadimethrine bromide	Sigma-Aldrich, Steinheim (Germany)
High-capacity RNA-to-cDNA Kit	Applied Biosystems, Waltham (USA)
H_2O_2	Merck, Darmstadt (Germany)
Horse serum (HS)	Gibco/Invitrogen, Grand Island (NY, USA)
Hydrogen peroxide 30%	Merck, Darmstadt (Germany)
Isopropanol	Merck, Darmstadt (Germany)
Kanamycin A monosulfate	Sigma-Aldrich, St. Louis (MO, USA)
Laemmli sample buffer 2x/4x	Bio-Rad Lab., Hercules (CA, USA)
LB broth base	Invitrogen, Grand Island (NY, USA)
LB Broth with agar (Miller)	Sigma-Aldrich, Steinheim (Germany)
Methanol	Merck, Darmstadt (Germany)

Mounting medium VECTASHIELD®	Vector Lab., Burlingame (CA, USA)
NaCl EMSURE®	Merck, Darmstadt (Germany)
NP-40 Tergitol	Sigma-Aldrich, Steinheim (Germany)
PageRulerTM prestained protein ladder	Fermentas, St. Leon-Rot (Germany)
Paraformaldehyde	Merck, Darmstadt (Germany)
PBS powder pH 7.4	Sigma-Aldrich, St. Louis (MO, USA)
Penicillin-Streptomycin, liquid	Gibco/Invitrogen, Grand Island (NY, USA)
Phenol Red	Sigma-Aldrich, Steinheim (Germany)
PhosSTOP™	Roche Diagnostics, Mannheim (Germany)
Photographic developer G153 A and B	Agfa Healthcare, Mortsel (Belgium)
Photographic fixer G354	Agfa Healthcare, Mortsel (Belgium)
PNGase F	New England Biolabs, Ipswich (MA, USA)
Ponceau S	Sigma-Aldrich, Steinheim (Germany)
Protease inhibitor cocktail tablets complete mini	Roche Diagnostics, Mannheim (Germany)
Protein A/G PLUS-Agarose	Santa Cruz Biotechnology, Dallas (USA)
Random primers	Promega, Mannheim (Germany)
Recombinant Human ANG-1	R&D Systems (USA, Canada)
Recombinant Human ANG-2	R&D Systems (USA, Canada)
Red blood cell Lysing Buffer	Sigma-Aldrich, Steinheim (Germany)
Reverse transcriptase SuperScript® II	Invitrogen, Grand Island (NY, USA)
RIPA buffer	Sigma-Aldrich, Steinheim (Germany)
RNase inhibitor RNaseOUT™	Invitrogen, Grand Island (NY, USA)
RNaseZAP®	Sigma-Aldrich, St. Louis (MO, USA)
RPMI 1640	Gibco/Invitrogen, Grand Island (NY, USA)
Roti®-Stock 10x TBS	Carl Roth, Karlsruhe (Germany
SDS 10% (w/v) solution	Bio-Rad Lab., Munich (Germany)
SDS-PAGE running buffer Rotiphorese® 10x	Carl Roth, Karlsruhe (Germany)
Sodium chloride	Merck, Darmstadt (Germany)
Sodium desoxycholate	Sigma-Aldrich, St. Louis (MO, USA)
Sodium hydroxide tablets EMSURE®	Merck, Darmstadt (Germany)
Stripping buffer for Western Blots Restore™ PLUS	Pierce / Thermo Sci., Rockford (IL, USA)

TaqMan® universal PCR master mix 2x	PE Applied Biosys, Weiterstadt (Germany
Taq DNA polymerase	Fermentas, St. Leon-Rot (Germany)
TBE Tris/Boric Acid/EDTA 10x	Bio-Rad Lab., Hercules (CA, USA)
TEMED	Amresco, Solon (OH, USA)
TKI (ab141270)	Abcam, Berlin, (Germany)
Triton X-100	Sigma-Aldrich, Steinheim (Germany)
Trizma® base	Sigma-Aldrich, Steinheim (Germany)
Trypan blue solution 0.4%	Sigma-Aldrich, St. Luis (MO, USA)
Trypsin, 0.05% with EDTA	Gibco / Invitrogen, Grand Island (NY, USA)
Tween 20	Carl Roth, Karlsruhe (Germany)
Wheat Germ Agglutinin	Vector Lab., Burlingame (CA, USA)
Xylene	Merck, Darmstadt (Germany)

2.1.4 Buffers and solutions

All solutions listed were prepared in bidest. water.

Agarose gel:

1% (w/v) agarose in 1x TBE
boil until dissolved, cool to approximately 60°C
add 0.005% (v/v) ethidium bromide

Isolation buffer (for EC isolation from pituitary adenoma tissue):

DPBS
2% FBS
0.5 M EDTA

NP-40 lysis buffer (IP):

20 mM HEPES
150 mM NaCl
1 mM EDTA
1% nonidet P-40 (NP-40)

Paraformaldehyde (2%, pH 7.4):

2% (w/v) paraformaldehyde in PBS
15 µl phenol red
add 10 M NaOH until dissolved (color change from pink to colorless)
adjust pH to 7.4 with HCl using pH indicator strips

PLA-washing buffer A (pH 7.4, steril):

8.8 g NaCl
1.2 g Tris Base
0.5 ml Tween 20
Ad 1 l MilliQ-H2O

PLA- washing buffer B (pH 7.5, steril):

5.84 g NaCl
4.24 g Tris Base
26 ml Tris HCl
Ad 1 l MilliQ-H2O

Running buffer 10x (pH 8.3):

500 mM Tris base
390 nM Glycin
0.039% (w/v) SDS

Separating gel (8%) for SDS-PAGE (10 ml):

2.64 ml 30% (w/v) acrylamide/bis
4.71 ml H2O bidest.
2.5 ml 1.5 M Tris (pH 8.8)
100 µl 10% (w/v) SDS
50 µl 10% (w/v) APS
5 µl TEMED

Separating gel (10%) for SDS-PAGE (10 ml):

3.3 ml 30% (w/v) acrylamide/bis
4.05 ml H2O bidest.
2.5 ml 1.5 M Tris (pH 8.8)
100 µl 10% (w/v) SDS
50 µl 10% (w/v) APS
5 µl TEMED

Stacking gel (4%) for SDS-PAGE (5ml):

0.66 ml 30% (w/v) acrylamide/bis
3.3 ml H2O bidest.
1.26 ml 0.5 M Tris (pH 6.8)
50 µl 10% (w/v) SDS
25 µl 10% (w/v) APS
5 µl TEMED

TBE buffer 5x (pH 8.3):

89 mM tris base
89 mM Boic Acid
3 mM EDTA

Transfer buffer 10x:

31.2 g Tris Base
144 g Glycin
Add 1 l MilliQ-H2O

Transfer buffer 1x:

10% (v/v) 10x Blotting buffer
20% (v/v) MeOH

2.1.5 Commercially available kits

Table 6: List of kits.

Avidin/Biotin Blocking System	Covance Inc., Princeton (USA)
BCA Protein Assay Pierce®	Thermo Sci., Rockford (IL, USA)
Caspase-Glo® 3/7 Assay Systems	Promega, Mannheim (Germany)
DSB-XTMBiotin protein labeling kit	Thermo Fisher Scientific, Waltham, USA
Duolink® in situ Detection Reagents kit red	Olink Bioscience Uppsala (Sweden)
Dynabeads FlowComp Flexi Kit	Thermo Fisher Scientific, Waltham, USA
Histo mark Biotin Streptavidin HRR- system Goat anti Rabbit IgG (H+L)	Kirkegaard & Perry Laboratories, (MD, USA)
Histo mark Biotin Streptavidin HRR- system rabbit anti goat IgG (H+L)	Kirkegaard & Perry Laboratories, (MD, USA)

Human Angiopoietin-2 Quantikine ELISA Kit	R&D Systems, (USA, Canada)
Miniprep Kit QIAprep® Spin (50)	Qiagen, Hilde (Germany)
Mycoplasma detetction kit	PromoKine, Heidelberg (Germany
RNeasy Micro Kit (50)	Qiagen, Hilde (Germany)
SF Cell Line 4D-Nucleofector^{tm} X Kit	Lonza, Basel (Switzerland)
WST-1 Cell Proliferation kit	Roche, Basel (CH)

2.1.6 Constructs

The pIREShyg vector containing human Ang-2/myc epitope/6x His was kindly provided by Dr. Katharina Detjen, Charité-Universitätsmedizin (Detjen *et al.* 2010) (Berlin) (Figure 5).

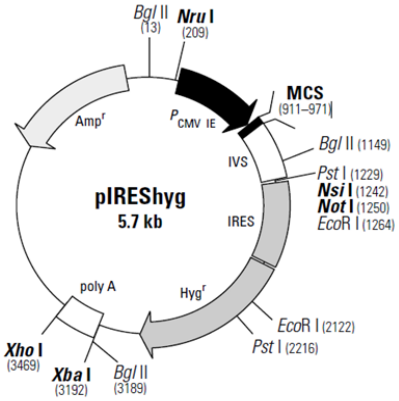

Figure 5: *ANG-2*:pIREShyg vector backbone map (dr. Detjen).

The EX-K4038-M09 vector with human *ANG-2* transcript variant 1 (Myc/DDK tagged) was purchased by GeneCopoeia, Rockville (MD, USA) (Figure 6).

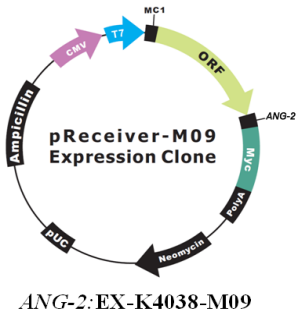

Figure 6: *ANG-2*:EX-K4038-M09 expression vector backbone map (GeneCopoeia).

pLKO.1-puro vector caring a shRNA was used for stable gene silencing of rat *Ang-2* using lentiviral particles (Figure 7). Three independent sequences was used to silence *Ang-2* as follow: Angpt2-1: GATTTTAGCACAAAGGATT; Angpt2-2: TGCAGCTTCTTCAACATTCTA; Angpt2-3: ACGGCTGTGATGATCGAGATT. Sense sequence, loop and anti-sense sequence form after transcription a hairpin structure in the nucleus. In the cytoplasm, the loop sequence will be removed by Dicer. From this point, they will be processed in the same manner as siRNAs to degrade the mRNA of interest.

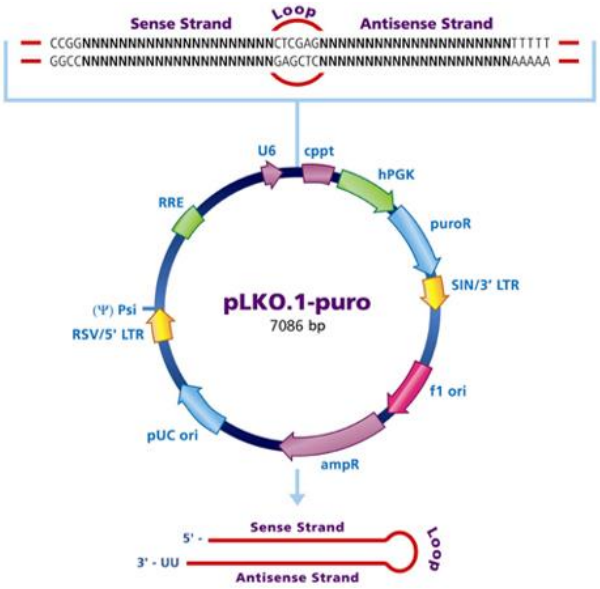

Figure 7: pLKO.1-puro vector map**.**

These lentiviral transduction particles and non-target shRNA control transduction particles were purchased from Sigma-Aldrich Chemie GmbH.

2.1.7 Assay primer for qRT-PCR

Table 7: List of assay primers for qRT-PCR (Thermo Fisher).

Gene symbol	Assay ID	Sequence 5'→3'
ANGPT1 (human)	Hs00375822_m1	GAGACCCAGGTACTAAATCAAACT
ANGPT2 (human)	Hs01048042_m1	GAACAGTTTCCTAGAAAAGAAGGT
VEGF (human)	Hs00900055_m1	ACATCACCATGCAGATTATGCGGAT
TBP-645 Fw (human)	090907-151	GCCCGAAACGCCGAATAT
TBP-717 Rev (human)	090907-151	CCGTGGTTCGTGGCTCTCT

TBP	1957174	CCAAGCGGTTTGCTGGGG
Angpt-1 (rat)	Rn00585552_m1	AAAAGAAGTTTTGCTAAAGGGAGG
Angpt-2 (rat)	Rn01756774_m1	GCTCACAGGAGGCTGGTGGTTCGA
β2m (rat)	Rn00560865_m1	GCTTGCCATTCAGAAAACTCCCCA

2.1.8 siRNAs

Table 8: List of siRNAs.

siRNA	Product number	Company
ON TARGETplus Non-targeting siRNA	D-001810-03-05	Thermo scientific Dharmacon Lafayette (CO,USA)
siPOOL targeting rat Angpt2	NM_134454	siTOOLs Biotech GmbH, München (Germany)

2.1.9 Antibodies

2.1.9.1 Primary and secondary antibodies used for Western blot:

Primary antibodies were diluted in 3% (w/v) BSA containing 0.1% sodium azide. Antibody dilutions were stored at 4°C and re-used several times.

Table 9: Primary antibodies used in Western Blot.

Antibody	Company	Product Nr.	Host	Dilution	Band size
anti-Ang-1	Abcam	Ab133425	mouse	1:500	~57kDa
anti-Ang-2	R&D	AF623	goat	1:200	~57kDa
anti-Integrin	Abcam	EP1041Y	rabbit	1:500	~140kDa
anti-Tie-2	Thermo Scientific	PA5-28582	rabbit	1:500	~140kDa
anti-Tie-2	Santa Cruz	sc-324	rabbit	1:500	~140kDa
anti-Tie-2	Santa Cruz	sc-31266	goat	1:500	~140kDa
anti-pTie-2 (pTyr1102/1108)	Millipore	PC449	rabbit	1:3000	~140kDa
anti-pTie-2 (pTyr 992)	Cell Signaling	4221	rabbit	1:1000	~140kDa
anti-Akt	Cell Signaling	9272	rabbit	1:1000	~60kDa
anti-pAkt (S473)	Cell Signaling	4060	rabbit	1:500	~60kDa
anti-Fak	Cell Signaling	3285	rabbit	1:1000	~125kDa
anti-pFak (Tyr397)	Cell Signaling	3283	rabbit	1:500	~125kDa
anti-Erk1/2	Cell Signaling	4695	rabbit	1:500	~44/42kDa

anti-pErk1/2 (Thr202/Tyr204)	Cell Signaling	4376	rabbit	1:1000	~44/42kDa
anti-c-Myc	Abcam	ab9106	mouse	1:400	~49kDa
anti-α-Tubulin	Sigma-Aldrich	T5168	mouse	1:1000	~55 kDa
anti-P38	Cell Signaling	9212	rabbit	1:1000	~43kDa
anti-pP38	Cell Signaling	4511	rabbit	1:1000	~43kDa

Secondary antibodies were diluted for each use in 5% (w/v) fresh skimmed milk in TBS-T.

Table 10: Secondary antibodies used in western blot. All antibodies are conjugated with horseradish peroxidase.

Antibody	Company	Product Nr.	Host	Dilution
anti-rabbit IgG	GE Healthcare	NA934-1ML	Donkey	1:3000
anti-mouse IgG	GE Healthcare	NA931-1ML	Sheep	1:4000
anti-goat IgG	R&D	HAF109	Donkey	1:3000

2.1.9.2 Immunohistochemistry

All primary antibodies used for immunohistochemistry were diluted freshly in Antibody Diluent Buffer (DCS Innovative Diagn. Sys., Hamburg).

Table 11: Primary antibodies used in immunohistochemistry.

Antibody	Company	Product Nr.	Host	Dilution
anti-Ang-1	R&D	AF923	goat	1:300
anti-Ang-2	Abcam	ab153934	Rabbit	1:400
anti-Tie-2	Thermo Scientific	PA5-28582	rabbit	1:600
anti-pTie-2	Millipore	PC449	rabbit	1:2000

2.1.9.3 Primary and secondary antibodies used for immunofluorescence on cells and tissues

All primary and secondary antibodies used for immunofluorescence were diluted freshly in Dako Antibody Diluent Buffer (Dako, Hamburg (Germany)).

All primary and secondary antibodies used for immunofluorescence on cells were freshly diluted in 5% normal goat serum.

Table 12: Primary antibodies used in immunofluorescence on cells and tissues.

Antibody	Company	Product Nr.	Host	Dilution
anti-Ang-2	Abcam	ab153934	rabbit	1:400
anti-Ang-2	R&D	AF623	goat	1:300
anti-Tie-2	Thermo Scientific	PA5-28582	rabbit	1:600
anti-Tie-2	Millipore	05-584	mouse	1:200
anti-pTie-2	Millipore	PC449	rabbit	1:2000
anti-Annexin V	Abcam	Ab14196	rabbit	1:200
anti-Na^+K^+ATPase	Abcam	Ab76020	rabbit	1:500
anti-Na^+K^+ATPase	Abcam	Ab7671	mouse	1:300
anti-Ki67	Abcam	Ab16667	rabbit	1:200

Table 13: Secondary antibodies used in immunofluorescence.

Antibody	Fluorochromes	Company	Product Nr.	Dilution
anti-rabbit IgG	FITC	Invitrogen	F2765	1:200
anti-rabbit IgG	Alexa Fluor 555	Cell Signaling	4413	1:200
anti-mouse IgG	FITC	Invitrogen	F2761	1:200
anti-mouse IgG	Alexa Fluor 555	Cell Signaling	4409	1:200
anti-goat IgG	Alexa Fluor 555	Abcam	ab150130	1:200
anti-guinea-Pig IgG	Alexa Fluor 555	Invitrogen	A21435	1:500

2.1.10 Bacteria and cell lines

Bacteria

One Shot® TOP10 E. coli competent cells, Invitrogen, Grand Island (NY, USA)

Cell lines

All cells were handled in a sterile hood with controlled airflow and incubated at 37°C in a humidified atmosphere of 5% CO2. When the cells reached a confluence of approximately 80-90% they were split in a ratio between 1:8 and 1:6 depending on their growth kinetics. The compositions of the medium for each cell line are described below.

GH3 cells (ATCC):

500 ml FK-12 medium

15% (v/v) horse serum

2.5% (v/v) ml FBS

100 units/ml of penicillin G sodium and 100 µg/ml streptomycin

HUVEC (Gibco, invitrogen cell culture):

Endothelial cell growth medium (Sigma Aldrich)

Att20 (ATCC):

500 ml DMEM medium

10% (v/v) FBS

100 units/ml of penicillin G sodium and 100 µg/ml streptomycin

αT3 (Pamela Mellon; University of San Diego, CA, USA):

500 ml DMEM medium

10% (v/v) FBS

100 units/ml of penicillin G sodium and 100 µg/ml streptomycin

LβT2 (Pamela Mellon; University of San Diego, CA, USA):

500 ml DMEM medium

10% (v/v) FBS

100 units/ml of penicillin G sodium and 100 µg/ml streptomycin

2.1.11 Tissues and serum

Human non-functioning pituitary adenomas (HNFPA)

HNFPAs were obtained from 37 patients, who underwent transsphenoidal surgery at Imperial College, London, UK or Department of Neurosurgery, University of Tübingen. Healthy adenohypophysis samples were received from the Parkinson's UK brain Bank, obtained post-mortem (within 2–18 h from death).

Serum

Serum samples of 60 healthy volunteers and 60 NFPA patients were provided by Carl Gustav Carus University Clinic, Dresden and the Neurosurgery Department of Tübingen, respectively.

2.1.12 Software

Table 14: List of used softwares.

7300 System SDS v1.4	Applied Biosystems, Carlsbad (CA, USA)
AimImageBrowser Version 4.0	Carl Zeiss, Jena (Germany)
Axio Vision 4.6	Carl Zeiss, Jena (Germany)
LabSens Version 1.7	Olympus Soft Imaging Solutions, Münster (Germany)
Microplate Manager 5.2.1	Bio-Rad Laboratories, Munich (Germany)
MS Office 2010	Microsoft, Unterschleißheim (Germany)
ND-1000 V3.7.1	Thermo Fisher Sci., Waltham (MA, USA)
GraphPad Prism 7	GraphPad Software Inc., La Jolla (USA)
Fiji	https://fiji.sc/
Photoshop CS5	Adobe, San Jose (USA)

2.2 Methods

2.2.1 Bacteria

2.2.1.1 Transformation of Eschericha Coli (*E. coli*)

E. coli TOP10 competent cells were used for amplification of plasmids. The bacteria were transformed by heat shock. Therefore, 50 µl of One Shot TOP10 *E. coli* competent cells were thawed on ice and incubated with 1 µg of plasmid DNA for 30 min on ice. After a heat shock of 45 sec at 42°C in a heating block the cells were cooled for 5 min on ice. Bacteria were then allowed to recover in 250 µl pre-warmed SOC medium for 1 h at 37°C. Afterwards, 20 µl of the bacterial suspension were spread on LB agar plates containing 100 µg/ml ampicillin and incubated at 37°C over night. The next day, single clones were picked and transferred

individually to 10 ml LB medium. After a further overnight incubation at 37°C, bacteria were harvested for either plasmid isolation or preparation of glycerol stocks.

2.2.1.2 Plasmid isolation and determination of the DNA content

Plasmids were isolated from bacteria using a miniprep kit from Qiagen following the manufacturer's instructions.

2.2.1.3 Glycerol stocks

For glycerol stocks, 20 ml selective LB overnight cultures were inoculated. The next day, bacteria were harvested at 2500 g and 4°C for 30 min. The cell pellet was resuspended in 4 ml LB containing 20% (v/v) glycerol. The suspension was divided into four cryo vials and stored at -80°C.

2.2.2 Culture of established cell lines and HUVECs

Rat pituitary cell lines (GH3, αT3, LβT2 and AtT-20) and HUVECs were cultivated in cell specific medium (see 2.1.10). Cells were handled separately to minimize the risk of cross-contamination. All media and trypsin were warmed to 37°C before use. Cells were cultivated in 6-, 12- or 24-well plates or culture flasks.

2.2.2.1 Freezing and thawing of cells

For long-term storage, cells with low passage numbers were expanded in 75 cm^2 flasks to approximately 80% confluency. Cells were harvested (see 2.2.2.2) and pelleted in 15 ml tubes at 1000 g and 25°C for 5 min. The cell pellet was resuspended in 1 ml horse serum containing 10% (v/v) DMSO. As DMSO is cytotoxic at room temperature, all subsequent freezing steps were carried out as quickly as possible. The cell suspension was divided into cryogenic vials (1 ml/vial) and quickly transferred to a freezing container filled with isopropanol, which was then placed at -80°C. The container ensured a continuous temperature reduction of 1°C per minute. After approximately 72 h, the vials containing frozen cells were transferred to liquid nitrogen tanks (-196°C) for long term storage.

To prevent changes in phenotype and functional differentiation, cells were maintained for 20 passages before being replaced with fresh stocks. To thaw the cryoconserved cells, the cell vials were placed in a 37°C water bath for 2 min and the thawed suspension transferred to 10

ml of cell-specific prewarm medium. Rapid dilution of the freezing medium is essential due to the toxicity of the cryoprotectant DMSO at room temperature. To remove the DMSO, cells were centrifuged at 1000 rpm and 25°C for 5 min, resuspended in fresh medium and transferred to 25 cm^2 tissue culture flasks.

2.2.2.2 Passage and harvesting of cell lines

In order to avoid growth inhibition and cell death due to cell overcrowding, the cell density was always kept at 70-80% (maximum) by either plating cells in larger flasks or by passaging the cells before confluency was reached. Cells were passaged in a split ratio of 1:2 - 1:5 every three days. Medium was aspirated and cells were washed with PBS to remove calcium and magnesium as well as trypsin inhibitors from the serum-containing medium and incubated with 1 ml of 0.05% trypsin/EDTA for approximately five minutes at 37°C to break cell-cell and cell-matrix contacts. Then, 5 ml of the cell type specific culture medium were added and the cells removed from the surface of the culture flask or dish by gentle pipetting. To harvest the cells, after trypsinization, the cells were resuspended in 5 ml medium and centrifuged at 1000 rmp for 5 min at 25°C. The pellet was washed with 1 ml sterile PBS and centrifuged for 5 min at 8000 rpm and 25°C. PBS was removed and the pellet was stored at -20°C or used immediately for protein extraction or RNA isolation.

2.2.2.3 Mycoplasma test

The cells were regularly tested for the mycoplasma contamination using a mycoplasma test kit (PromoKine). For the preparation of the test sample, 1 ml of cell culture supernatant was transferred into a 1.5 ml centrifuge tube. The supernatant was briefly centrifuged at 250 g to pellet cellular debris. The supernatant was then transferred into a fresh sterile tube and centrifuged at 20000 g for 10 min to sediment mycoplasma. The supernatant was carefully discarded and the pellet resuspended in 50 µl of the buffer solution. The mixture was heated to 95°C for 3 min. For PCR amplification, following reagents were prepared in a PCR tube:

Table 15: The components of mycoplasma test.

Reagent	Volume
H2O	35 µl
Reaction Mix	10 µl
Test sample	5 µl

The tubes were placed in a PCR thermal cycler with the following program (Table 16): steps 2-4 were repeated for 35 cycles.

Table 16: PCR program for mycoplasma test.

Step	Temperature [°C]	Time
1	94	30 sec
2	94	30 sec
3	60	120 sec
4	72	60 sec
5	94	30 sec
6	60	120 sec
7	72	5 min

2.2.3 Rat pituitary adenoma primary cell culture

MENX rats were sacrificed at around 8 months of age and the isolated pituitary gland was washed twice with ice cold Hank's Balanced Salt Solution (HBSS), minced with a sterile scalpel into small pieces and incubated in serum free RPMI 1640 containing collagenase IV (0.45 mg/ml) for 2 h at 37°C. The cell suspension was dispersed by passing through a sterile 0.8 mm and then 0.6 mm injection needle 10 times each and filtered through a 70 µm cell strainer and centrifuged at 1000 rpm for 5 min. The cell pellet was resuspended in 1-3 ml red blood cell lysing buffer and incubated for 3 min at RT. After adding 8 ml RPMI 1640 supplemented with 10% FBS, 1% (v/v) penicillin-streptomycin, cells were centrifuged and resuspended in 2 ml medium, and the cell number was determined using a Neubauer cell counting chamber. The cells were seeded in 96-well plates (10^4 cells per well), and left for 48 h at 37°C in a humidified incubator with 5% CO_2 before beginning the treatments.

2.2.4 Separation of RPA cells and ECs

To isolate the ECs from rat pituitary adenoma, the final cell pellet from the last step (see paragraph 2.2.3) was resuspended in 400 µl ice cold isolation buffer and transferred into 1.5 ml tube. Then, 40 µl (0.5 mg/ml) of DSB-X biotin-labeled anti-rat CD31 antibody (BD Pharmingen, Product Nr. 555025) was added to the cell suspension and incubated for 10 minutes at 4°C under gentle rotation (3 rpm). CD31 is highly expressed in ECs (Sievert *et al.* 2014) . The antibody was biotin labeled following the manual instructions of Dynabeads FlowComp Flexi Kit. The cell suspension was centrifuged for 8 min at 350 g and resuspended

in 700 µl ice cold isolation buffer. 80 µl of magnetic dynabeads coated with streptavidin were added and incubated for 15 min at 4°C under gentle rotation (3 rpm). Afterwards the tube was placed in the magnetic rack. After 2 min, the bead-free, unbound CD31 negative cells were removed carefully and collected in a separate 15 ml tube. The CD31-positive cells, which were immobilized in the DSB-X-streptavidin-bead-complex, remained on the wall of the tube due to the magnetic field. The tube was removed from the magnetic rack and the bead-bound cells were further enriched for CD31 positivity by washing with 1 ml ice cold isolation buffer by pipetting the suspension up and down and placing the cells back in the magnetic rack. After at least 5 washing steps, cells attached to beads were resuspended in 1 ml release buffer (provided by kit) and incubated for 10 min at RT. The cell suspension was mixed by pipetting up and down; the cells were detached from the beads by biotin-streptavidin competition. Then the tube was placed in the magnetic rack (Figure 8).

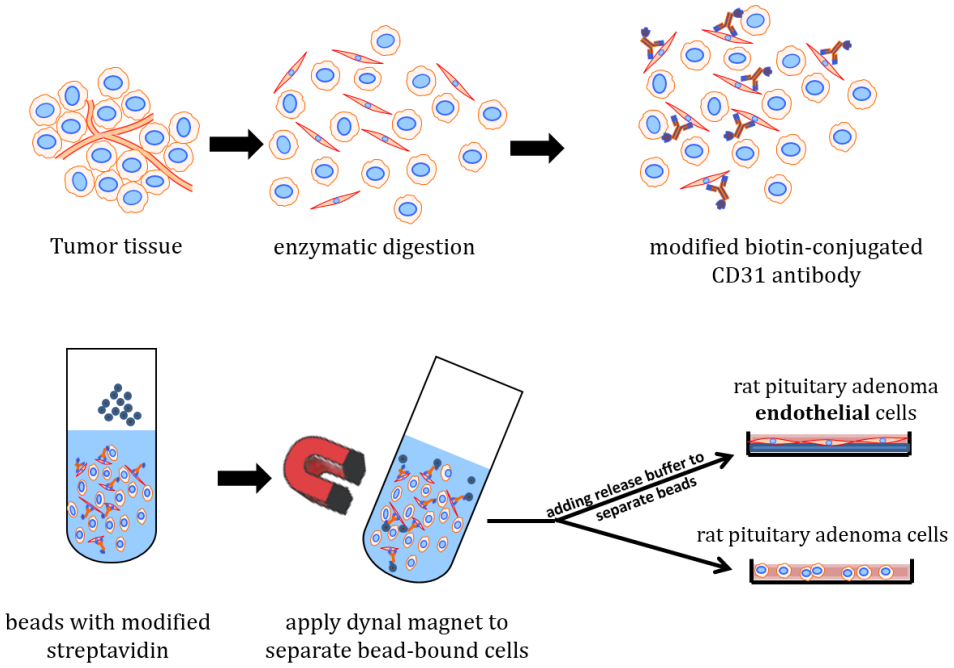

Figure 8: EC isolation from rat pituitary adenoma.

After 1 min, bead free CD31-positive ECs were isolated, while the magnetic beads remained on the wall of the tube. Both EC and PA cell populations were centrifuged for 8 min at 350 g and RT. The cell culture flask for culturing rat pituitary adenoma ECs was coated with 2% gelatin. The cell pellet was resuspended in cell specific medium and placed in a humidified incubator with 5% CO_2 at 37°C.

2.2.5 Concentration of supernatant of primary and established cells

Ang-2 is a secretory protein. To determine its presence in cell culture medium of primary or established cells, the supernatant of these cells was analyzed by western blot and ELISA. Therefore, 5×10^5 cells were cultured in 24 well plates and the supernatant collected after 48 h. 500 µl of cultured cells supernatant was concentrated by Amicon Ultra-0.5 ml Centrifugal Filters (30 K) following the manual instructions. The supernatant was centrifuged for 20 min in RT. The concentrated supernatants were stored at -20°C for further experiments. Same cell and culture medium amount was used for all experiments.

2.2.6 Transfection of GH3 cells with siRNA or expression vector

GH3 cells were transfected either with an Ang-2 expressing vector or with siRNA against Ang-2. Each time a negative control (mock vector or scrambled RNA) was included. The transfection was performed using Amaxa 4D-Nucleofector (Lonza, Cologne, Germany). For each transfection 2×10^6 cells were used. The cells were centrifuged at 1000 rpm for 5 min. The supernatant was removed, and the cells were resuspended in 82 µl SF solution and 18 µl supplement 1. Depending on the experiment, 2 µg plasmid DNA or 700 pmol siRNA were added into the mixtures, which were transferred into nucleofection cuvettes. The electroporation was performed with the DS131 program. The electroporated cells were resuspended in 400 µl warm cell culture medium and gently transferred into the warm 6-well plate (final volume 2 ml/well). 48 h after transfection the cells were used for further studies.

2.2.7 Lentiviral transduction

To permanently downregulate Ang-2 in GH3 cells and generate Ang-2-silenced GH3 clones, we used MISSION® lentiviral transduction particles provided by Sigma Aldrich. Cells were infected with one of three different shRNAs against Ang-2 cloned in pLKO.1-puro vector or shRNA non-target control particles. For transduction, GH3 cells ($1.6x10^4$ cells/well) were plated in a 96-well plate and 24 h later the medium was removed and 110 µl fresh media and Hexadimethrine bromide (8 µg/ml) were added to each well to enhance transduction efficiency. Then, the appropriate number of viral particles to give a suitable multiplicity of infection (MOI= the number of transducing lentiviral particles per cell) was added to the wells and the plate was swirled to mix. The cell-viral particle mixture was incubated at 37°C overnight. The MOI was calculated as follow:

(total number of cells per well) x (desired MOI) = total transducing units needed (TU)

(total TU needed) / (TU/ml reported on vial) = total ml of lentiviral particles to add to each well

We used 6 different MOIs (0.5-10) for the infection of the cells. 24 h after infection, the medium was changed and fresh medium was added to each well. On the next day, medium was replaced with fresh medium containing puromycin (4 µg/ml) to select resistance colonies. A puromycin titration (kill curve) was performed on parental cells to establish the appropriate dosage prior to infection.

The cells were expanded over 2 weeks and the transduction efficiency was determined using qRT-PCR (Taqman) or ELISA.

2.2.8 Cell viability assay

To study the effect of upregulated or downregulated Ang-2 or the efficacy of drug treatment (AMG386 and TKI) on primary pituitary adenoma or GH3 cells, proliferation assays were conducted. The cells were plated in 96-well plates (10^4 cells/well). Cell viability was measured 48 h after transfection or treatment by using WST-1 colorimetric assay reagent (Roche, Mannheim, Germany) according to the manufacturer's recommendations. If the cells were transfected with siRNA against Ang-2, 24 h after transfection, the medium was removed and the cells were cultivated in serum free medium for further 24 h. Thereafter the cell viability was determined by measuring the absorbance at 450 nm using a microplate reader.

2.2.9 Apoptosis assay

To assess the effects of Ang-2 modulation or drug treatment (AMG386 or Tie-2 kinase inhibitor) on the apoptosis of GH3 or primary pituitary cells, the activity of caspase 3/7 was measured using the Caspase-Glo ® 3/7 Assay kit (Promega). Cells were plated in 96-well white bottom plates and 48 h after transfection or treatment the activity of caspase 3/7 was measured. The reagent used in this assay was added directly to the wells, resulting in cell lysis and cleavage of the substrate containing a tetrapeptide sequence, DEVD, by caspase-3/7 and generation of a luminescent signal, which was measured using a luminometer.

2.2.10 Nucleic acids analytics

2.2.10.1 RNA isolation

RNA was isolated from rat and human pituitary tissues using the RNeasy Micro Kit from Qiagen and following the manual instructions.

2.2.10.2 Nucleic acid quantification

Concentration and quality of RNA and plasmid DNA samples were analyzed using the NanoDrop device. An OD of 1.0 at a wavelength of 260 nm corresponds to 50 µg/ml for double-stranded DNA and to 40 µg/ml for RNA. To evaluate the purity of the nucleic acid sample, the ratio of the absorbance at 260 nm and 280 nm is measured. This ratio amounts to 1.8 for pure DNA and 2.0 for pure RNA.

2.2.10.3 Reverse transcription

In order to perform qRT-PCR-based analysis on RNA extracts, reverse transcription was performed to make cDNA from RNA templates. To this end, 300 ng of total RNA was incubated for 10 min at RT with 1 µg random primers in an 11 µl reaction volume. Then the following components were added to each reaction:

Table 17: The components of reverse transcription.

Reagent	Volume
5x first strand buffer	4 µl
DTT (0.1 M)	2 µl
dNTP Mix (10 mM each)	1 µl
RNaseOUT ribonuclease inhibitor	1 µl
SuperScript™ II reverse transcriptase	1 µl

RT-Mixtures were incubated for 1 h at 42°C followed by incubation at 95°C for 5 min to stop the reaction. cDNA was stored at -20°C until further use.

2.2.10.4 Quantitative real time PCR (qRT-PCR)

After generating cDNA from RNA, the gene of interest was amplified by TaqMan PCR using gene expression assays from Applied Biosystems.

The following components were prepared for each sample:

Table 18: The components of qPCR.

Reagent	Volume
2x TaqMan PCR master mix	10 µl
Assay Primer	1 µl
Ampuwa	5 µl

16 µl of mixture was used for each well of 96-well PCR plate. 4 µl of Ampuwa-diluted reverse transcription product (1:1) was added (diluted cDNA as template). Calibrator DNA was diluted 1:25. All samples were pipetted in duplicate. For each gene a negative control (16 µl mix plus 4 µl Ampuwa) and a calibrator reverse transcription product were also included. cDNA from rat pituitary for rat samples and human adrenal gland for human samples (calibrator) was used to create standard curves for the genes of interest. In addition to the genes of interest, an endogenous control, *β2m* (encoding β2 microglobulin) for rat samples and *TBP* (encoding TATA box binding protein) for human samples, was run for normalization of cDNA input.

The 7300 Real Time PCR System was run for 40 cycles (steps 3 to 4) as followed:

Table 19: qRT-PCR program.

Step	Temperature [°C]	Time
1	50	2 min
2	95	10 min
3	94	15 sec
4	60	1 min
5	4	Pause

To quantify PCR reaction products during each cycle, the cycle threshold (Ct) value for each sample was calculated. Relative quantification was performed using the pre-recorded standard curve and analysis data of the 7300 detection system. Linear regression analysis was used to calculate the relative amount of mRNA in samples. Values were normalized against *β2m* or *TBP*. The relative mRNA expression level of the target genes was calculated with the 2-ΔΔCt formula.

2.2.11 Protein extraction and western blotting

2.2.11.1 Protein extraction

Frozen or fresh cell pellets were placed on ice and resuspended in 20-60 µl RIPA (depending on pellet's size) buffer containing kinase and protease inhibitors. After 20 min on ice, the cell lysate was inverted 2-3 times and spun down at 12000 rpm and 4°C for ten minutes to remove cell debris. The supernatant containing the extracted proteins was transferred into a fresh tube for determination of protein concentration or storing at -20°C.

2.2.11.2 Protein quantification

The protein concentration was determined using the bicinchoninic acid (BCA) assay. For quantification of proteins a standard curve using BSA was created. 2 µl of each sample and standard were added to 98 µl H_2O bidest. For the baseline correction, 2 µl RIPA buffer were added to 98 µl H_2O bidest. 1 ml BCA solution (1:50 mixture of reagent A and B from Pierce kit) were added to standard curve and each sample, the tubes were closed, vortexed and incubated at 60°C for 30 min. The OD of the solution was measured on a spectrophotometer at 560 nm. The amount of protein in the given sample was estimated by comparing the value for OD_{560} to the standard curve.

2.2.11.3 SDS-PAGE and western blot transfer

To identify and quantify a specific protein through antibody detection, the cell lysates were separated by polyacrylamide gel electrophoresis. Prior to loading samples on to prepared gels 50 µg of each sample protein was mixed 1:1 with 2x Laemmli buffer containing 5% (v/v) β-mercaptoethanol and denatured for 5 min at 95°C.

Samples were separated in SDS running buffer on discontinuous gels, 4% stacking and 10% separating gels (depending on the molecular mass of protein of interest). Gels were first run at 90 V until the tracking stain had passed the interface between stacking and separating gel, then the voltage was increased. A pre-stained protein ladder was also included in each gel. After running for about 2 h at 140 V, gels were placed into a western blot sandwich. Proteins were blotted onto nitrocellulose membrane (NC) using the wet blot system. NC membranes were activated with water prior to use. The components of the blotting sandwich were soaked in transfer buffer and assembled as follows: sponge pad, Whatman paper, gel, NC membrane, Whatman paper and sponge pad. The sandwich was placed into a blotting chamber with

transfer buffer. Transfer was performed either for 2 h at 100 V or overnight at 4°C and 50 V. Thereafter, the sandwich was dissembled. To determine the quality of the transfer, the membrane was reversibly stained with Ponceau S. The staining was removed by washing the membrane three times for 5 min in TBS-T. Membranes were subsequently blocked by incubation in 5% milk dissolved in TBS-T for 1 h. After washing 3 times each 5 min with TBS-T, specific primary antibodies diluted in 3% BSA were incubated with the membranes overnight at 4°C. The membranes were washed with TBS-T and incubated with the appropriate horseradish peroxidase conjugated secondary antibody for 1 hour at RT followed by washing 5 min for three times with TBS-T. To detect specific bands a chemiluminescence agent (Pico West solution) was applied for 5 min in the dark. The membrane was exposed on a sheet of photo film. To detect other proteins with different primary antibodies, the membranes were incubated with stripping buffer for 15 min at RT. After three washes for five minutes each with TBS-T. The whole detection-process, starting from blocking with milk, was repeated. The housekeeping gene α-Tubulin was always probed as the loading control except in experiments in which the ratio of phospho-/total-proteins (for example pAkt/Akt) was calculated to monitor progression (activation or inactivation) of a signaling pathway after changing some parameters which may have an impact on signaling molecules, and an increase or a decrease of phosphorylated protein was the main focus of the experiment. Moreover, this ratio is not affected by the amount of loaded proteins, since the same membrane was probed to detect phosphorylated protein and reprobed to detect the total amount of it.

2.2.11.4 Isolation of cell membrane-bound receptors

GH3 cells ($2x10^6$ cells/well) were cultured in 6-well plates. The medium was removed and the cells were washed twice with ice-cold PBS. Cell culture plates were placed on ice and 500 µl of RIPA buffer including phosphatase- and protease inhibitors were added and incubated for 10 min at 4°C on rocking shaker. Cells were collected using a cold plastic cell scraper and transferred into a pre-cooled 1.5 ml tube and incubated at 4°C with shaking for an additional 20 min. The cell lysate was centrifuged for 30 min at 14000 g. After transferring the supernatant into a fresh 1.5 ml tube, the protein concentration was measured as described in 2.2.11.2. 50 µl of Wheat Germ Agglutinin (WGA) beads was washed with 200 µl RIPA buffer and centrifuged for 2 min at 14000 g. WGA can bind oligosaccharides containing terminal N-acetylglucosamine or chitobiose, structures which are common to membrane

glycoproteins, and helps to enrich and separate them from cytoplasmic proteins. Supernatant was discarded and 300 µg proteins was added to WGA beads followed by incubation on rotator at 4°C overnight. On the following day the WGA beads were washed for 2 min at 14000 g for 3 times with ice-cold RIPA buffer. The supernatant was discarded and 70 µl of 2x Laemmli sample buffer containing 10% (w/v) 2-Mercaptoethanol was added to the beads and incubated at 60°C for 20 min and subsequently analyzed by 8% SDS-PAGE western blot.

2.2.12 Co-immunoprecipitation of Tie-2 and Ang-2

For co-immunoprecipitation, GH3 cells or primary rat pituitary cells cultured in 10 cm cell culture dishes or 12 well plates, respectively, were washed twice with ice-cold PBS and incubated with cross-linker 3,3′-dithiobis [sulfosuccinimidylpropionate] (DTSSP) dissolved in PBS (0.5 mM) for 20 min, followed by incubation with 20mM Tris (pH=7.5). After washing, cells were incubated with lysis buffer (NP-40) for 30 min. The cells were incubated on ice for 30 min followed by centrifugation at 15.000 rcf for 5 minutes at 4°C. After pre-clearing with 20 µl Agarose beads, the protein concentration was measured as described in 2.2.11.2 and 300 µg of total protein were incubated with 3 µl of anti-phospho-Tie2 Tyr1102/1108 antibody (Calbiochem) or 5 µl anti-Ang-2 antibody (R&D systems) for 1 h. Subsequently, 30 µl of Agarose beads were prepared by washing 3 times with 200 µl NP-40 and centrifuged at 300 rpm. After washing, the beads were added to the lysate and incubated overnight at 4°C. Bound proteins were eluted from the beads by adding 50 µl of Laemmli sample buffer containing 10% (w/v) 2-Mercaptoethanol and incubated for 20 min at 60°C. Samples were analyzed by 8% SDS-PAGE Western blotting. When the immunoprecipitation was performed with anti-phospho-Tie2 antibody the membrane was blotted with anti-Ang-2 and vice versa.

2.2.13 Immunhistochemical staining (IHC) of tissue sections

Immunohistochemistry (IHC) is a method used to determine the localization and level of expression of specific proteins in tissues. Pituitary sections (3 µm thick) were cut from paraffin-embedded tissue blocks. The sections were deparaffinized 2x10 min in xylol and rehydrated by incubation in decreasing concentrations of ethanol (100%, 100%, 96%, 70%, each step 5 min). Afterwards, the tissues were washed in distilled water and then in TBS-T (Tris-buffered saline, 0.05% Tween, pH=7) for 5 min. To block endogenous peroxidase and reduce non-specific signals the tissues were pre-incubated in 3% hydrogen peroxide (H_2O_2) in

methanol for eight minutes and washed 2x5 min in TBS-T. The fixation and processing steps involved in the preparation of tissues often results in loss of immunoreactivity of antigens. Therefore, the tissues were boiled in a pressure cooker in the microwave with 0.01 M citrate buffer (pH=6) for 30 min to unmask the antigens. The tissues were washed again for 5 minutes in TBS-T. After Avidin/Biotin block, each step 15 min, the samples were blocked for 30 min in normal serum to mask unspecific binding, the tissues were incubated with primary antibodies against the specific proteins overnight at 4°C.

Afterwards, the tissues were washed three times in TBS-T for 5 min and incubated with biotinylated secondary antibodies for 45 min, followed by washing (3 x 5 min) in TBS-T. Then Streptavidin-horseradish peroxidase (KPL kit) was added to the tissues. After 30 min the tissues were washed three times for 5 min in TBS-T, followed by incubation with DAB staining solution for ca. 2 min. The DAB reaction was monitored on microscope to achieve proper signal intensity. The reaction was stopped by placing the sections into water and subsequently they were counterstained in Haematoxylin for 20 sec. The slides were finally washed under running water for 4 min and dehydrated in increasing concentrations of ethanol (70%, 96% and 100%) 2 min incubation in each concentration. Subsequently the sections were incubated in xylol twice for 10 min and mounted with cover slips. To detect Ang-2 in human and rat tissues, IHC was performed on an automated immunostainer (Ventana Medical Systems). After Avidin/Biotin block, the tissues were placed into the automated immunostainer and the standard protocol #92 was run (the steps were the same as explained for the manual staining). Images were recorded using an Olympus BX 43 microscope.

2.2.14 Immunofluorescent staining of tissue sections

Paraffin-embedded tissue sections were deparaffinized in xylol twice and each time for 10 min and then incubated for 10 min in isopropanol. The rehydration and cooking steps are described in 2.2.13, but without incubation in H_2O_2. After boiling, the tissue sections were transferred into TBS-T. To reduce tissue autofluorescence the sections were incubated in 0.1% Sudan Black in 70% Ethanol for 20 min. After washing three times with TBS-T, the tissue sections were incubated in serum to mask unspecific epitopes, followed by an overnight incubation at 4°C with primary antibody diluted in Dako REAL solution. If co-immunofluorescent staining was performed, both primary antibodies were added on the tissue sections. On the following day the samples were washed three times in TBS-T for 5 min. The

secondary antibody or antibodies if co-immunofluorescent staining was done, were diluted in Dako REAL solution and added to the tissues followed by incubation for 45 min and washed 3 times each 5 min in TBS-T. The nuclei were stained with DAPI in the dark for 3 min followed by 8 min washing in distilled water. Afterwards, the tissue sections were covered with 1 drop of vectashield mounting medium and a cover glass. Tissue slides were stored at -20°C in the dark.

2.2.15 Immunofluorescence of cells

Coverslips were coated with poly-L-lysine for 10 min in a 24-well plate. They were washed with PBS and allowed to dry. $8x10^5$ cells were cultured on coverslips in the appropriate medium and incubated overnight at 37°C. On the following day the medium was removed and the cells were washed three times with PBS, followed by fixation process with 2% paraformaldehyde in PBS for 30 min. After fixation cells were washed three times in PBS. 1 ml PBS was added to each well and the cells were incubated over night at 4°C. On the following day the cells were incubated in 0.1% Triton X-100 (in PBS) for 3 min to improve the penetration of the antibodies inside the cells. The cells were washed five times with PBS and blocked in 5% normal goat serum (in PBS) for 30 min followed by incubation with the primary antibody overnight at 4°C. After the antibody was removed and the cells were washed three times with warm PBS (37°C), the appropriate secondary antibody (1:200), diluted in 5% normal goat serum, was added to the cells and incubated for 1 h at RT. Then cells were washed three times with PBS. Afterward the nuclei were stained with DAPI in the dark for three minutes and the washing procedure (3x PBS) repeated. The coverslips were mounted onto slides using vectashield. The slides were stored at -20°C in the dark.

2.2.16 Proximity Ligation Assay (PLA)

Formalin fixed paraffin embedded rat PA samples were deparaffinized, rehydrated and cooked in citrate buffer as described in 2.2.13. After cooking, the tissue samples were washed twice in TBS-T + 1 M Glycin (2x5 min) and once in TBS-T. Then the blocking solution (provided by the PLA kit) was added to each sample followed by incubation at 37°C for 30 min (Sigma-Aldrich). After incubation the primary antibodies, anti-Ang-2 and anti-Tie-2 or the combination of anti-Ang-2 and anti-pTie-2 was added to each sample and incubated overnight at 4°C. Afterward the tissue samples were washed twice with washing buffer A

(Sigma-Aldrich). Then the specific proximity probes targeting goat and rabbit IgGs (secondary antibodies attached to single stranded DNA oligonucleotides) were added at a 1:5 dilution using the antibody diluents supplied by kit. After 1 h incubation at 37°C in a humidity chamber, the tissue samples were washed and the ligation solution (included in the kit) was added to the samples and incubated for 30 min at 37°C in a humidity chamber. After ligation, the samples were washed again using the same washing buffer. Then the samples were treated with the amplification and detection solution (Sigma-Aldrich) and were incubated for 100 min in a humidity chamber at 37°C. Afterwards the samples were washed in washing buffer B and for 1 min in diluted (1:100) washing buffer B in dark Sigma-Aldrich. The samples were left to dry at room temperature and were mounted using a mounting medium containing DAPI and stored at 4°C.

2.2.17 Determination of Angiopoietin-2 concentration in the human plasma or supernatant of cultured cells

Plasma ANG-2 levels and the concentration of secreted Ang-2 in the supernatant of cultured cells were determined using an ELISA kit (DANG20, R&D) following the manufacturer's instructions. 1:5 dilution of each human plasma sample was used for the measurement of absorbance at 450 nm. For the supernatant a dilution of 1:50 was used. Ang-2 concentrations were calculated afterwards using a standard curve from the standard provided in the kit.

2.2.18 *in vitro* and *in vivo* treatment using AMG386

AMG386 (Trebananib) was provided by Amgen research GmbH. The concentration of stock solution was 30 mg/ml. For *in vitro* experiments the final concentration was prepared in the culture medium immediately before use. For *in vivo* studies, the stock solution was diluted in 0.9% NaCl to reach a final concentration of 1.6 mg/ml. 2 mg AMG386 per kg body weight (2 mg/kgbw) was administered intraperitoneal to MENX rats as suggested by Amgen.

MENX-affected rats were maintained and treated with AMG386 or placebo in agreement with the procedures approved by the Helmholtz Zentrum München, by the Technische Universität München, and by the local government authorities (Bayerische Landesregierung) (Az.: 55.2.1.54-2532-39-13).

Animals received drug/placebo treatment daily for a total of three days to establish that the treatment was well tolerated and if we could observe any changes in the phosphorylation level of Tie-2 in pituitary cells (Figure 9).

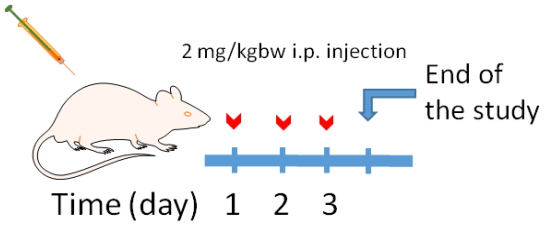

Figure 9: Scheme of the short-term AMG386 administration to MENX mutant rats. Rats were treated daily by i.p. injection of ANG386 (2 mg/kgbw) or placebo. After 3 days the rats were sacrificed and pituitary glands collected. Red arrows show the treatment with AMG386.

Then, the animals were treated with AMG 386 five times in 2 weeks as shown in Figure 10.

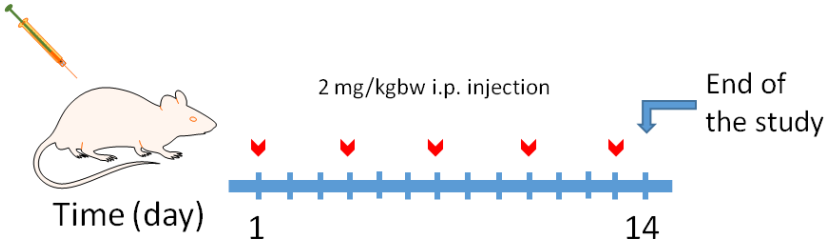

Figure 10: Scheme of the long term AMG386 administration to MENX mutant rats. Rats were treated once every three days by i.p. injection of ANG386 (2 mg/kgbw) or placebo. After two weeks the rats were sacrificed and pituitary glands collected. Red arrows show the treatment with AMG386.

2.2.19 Statistical analysis

Study endpoints from *in vitro* experiments, including cell proliferation, apoptosis, migration, colony formation, as well as primary cell viability, were displayed by bar graphs with means ± SEM. Unpaired nonparametric Mann Whitney test was used for detecting differences between series of data, separately at all time points. All statistical analyses were executed using GRAPHPAD (GraphPad Software Inc), with the level of statistical significance set at 0.05.

2.2.20 Quantification of IF

Quantification of Ang-2, Tie-2 or pTie-2 IF staining intensities in cells was performed using ImageJ. Images were subjected to the threshold function, and the same threshold for all images obtained with the same antibody, was used. Then, the intensity of the staining was

quantified for 30 cells in total for each experimental condition and is indicated as average ± SEM for each condition. The Ki67 labeling index (= nuclear immunoreactivity) of rat adenomas after treatment was determined semiquantitatively by counting the positive nuclei in 3x high-power fields per tissue (n=3 per group) and is indicated as the percent of positive cells against all neoplastic cells in the fields examined.

2.2.21 Scoring of ANG-1 and -2 immunostainings in human NFPAs

Semi-quantitative evaluation of human pituitary tissues was performed on the microscope. For the evaluation, we considered the intensity of the staining and the percentage of cells expressing the protein of interest. Tissues with no immunoreactivity for ANG-1 or ANG-2 were scored as (-), those with weak expression scored as (+). The moderate and strong expression of these two proteins were marked by (++) and (+++), respectively. In our cohort, in two samples the expression of ANG-1 was restricted to adenoma-associated vessels. No staining was found in the cytoplasm of adenoma cells. Therefore, they were scored (-).

3 Results

3.1 Characterization of angiogenesis-promoting proteins in MENX-associated pituitary gonadotroph adenomas

3.1.1 The expression of Ang-1 and -2 in MENX rats

Whole-genome transcriptome analysis of MENX- and wild type rat pituitary tissue has previously shown that the expression of *Ang-1* and *Ang-2* is deregulated in the pituitary tumors of MENX rat compared to wild-type animals (-3.4 and +2.4 fold, respectively) (Lee *et al.* 2013). To validate this array data, the mRNA expression levels of these two genes were evaluated by quantitative RealTime RT-PCR (qRT-PCR) in pituitary tumors of MENX rats and in wild-type rat pituitary tissues (Figure 11).

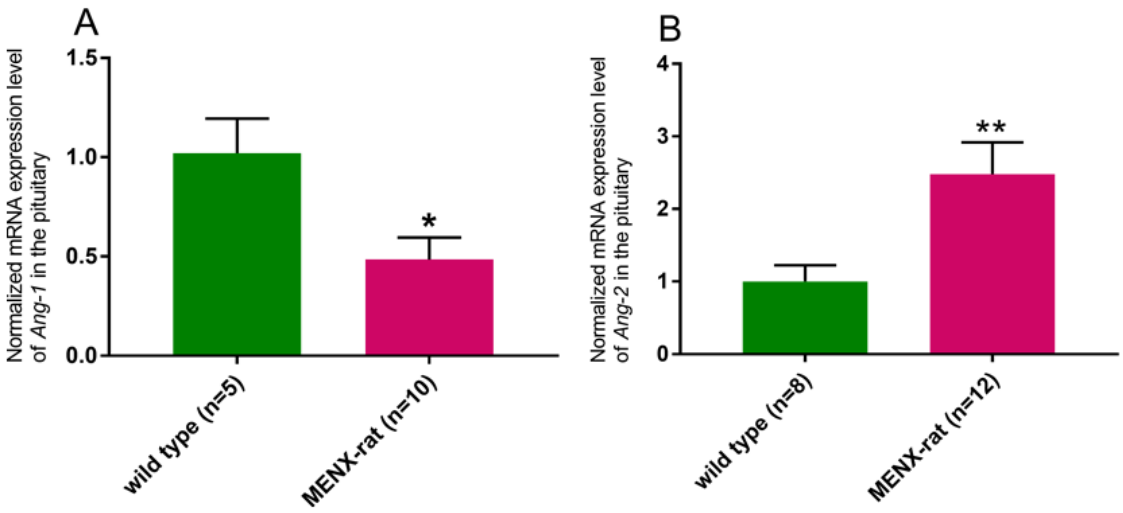

Figure 11: mRNA expression of *Ang-1* and *-2* in pituitary glands of wild-type and MENX rats. Total RNA from the pituitary tissue was extracted and, after reverse transcription, the levels of *Ang-1* and *-2* cDNA were analyzed in a PCR cycler using specific Taqman primers and probes (Assay-on-DemandTM). The relative mRNA expression level of the target genes was normalized for input RNA using rat *β2-microglobulin* gene expression (housekeeping gene). A calibrator rat pituitary RNA was always run in parallel. The relative mRNA expression was calculated with the 2-ΔΔCt formula. The obtained relative value was normalized against the average level of mRNA expressed in wild-type rat pituitary samples, arbitrarily, set to 1. (A) The expression of *Ang*-1 in MENX rats (n=10) was reduced about 50% when compared to wild type rats (n=5). (B) *Ang-2* was on average +2.5 fold higher expressed in MENX rats (n=12) compared to wild type animals (n=8). Data are expressed as mean ± SEM. (Mann Whitney test; *P< 0.05, **P<0.01).

This confirmed that *Ang-1* was significantly downregulated in pituitary tumors of MENX rats, whereas *Ang-2* was upregulated in these tissues when compared with normal pituitary.

To determine whether there is a correlation between the level of mRNA expression of *Ang-1* and *-2* with that of their corresponding proteins, IHC was performed on the pituitaries of wild-type and MENX rats (Figure 12).

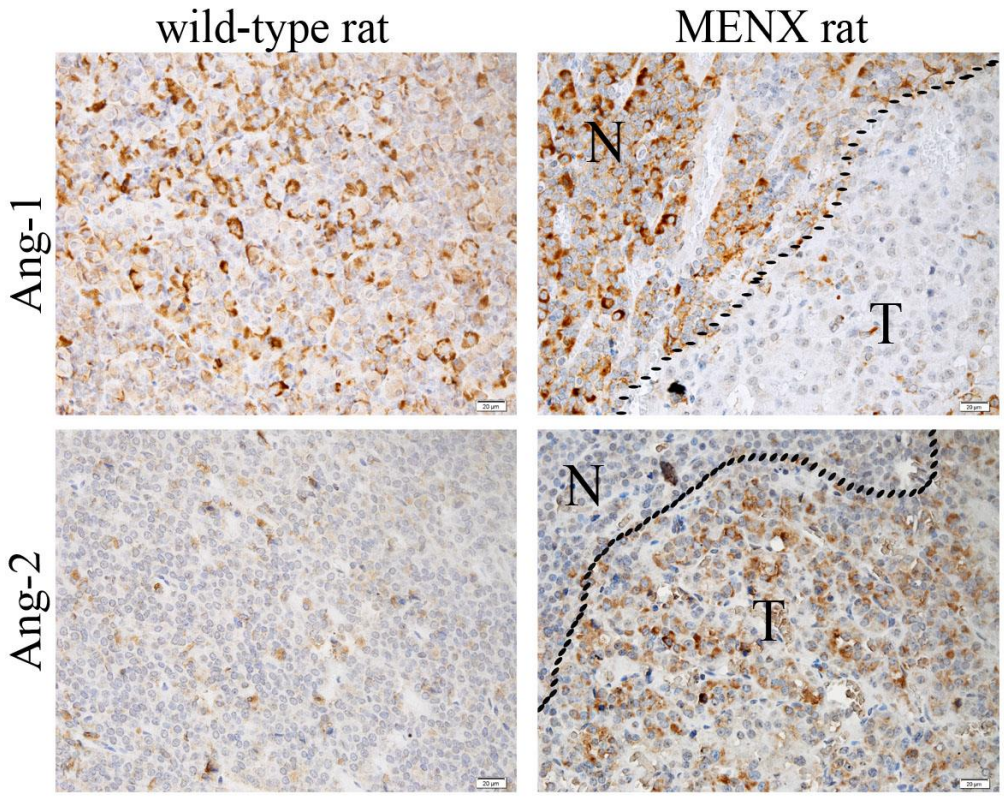

Figure 12: Expression of Ang-1 and Ang-2 in wild-type and MENX rat pituitary tissue. Immunohistochemical staining was performed on paraffin-embedded formalin-fixed pituitary tissues using antibodies against Ang-1 (1:300) and Ang-2 (1:400). The staining indicates a large number of cells, which strongly express Ang-1 in the pituitary of wild-type rats; in contrast the pituitary adenomas show almost no positive staining for Ang-1. Ang-2 is sporadically expressed in the cytoplasm of some pituitary cells in wild-type rat pituitary, but it is highly expressed in MENX rat pituitary adenomas. (Ang-1 staining, wild-type n=5 and MENX rat n=8; Ang-2 staining, wild-type n=5 and MENX rat n=10); N, normal; T, tumor. Original magnification: 400x; scale bar: 20 µm.

We observed that the expression of Ang-1 was present in the wild-type pituitary and non-tumorous pituitary tissues of MENX rats, but it was absent in rat pituitary adenomas. Conversely, the expression of Ang-2 was higher in pituitary adenomas compared to both the surrounding non-tumorous pituitary tissue in mutant rats and the wild-type rat pituitaries. Moreover, PAs among mutant rats of different ages (4-8 months of age) all express Ang-2, and expression of this protein was not age- or tumor size-dependent. Negative controls without primary antibodies were always included to verify the specificity of positive staining.

3.1.2 The expression of Tie-2 and pTie-2 in MENX rats

Usually, Ang-2 is expressed in EC cells, but we observed its expression also in PA cells. We wondered if the receptor of this ligand is also expressed in the adenomas. Thus, we assessed the expression of Tie-2 in MENX and wild-type rat pituitary tissues (Figure 13). The immunohistochemical staining was performed on 3 wild-type tissues and 3 rat pituitary adenomas.

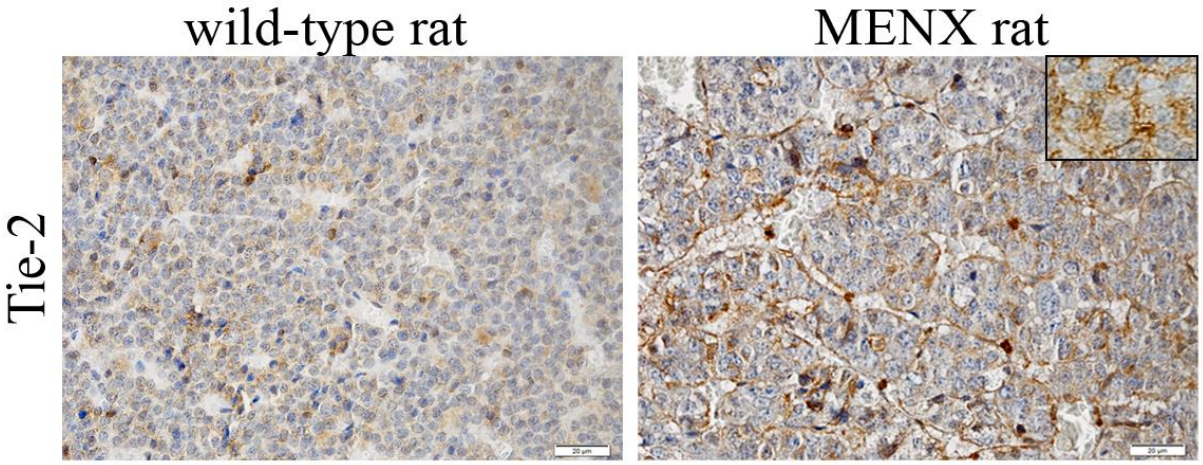

Figure 13: Expression of Tie-2 in wild-type and MENX rat pituitary adenoma. Immunohistochemical detection of Tie-2 was performed with anti-Tie-2 Antibody (1:600). A few pituitary cells in the wild type rats express Tie-2 in the cytoplasm and cell membrane. Both pituitary adenoma cells and ECs (tumor area) show pronounced expression of Tie-2 with membranous localization. Original magnification: 400x; scale bar: 20 µm.

The Tie-2 receptor was only highly expressed in tumor areas of MENX rat pituitaries, where it associated with the cell membrane of both endothelial and adenoma cells. A few Tie-2 expressing cells were also found in wild-type rat pituitary tissues. Then, we wondered if Ang-2 and Tie-2 are co-localized in pituitary adenomas. IHC was performed on consecutive sections of MENX rat pituitaries to detect the expression of Ang-2 and Tie-2. After staining, a tissue scanner was used to analyze the localization of Ang-2 and Tie-2. These results indicate that the 2 proteins are co-localized (Figure 14).

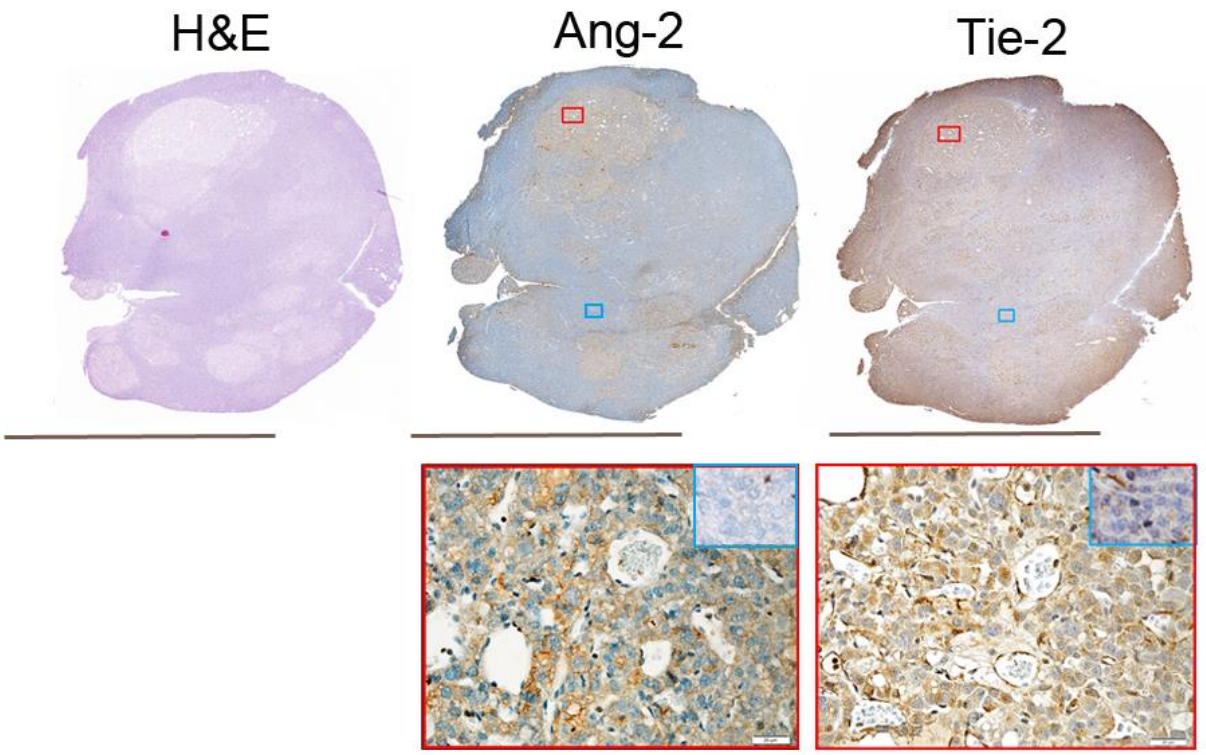

Figure 14: Co-localization of Ang-2 and Tie-2 in MENX rat pituitary adenoma. Three consecutive sections of paraffin-embedded formalin fixed MENX rat pituitary adenoma were used for H&E staining and detection of Ang-2 and Tie-2 by immunohistochemistry. H&E staining showed multifocal pituitary adenoma. Whole scan of pituitary tissue indicates expression of Ang-2 only in tumors, co-localized with Tie-2 receptor (red boxes). Blue boxes show a non tumorous area of MENX rat pituitary without any reactivity for Ang-2 or Tie-2. Immunohistochemical detection of Ang-2 and Tie-2 was performed with anti-Ang-2 (1:400) and anti-Tie-2 Antibodies (1:600). Scale bar for whole tissue scan: 5 mm. Original magnification of figures with red border: 400x; scale bar: 20 µm (n=3).

Previous studies done in human ECs demonstrated that Ang-2 at high concentrations and in the absence of Ang-1 can also phosphorylate Tie-2 receptor and act as an agonist (Yuan *et al.* 2009). Our data indicated that Ang-2 and Tie-2 were highly expressed in MENX rat gonadotroph adenomas, whereas no immunoreactivity was observed for Ang-1 in MENX rat pituitary adenomas. Therefore, we wondered whether Tie-2 is activated by Ang-2 also in pituitary adenomas. We performed Co-IF on MENX rat pituitary adenoma to confirm the localization of Ang-2, Tie-2 and pTie-2 (Figure 15).

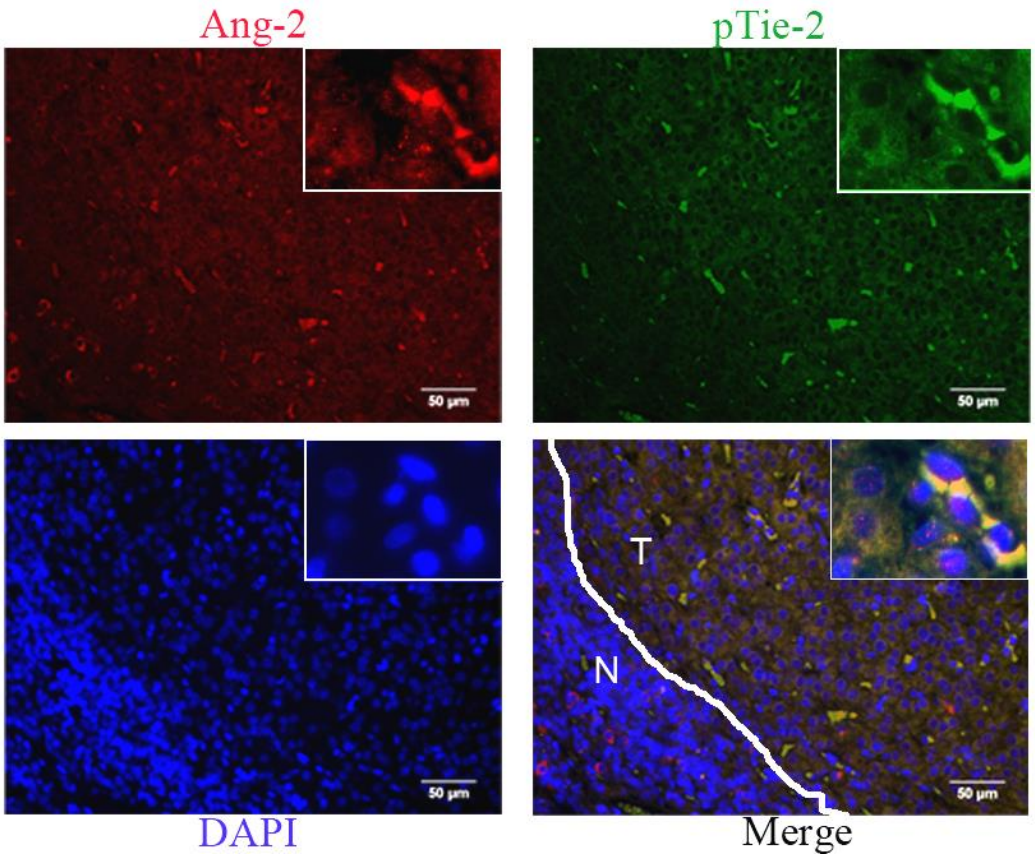

Figure 15: Co-localization of Ang-2 with pTie-2 in MENX rat pituitary adenoma. Antibodies against Ang-2 (1:300) and pTie-2 (1:2000) were used to determine their localization in RPAs. Ang-2 is co-localized with pTie-2 in MENX rat pituitary adenomas. Original magnification: 200x; scale bar: 50 µm.

Ang-2 was found to be co-localized with pTie-2 in cells of PAs in MENX rats. Moreover, Tie-2 was phosphorylated and thereby activated in PAs. Given that the tumor cells express Ang-2 but not Ang-1 (Figure 12), this finding suggests that Ang-2 may activate Tie-2.

3.2 Characterization of angiogenesis promoting proteins in human pituitary gonadotroph adenomas

3.2.1 The expression of Angiopoietin-1 and -2 and their corresponding receptor in human gonadotroph adenoma

Previous results from genome-wide transcriptome analysis of human pituitary tumors indicate that *ANG-1* is downregulated in human NFPAs (Moreno *et al.* 2005, Evans *et al.* 2008). To validate this finding in human gonadotroph adenomas, we measured the mRNA expression level of *ANG-1* in frozen samples of 14 NFPA (11 males and 4 females) and in two healthy

pituitary mRNAs, commercially available (BioChain), as control, using quantitative RT-PCR (TaqMan-PCR).

The clinical information of the patients used for TaqMan is summarized in Table 20.

Table 20: Clinical characteristics of NFPA patients used for qRT-PCR (Imperial College).

Sample ID	Sex	Age	Tumor biology	% Ki67
296	M	56	invasive	2%
286	M	59	invasive	1%
263	M	58	invasive	2%
271	F	44	non-invasive	1%
41	M	57	invasive	2%
224	M	59	non-invasive	2%
276	F	62	invasive	2%
297	M	50	invasive	3%
283	M	47	non-invasive	<1%
285	F	71	non-invasive	1%
288	M	76	invasive	1-2%
289	M	56	invasive	3%
301	F	47	non-invasive	1-2%
267	M	58	invasive	4%

The normalized *ANG-1* mRNA expression level in patients was calculated using TBP as control and compared with normal pituitary samples. We found the expression of *ANG-1* to be downregulated in the adenomas compared to normal pituitaries. In all cases except one (case 296) the expression of *ANG-1* was more than two fold reduced when compared to the human healthy controls (Figure 16). Since the ANG-1/-2 act as context-dependent antagonists or agonists, we also investigated the expression of *ANG-2* mRNA in these samples. *ANG-2* expression was elevated (> 2 fold) in 6 out of 14 pituitary adenomas compared with normal pituitaries (Figure 16). The patients with elevated *ANG-2* levels were all males, and 4 out of 5 had an invasive adenoma. In contrast, only 5 out of 9 samples with no *ANG-2* upregulation showed an invasive behavior.

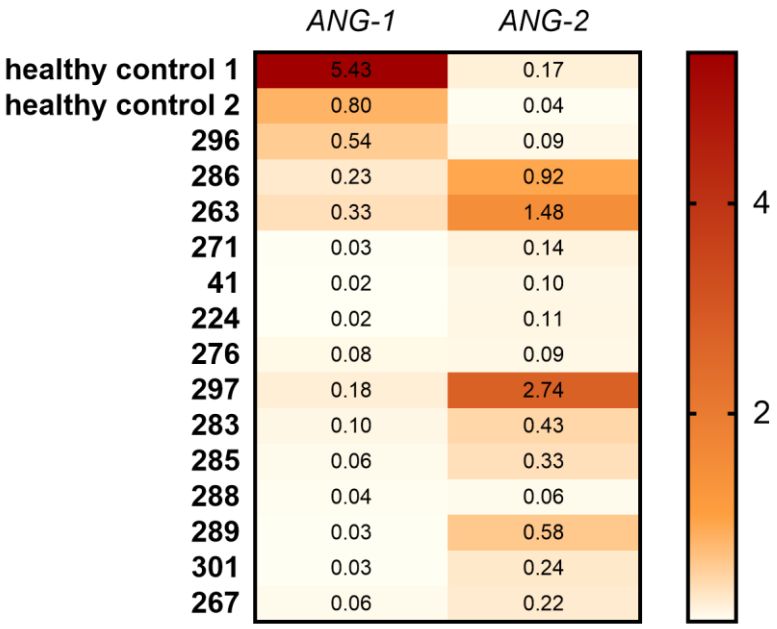

Figure 16: mRNA expression of *ANG-1* and *ANG-2* in normal pituitary and NFPA patients. Total RNA was extracted from the pituitary adenoma samples, reverse transcribed, and the level of *ANG-1* and *ANG-2* cDNA was analyzed in a PCR cycler using specific TaqMan primers and probes (Assay-on-DemandTM). The relative mRNA expression level of the target genes was normalized for input RNA using *TBP* gene expression (housekeeping gene). A calibrator human adrenal RNA was run in parallel. The relative mRNA expression was calculated with the 2-ΔΔCt formula. Normalized ct-values are demonstrated in the figure. *ANG-1* was downregulated in all NFPA patients compared to the healthy controls. *ANG-2* was upregulated in 5 out of 14 patients (> 2 fold).

Given that an increased ratio of ANG-2 to ANG-1 (mRNA and protein) correlates with enhanced tumor angiogenesis and poor prognosis in many cancer types (Tait and Jones 2004), we calculated the ratio of *ANG-2* to *ANG-1* for NFPAs. In our tumors, the ratio of *ANG-2* to *ANG-1* gene expression was shifted toward *ANG-2* (i.e. >1) in 13 out of 14 pituitary adenoma samples (Figure 17).

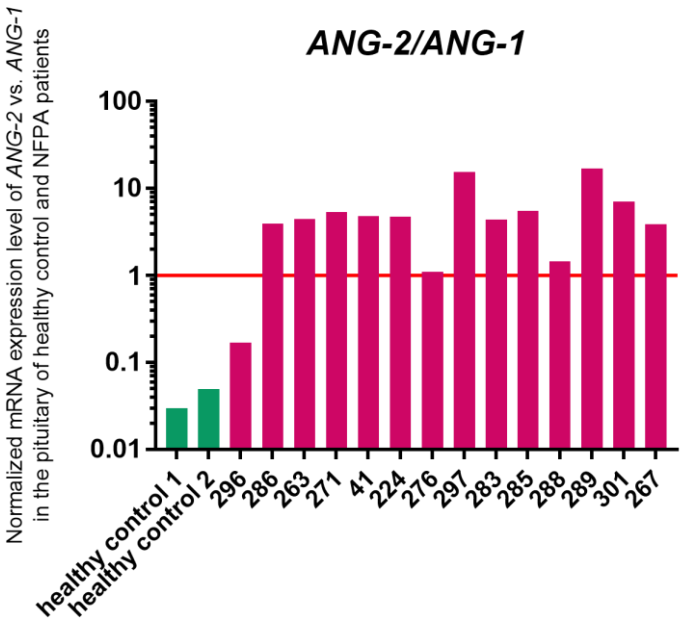

Figure 17: *ANG-2/ANG-1* ratio in normal pituitary and pituitary adenomas. In human NFPAs, the ratio of *ANG-2/ANG-1* is shifted toward *ANG-2*, which correlates with our findings in MENX rats.

To verify whether there was a correlation between the levels of *ANG-1* and *ANG-2* mRNA and the encoded proteins, we compared their expression at the mRNA and the protein levels. 15 and 37 NFPAs were analyzed by IHC to evaluate the expression of ANG-1 and ANG-2, respectively. In each run 3 healthy pituitary controls were also included. The expression of these two proteins in NFPAs correlated with the qRT-PCR data (Figure 18).

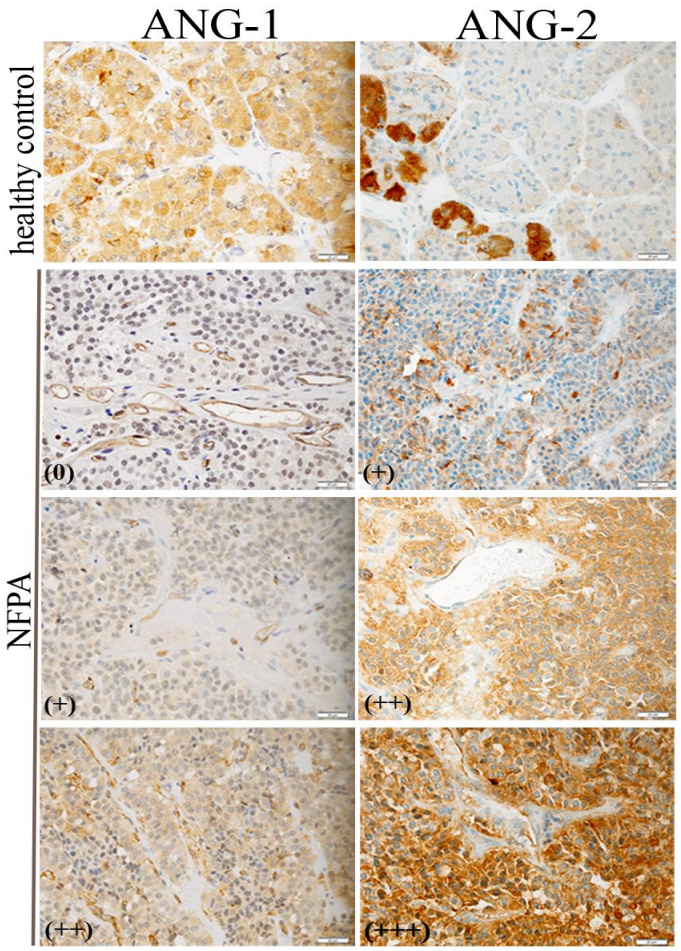

Figure 18: ANG-1 and ANG-2 are differently expressed in human NFPA and healthy control. To assess the expression of ANG-1 and ANG-2 in our cohort, formalin fixed paraffin-embedded human pituitary tissues were analyzed by IHC using anti-ANG-1 (1:300) and anti-ANG-2 (1:400) antibodies. 4 representative tissue sections show the range of observed expression intensity from (0) to (+++). Original magnification: 400x; scale bar: 20 µm.

Most human NFPAs demonstrated a weak or moderate expression of ANG-1, whereas ANG-2 was highly expressed in the majority of our samples (Figure 19).

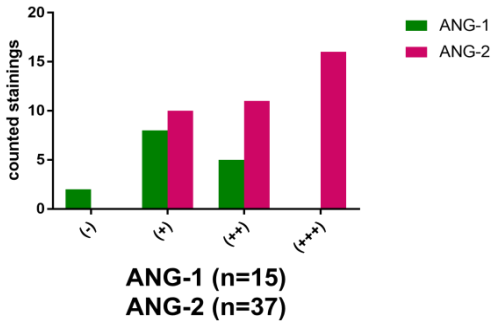

Figure 19: Summary of semi-quantitative evaluation of ANG-1 and ANG-2 expression in human NFPAs. The graph demonstrates the distribution of each score given to ANG-1 and ANG-2 expression in NFPA samples.

We observed a weak (+, n=8) or moderate (++, n=5) expression of this protein in adenoma cells of the remaining samples with sporadic positivity for ANG-1 expression in the vessels. The control healthy tissues showed the highest expression of ANG-1. All NFPAs expressed ANG-2, the majority of them displaying a moderate (++, n=11) or strong (+++, n=16) expression level. We found a weak (+) expression of ANG-2 only in 10 samples, whereas healthy controls showed no immunoreactivity for ANA-2.

In healthy pituitary control tissues, some cells strongly expressed ANG-2 as was seen in rat pituitary tissues (Figure 12). We wondered whether they belong to the gonadotroph lineage. Therefore, co-IF was performed for α-subunit (α-SU), a marker of gonadotroph cells, and ANG-2 (Figure 20).

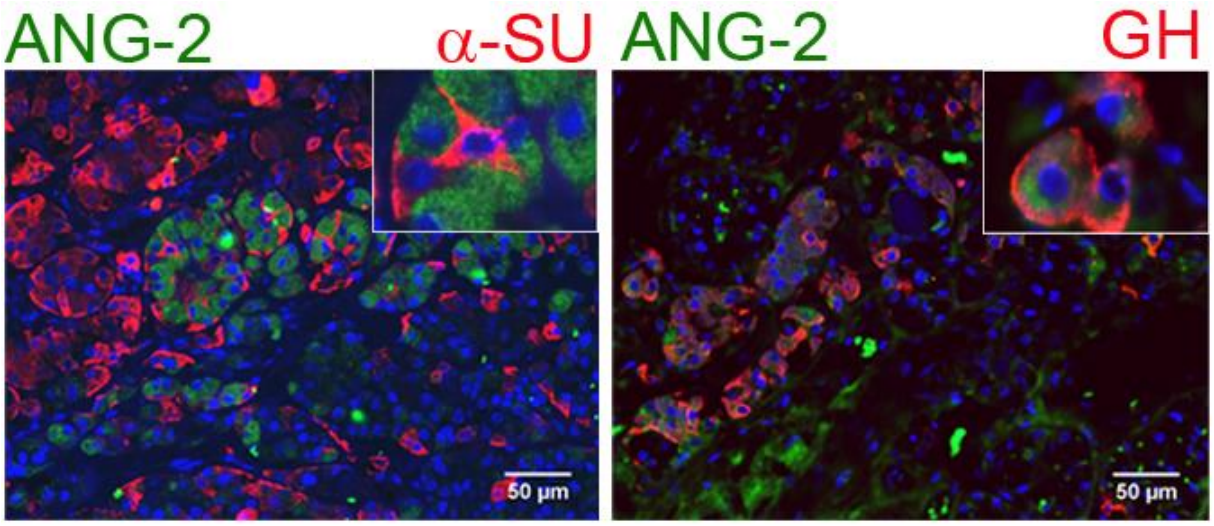

Figure 20: Co-immunofluorescence staining performed on human healthy pituitary tissue. Antibodies against Ang-2 (1:300) and α-SU (1:1000) were used to assess their localization in healthy pituitary (left figure). ANG-2 and α-subunit are not co-expressed in gonadotroph cells of healthy pituitary. Antibodies against ANG-2 (1:300) and growth hormone (GH) (1:500) were used to determine the localization of ANG-2 and GH (right figure). The staining shows co-expression of ANG-2 and GH in somatotroph cells of healthy pituitary but not in gonadotrophs. Original magnification: 200x; scale bar: 50 µm.

The gonadotroph cells expressing α-SU showed no immunoreactivity for ANG-2. In contrast, the cells belonging to somatotroph lineage (growth hormone (GH)-producing cells) displayed high immunoreactivity for ANG-2 (Figure 20).

Next, TIE-2 expression in human NFPA was assessed (Figure 21).

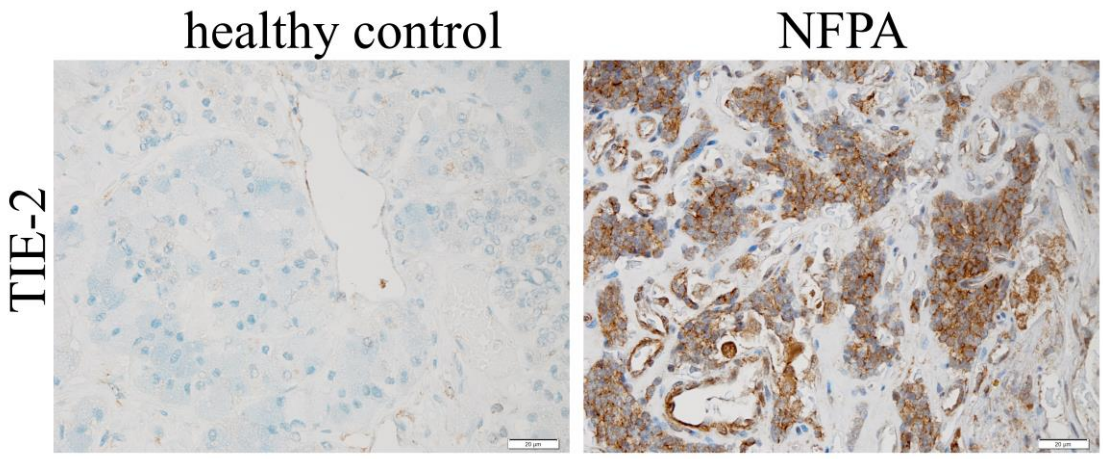

Figure 21: TIE-2 is highly expressed in human PAs. Expression of TIE-2 receptor in human healthy pituitary and human NFPA was assessed using formalin fixed paraffin-embedded tissues by IHC (anti-Tie-2 antibody, 1:600). Original magnification: 400x; scale bar: 20 μm.

Whereas in control non-tumourous pituitaries TIE-2 was expressed only in sparse ECs, the receptor was present in tumor-associated ECs. Moreover, TIE-2 was also found expressed both in the cytoplasm and on the membrane of NFPA cells (Figure 21).

3.2.2 Circulating ANG-2 level is elevated in NFPA patients

As mentioned previously, in some tumor types the amount of circulating ANG-2 is elevated when compared with healthy controls. For example, in melanoma and myeloma increased plasma levels of ANG-2 could predict the disease prognosis and survival of patients (Helfrich *et al.* 2009, Terpos *et al.* 2012). Since ANG-2 is a secreted protein, and, based on our previous results, it is highly expressed in NFPAs at the mRNA and the protein levels, we analyzed the concentration of ANG-2 in the pre-operative plasma of patients with NFPA (n=60). The plasma of healthy volunteers served as control (n=60).

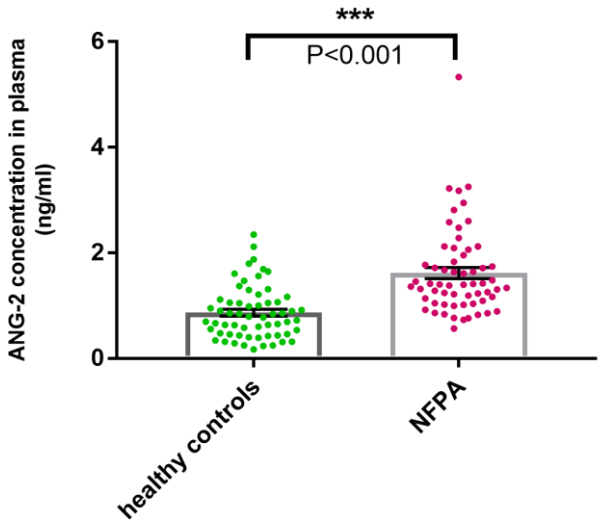

Figure 22: ANG-2 plasma levels of healthy controls and NFPA patients. Plasma samples of 60 healthy donors and 60 NFPA patients were analyzed using the human ANG-2 ELISA kit. ANG-2 was significantly increased in NFPA patients compared to healthy controls. Each dot in the plots represent the value measured for one individual (Mann Whitney test; P<0.001).

Age and gender of the control group were matched to those of the patients. ANG-2 plasma level was significantly elevated (on 1.9 fold) in NFPA patients when compared with healthy controls (mean 1.61 ng/ml vs. 0.87 ng/ml) (Figure 22). The data was still statistically significant even if we excluded the one outlier in the NFPA group (P = 4.89E-09). The plasma concentration of ANG-2 does not correlate with nodule size, age and gender or the invasiveness of the samples.

3.3 VEGF mRNA expression in HPAs

We measured the mRNA expression level of *VEGF-A* in the previously mentioned NFPA frozen samples (11 males and 4 females) (Table 20) and two normal pituitary mRNA samples, commercially available (BioChain), as control, using quantitative RT-PCR (TaqMan-PCR).

The normalized *VEGF-A* mRNA expression level in patients was calculated and compared with normal pituitary samples. We found no differences in expression level of *VEGF-A* in pituitary adenomas compared to one of the healthy normal control tissues, but if we considered the other healthy control, 9 adenoma samples showed a greater (>2 fold) expression of this gene (Figure 23).

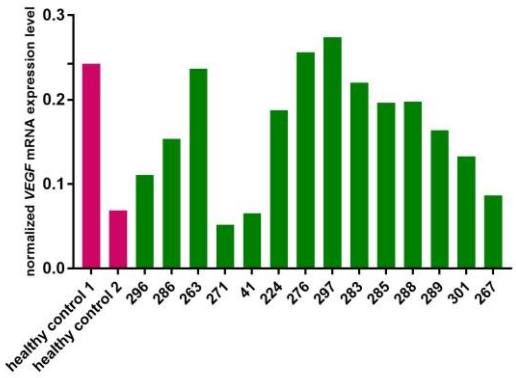

Figure 23: mRNA expression of *VEGF* in healthy control pituitary and NFPA patients. Total RNA from the pituitary gland was extracted, reverse transcription performed and the level of *VEGF* cDNA was analyzed in a PCR cycler using specific TaqMan primers and probes (Assay-on-DemandTM). The relative mRNA expression level of the target genes was normalized for input RNA using *TBP* gene expression (housekeeping gene) and a calibrator human adrenal RNA always run in parallel and was calculated with the 2-ΔΔCt formula. Normalized ct-values are demonstrated in the figure.

Since the healthy samples did not show the same trend regarding *VEGF-A* expression, we should have analyzed more healthy samples to draw a conclusion concerning the expression levels of *VEGF-A* in healthy and PA tissues. Despite our efforts, we could not find any additional provider for either healthy fresh pituitary samples or already extracted mRNA from this gland to expand our experiment.

3.4 *in vitro* functional experiments

3.4.1 Characterization of established pituitary adenoma cells expressing Ang-2

To understand the role of ANG-2 overexpression in pituitary adenomas, we performed further *in vitro* studies. We found that rat pituitary adenoma cells express Ang-2, Tie-2 and the receptor was phosphorylated (see Figure 15). We tested additional cell lines for Ang-2 expression. The cells tested were Att20, GH3, LβT2 and αT3, derived either from somatotroph- (Att20, GH3) or gonadotroph cells (LβT2, αT3). All cells were found to express Ang-2. α-Tubulin served as an internal loading control (Figure 24A). Since, we wanted to modulate the expression of Ang-2 to investigate its function in pituitary tumorigenesis, we determined if these cells also express the Tie-2 receptor. Therefore, western blot was performed to analyze the expression of this protein in our cell lines. A special protocol was

used to extract membrane proteins to analyze Tie-2 expression (Figure 24B). For further studies, we decided to work with GH3 cells because they were the only cells expressing both Ang-2 and Tie-2.

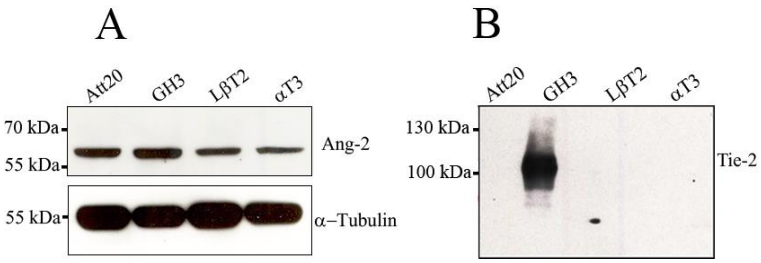

Figure 24: Western blot analysis of cell lines which may express Ang-2 and Tie-2. The expression of A) Ang-2 (1:200) and B) Tie-2 (1:500) was assessed in Att20, GH3, LβT2 and αT3. α-Tubulin (1:1000) is used as loading control. All four cell lines express Ang-2 but Tie-2 was detected only in GH3 cells.

Moreover, we performed IF staining to ascertain the localization of Ang-2 and Tie-2 in GH3 cells (Figure 25).

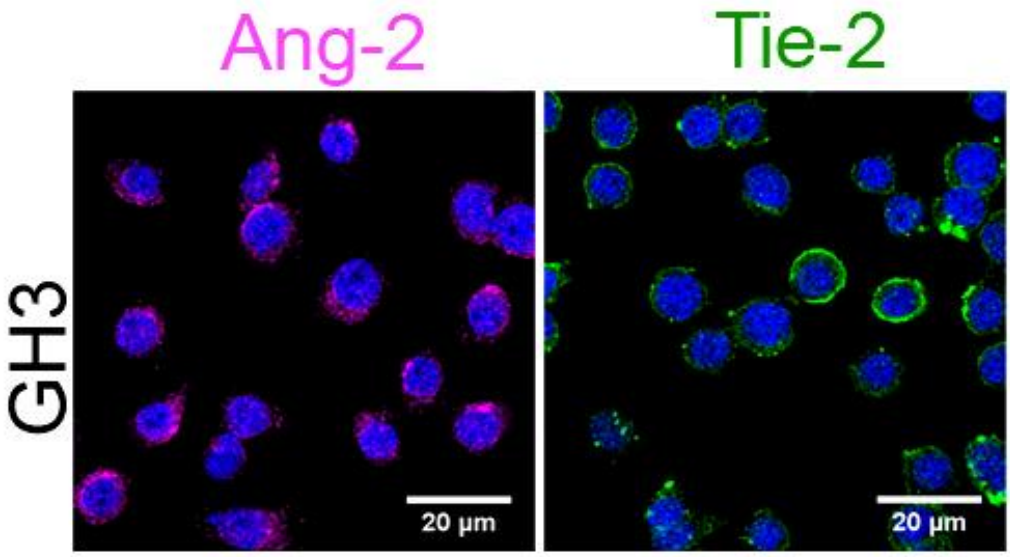

Figure 25: Immunofluorescence to detect Ang-2 and Tie-2 expression in GH3 cells. Expression of Ang-2 (1:400) and Tie-2 (1:200) was evaluated in GH3 cells. Ang-2 is detected in cytoplasm whereas Tie-2 is highly expressed in cell membrane. Cell nuclei were counterstained with DAPI. Original magnification: 400x; scale bar: 20 µm.

We observed cytoplasmic localization of Ang-2 and membranous localization of Tie-2 receptor as expected.

Since in rat and human pituitary adenomas Ang-1 was downregulated, we evaluated the expression of this protein in GH3 cells by western blot (Figure 26). HUVECs were included as positive control.

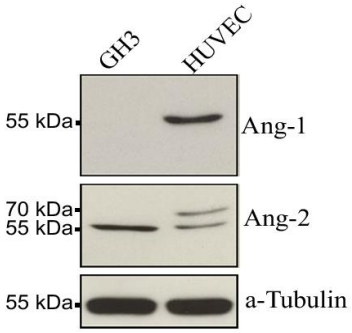

Figure 26: Expression of Ang-1 and Ang-2 in GH3 and HUVEC cells. The expression level of endogenous Ang-1 (1:500) and Ang-2 (1:200) in GH3 and HUVEC cells is identified by western blot. α-Tubulin (1:1000) is used as loading control.

Interestingly, we found that Ang-1 was also down regulated in GH3 cells similar to our findings in rat and human NFPAs, whereas Ang-2 was expressed in these cells. Angiopoietins possess several glycosylation sites. When they are glycosylated, the observed protein band in a western blot can appear at a size higher than the predicted one. Therefore, we assumed that the upper Ang-2 band in HUVECs is a glycosylated form, as reported for rhAng-1 (Davis *et al.* 1996).

Based on our results, GH3 cells expressed both Ang-2 and Tie-2 receptor, whereas Ang-1 was absent at the protein level. Thus, these properties made this cell line a proper model for further experiments as it mimics PAs *in vivo* and for modulation of Ang-2 expression.

3.4.2 Overexpression of Ang-2 in GH3 cells and functional analysis

To study a possible effect of Ang-2 overexpression on pituitary adenoma progression, we transfected GH3 cells with the mammalian expression vector pIREShyg, which carries human *ANG-2* full-length cDNA fused to a Myc- and a His-Tag (*ANG-2:*pIREShyg). This plasmid was a kind gift from Dr. Detjen (Charité - Universitätsmedizin Berlin).

First, we established transfection condition for GH3 cells using a pmaxGFP™ control vector, provided in the kit for the Lonza Nucleofector device. The DS-131 pulse gave the highest

transfection efficiency and a high number of viable cells after transfection (Figure 27A). HeLa cells were transfected in parallel as transfection control. *ANG*-2:pIREShyg or empty mock-vector were used for the transfection. 48 h after transfection, we were able to detect Ang-2 only in HeLa cells but the observed molecular mass of this protein was bigger than the predicted size for Ang-2 (56kDa) (Figure 27B).

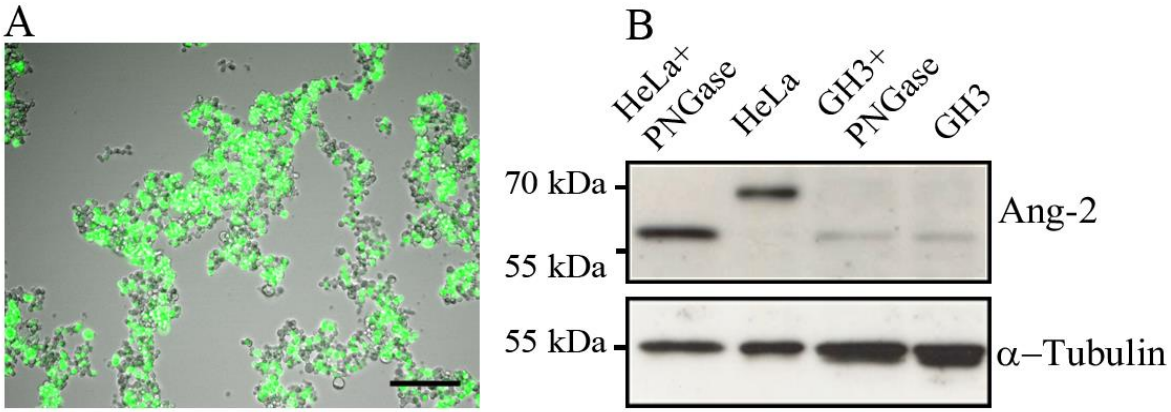

Figure 27: Transfection efficiency of GH3 cells using nucleofector (A) and evaluation of exogenous expression of ANG-2 in HeLa and GH3 cells (B). A) Optimized GH3 transfection conditions using pmaxGFP™ control vector and Lonza nucleofactor. The green signal indicates transfected GH3 cells. Original magnification: 200x; scale bar: 200 µm. B) The figure shows detection of Ang-2 (1:200) and the loading control α-Tubulin (1:1000). HeLa and GH3 cells were transfected with *ANG-2*:pIREShyg plasmid and collected 48 h later. Western blot indicates exogenous expression of glycosylated ANG-2 in HeLa cells (70kDa). Treatment of transfected Hela cell-lysate with PNGase-F leads to deglycosylation of exogenous ANG-2 and observation of a band with the predicted size of 56kDa for Ang-2. GH3 cells show no expression of exogenous ANG-2 but an endogenous expression of Ang-2 is detectable by treated and untreated lysate with PNGase-F.

This observation indicates that exogenous human ANG-2 undergoes post-translational modifications in transfected cells. Angiopoietin-2 is a glycoprotein, and its amino acid sequence contains several potential glycosylation sites (at amino acids 89, 119, 133, 151, 240, and 304) (Kim *et al.* 2000d). After treatment of HeLa protein lysate with PNGase-F, which is an amidase able to remove glycosyl residues, we observed that deglycosylation reduced the originally detected molecular mass of exogenous ANG-2 from 70kDa to the predicted 56kDa.

The overexpression of ANG-2 in GH3 cells was unsuccessful and no expression of exogenous protein could be detected in these cells (Figure 27B).

Therefore, we changed the vector to overexpress Ang-2 exogenously. The same transfection conditions were used to transfect GH3 cells with the vector *ANG-2*:EX-K4038-M09

expressing human ANG-2 with a c-Myc tag. GH3 cells were collected 48 h after transfection to analyze the expression of this construct (Figure 28).

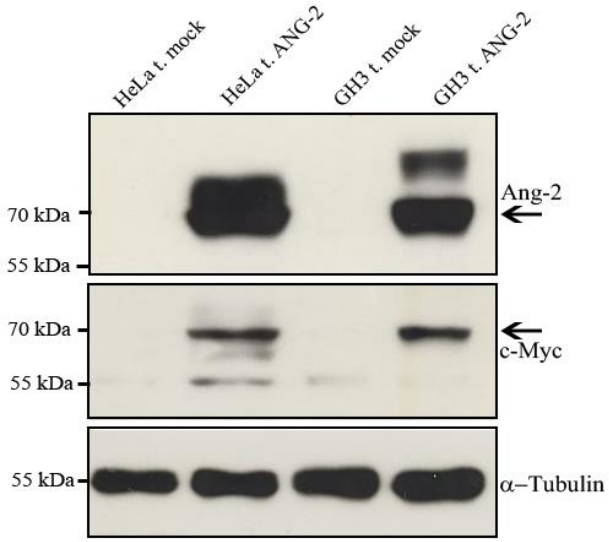

Figure 28: Validation of ANG-2 over-expression in HeLa and GH3 cells. The cells were transfected with mock or ANG-2:EX-K4038-M09 vector. 48 h after transfection, HeLa and GH3 cells were analyzed by western blot to assess transfection efficiency. Exogenous ANG-2 is detected in both cell lines. Specific anti-Ang-2 (1:200) and Myc-tag (1:500) antibodies were used to detect corresponding proteins. α-Tubulin (1:1000) was used as loading control.

In both GH3 and HeLa cells, the exogenous ANG-2 could be expressed and detected by western blot and the bands specificity was verified with an antibody against the c-Myc-tag. Due to the very short exposure time (30 s) the bands of endogenous Ang-2 in GH3 cells were not visible in this blot. Endogenous Ang-2 band was usually detected after 3 min. If we prolonged the exposure time, the strong signal of exogenous ANG-2 would covere the signal of endogenous one. With this construct, we detected again the glycosylated form of ANG-2, which possessed a molecular weight of 70kDa.

Since Ang-1 expression was undetectable in GH3 cells, we wondered if Ang-2 is able to activate Tie-2 in these cells as described in EC. This could have an impact on cell viability by activating PI3K and MAPK pathways (Bogdanovic *et al.* 2006, Kim *et al.* 2000c).

Thus, we investigated whether signaling pathways known to be activated upon binding of Ang-2 to Tie-2 in ECs, were also activated in Ang-2-overexpressing GH3 cells. Transfected cells either with *ANG-2*:EX-K4038-M09 or mock vector were collected 48 h later to study the effects of upregulated Ang-2 on downstream components by western blot (Figure 29).

Endogenous Ang-2 was detected in both cell lines (56kDa) and exogenous ANG-2 (70kDa) was present in ANG-2-overexpressing cell line.

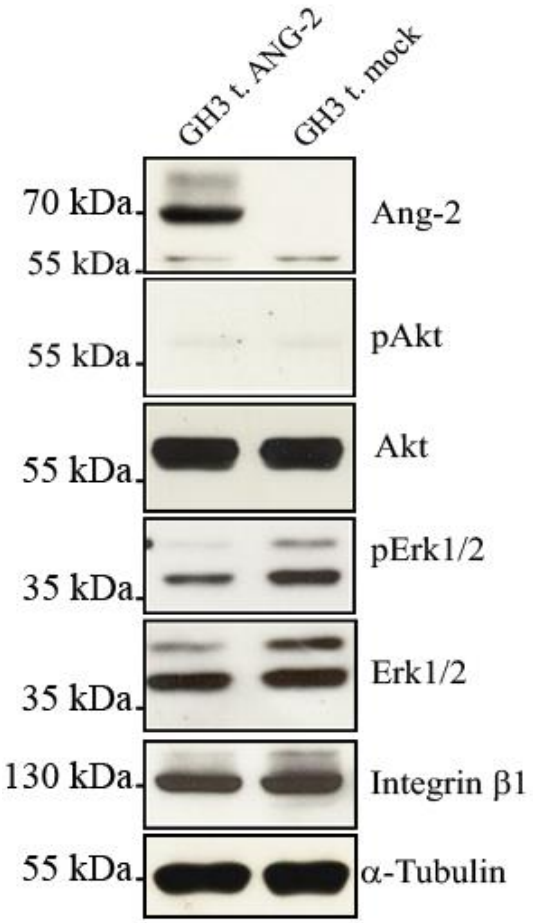

Figure 29: Exogenous ANG-2 has no effect on activation of downstream signaling molecules. GH3 cells were transfected with ANG-2:EX-K4038-M09 or mock vector and 48 h after transfection the lysates were analyzed by western blot. ANG-2 (1:200) is expressed in transfected GH3 cells. Western blot shows no changes in the amounts of pAkt (1:500), Akt (1:1000), pErk1/2 (1:1000), Erk (1:500) and Integrin β1 (1:500) in transfected cells compared to cells transfected with mock vector.

Akt is one of the downstream molecules activated by angiopoietins (Kontos *et al.* 1998, Kim *et al.* 2000c, Kim *et al.* 2000b). Therefore, we investigated the possible activation of this molecule in transfected GH3 cells, but we could not observe any effect on Akt. Moreover, pAkt is hardly detectable in GH3 cells.

Studies done in HUVECs have shown that both Ang-1 and Ang-2 stimulation resulted in the activation of Erk1/2 (Harfouche and Hussain 2006b). Based on these findings we checked whether there were any changes in the amounts of pErk1/2 in transfected cells compared to cells transfected with mock vector. We calculated the western blot band intensity of pErk1/2

using Fiji software in these two cell population and normalized it against total amount of Erk1/2 in the same cell lysate (Ang-2-overexpressing cell line=0.43 and mock transfected=0.65). Thus the ratio of pErk1/2 / Erk1/2 was decreased in the cells expressing exogenous ANG-2. Ang-2 activates Erk1/2 via β1 integrin/FAK/p130Cas signaling pathway (Hu *et al.* 2006). Therefore, we also checked if the expression of integrin β1 is altered in Ang-2 overexpressing GH3 cells, but its expression was unchanged in both cell groups (Figure 29). Thus, we wondered if we had assessed the effect of exogenous ANG-2 on signaling molecules at the wrong time point. Therefore, we tried to investigate its long-term effect on cell viability (Figure 30).

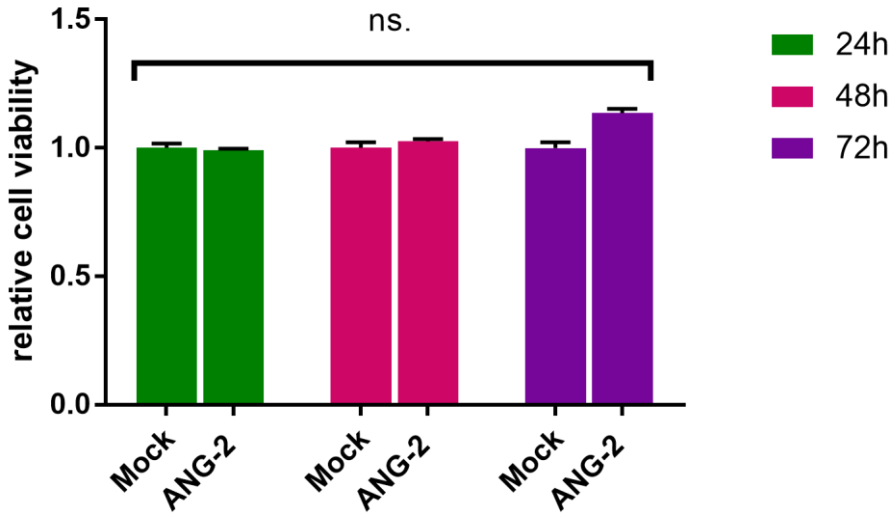

Figure 30: Effect of exogenous ANG-2 expression on the cell viability of GH3 cells. GH3 cells were transfected with ANG-2:EX-K4038-M09 or mock vector and cell viability was assessed 24 h, 48 h and 72 h after transfection. Cell viability of ANG-2 overexpressing cells was normalized against the values of cell viability of mock-transfected cells arbitrarily, set to 1. The experiment was performed independently with six technical and two biological replicates each and is expressed as the mean ± SEM. Statistical comparisons were performed using the Mann Whitney test. ns. = not statistically significant.

If we compared GH3 cells transfected with *ANG-2*:EX-K4038-M09 with those transfected with empty vector, no significant differences were observed in downstream signaling nor in the cell viability. Therefore, we wondered if the vector-encoded ANG-2 is biologically active in our system. There was also another possibility that the cells overexpressing Ang-2 tried to compensate the effect of permanently produced high amounts of ANG-2 (197 ng/ml in supernatant, which was more than 500 fold elevated compared to the parental cell line, measured by ELISA, 9×10^5 cells/well). To test this hypothesis we used a selected ANG-2

overexpressing clone (named "K9OE") and the parental cells as control (ctrl.) to check first the expression of Ang-2 and then the localization of Tie-2 receptor (Figure 31).

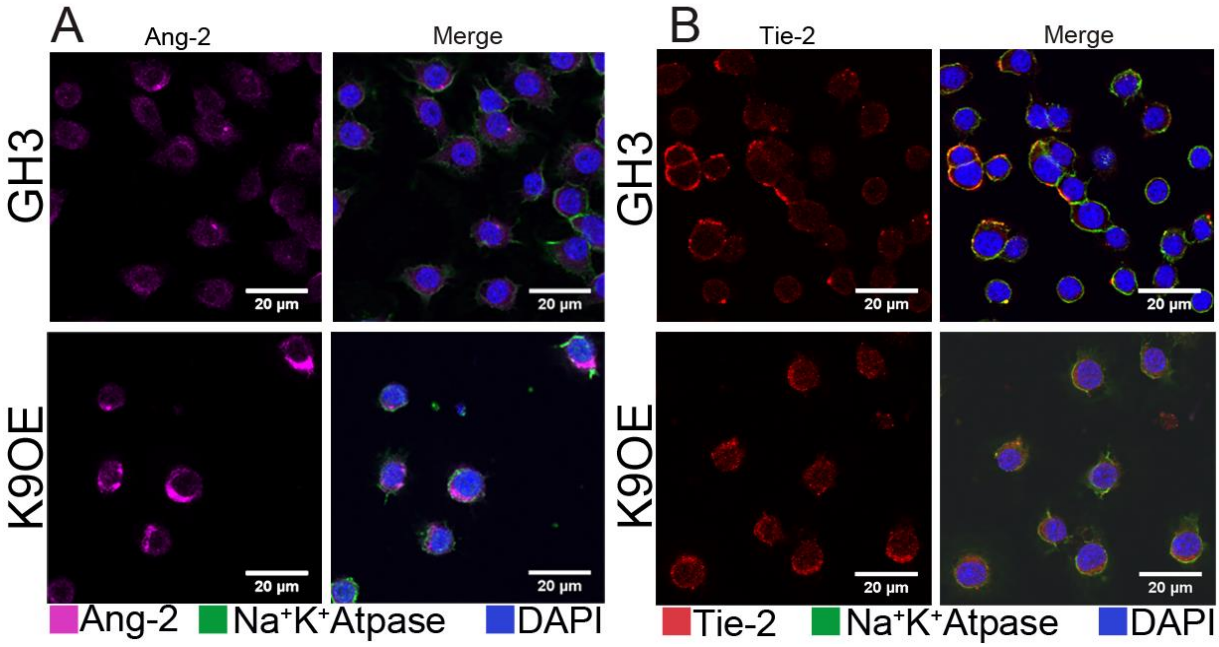

Figure 31: Immunofluorescence on K9OE and parental GH3 cells. Expression of Ang-2 (1:400) and Tie-2 (1:200) was evaluated in GH3 cells. Ang-2 is highly expressed in K9OE. Tie-2 is mainly localized in the membrane of parental cells, whereas in K9OE the receptor is distributed in the cytoplasm. Na^+K^+ ATPase served as membrane marker (1:300/1:500). The experiment was performed with three technical replicates. Cell nuclei were counterstained with DAPI. Original magnification: 400x; scale bar: 20 µm.

Similar to what we observed by western blot, ANG-2 overexpression was confirmed in K9OE cells by IF. However, the most interesting observation was the localization of Tie-2 in these two cell population. In parental cells, Tie-2 was almost exclusively localized in the cell membrane, whereas in K9OE cells the receptor was mostly internalized and distributed in the cytoplasm, which indicated that exogenously produced ANG-2 might be able to bind to Tie-2 and this results in the internalization of the receptor. Moreover, in excess of ANG-2, Tie-2 signaling was permanently activated. Probably, the cells tried to compensate the effect of constantly activated pathway therefore; we were not able to detect any activation of downstream signaling molecules in ANG-2-overexpressing cells.

3.4.3 Ang-2 is secreted into the culture medium and may bind Tie-2

Next, to prove our hypothesis that ANG-2 expressed by GH3 cells is released into the culture medium and might activate Tie-2, GH3 (parental), K9OE, and HUVECs as control were cultivated in 6 well plates for 48 h in serum-free condition to avoid the interference of components in FBS or horse serum on ELISA measurements of the supernatant. The supernatant was briefly centrifuged and concentrated using Amicon columns. The concentrated supernatant was analyzed by western blot and ELISA using a kit specific for ANG-2 (Figure 32 & Table 21).

Fifty µg of the concentrated supernatant was loaded onto a gel, after electrophoresis blotted and then the membrane was incubated with an antibody against Ang-2. The molecular mass of the observed band correlated with the predicted size of glycosylated Ang-2 (70kDa) (Figure 32).

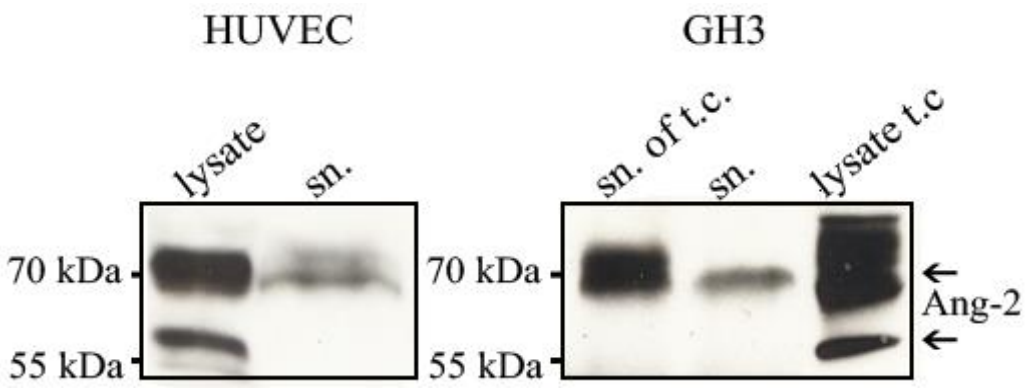

Figure 32: Exogenous and endogenous Ang-2 is released into the culture medium. HUVECs express ANG-2 and this protein is in both glycosylated (70kDa) and not glycosylated (56kDa) forms detectable by western blot. In the supernatant (sn.) of these cells, only glycosylated form of ANG-2 was observed. For GH3 cells, we used supernatant of transfected cells (sn. of t.c.), supernatant of untransfected cells (sn.) and cell lysate of transfected cells (lysate t.c). Secreted Ang-2 in GH3 cells is also glycosylated. In the cell lysate of transfected GH3 cells, we could observe both endogenous Ang-2 (56kDa) and exogenous glycosylated form (70kDa). Specific anti-Ang-2 (1:200) antibody was used to detect Ang-2 in HUVECs and GH3 cells.

Moreover, by ELISA we could also detect Ang-2 secreted in the supernatant of parental GH3 cells (Table 21).

Table 21: ANG-2 levels in the supernatant of HUVEC and GH3 cells (parental and transfected with ANG-2:EX-K4038-M09) measured by ELISA. Measured ANG-2 concentration is the average of 3 technical replicates for each cell line.

	GH3	C9OE	HUVEC
Cell number	9×10^5	9×10^5	9×10^5
ng/ml±SD	2.97±0.05	194.75±0.83	29.86±0.74

To investigate whether phosphorylated Tie-2 could be detected in GH3 cells, we immunoprecipitated Tie-2 in these cells. HUVECs served as control. Then western blot was performed and the membrane was probed using an antibody against pTie-2 (Tyr 1102/1108) (Figure 33).

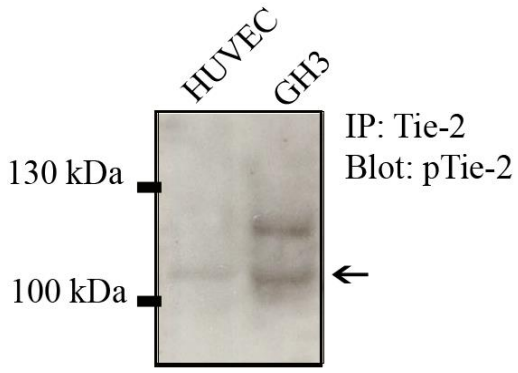

Figure 33: Tie-2 receptor is activated in GH3 cells. Western blot indicates that Tie-2 is phosphorylated on Tyr 1102/1108 in GH3 cells. Specific Antibody was used to immunoprecipitate Tie-2 in GH3 and HUVEC. Afterward, the membrane was probed with an anti-pTie-2 (Tyr 1102/1108) antibody (1:2000).

Our results showed that Tie-2 was phosphorylated at Tyr 1102/1108 in parental GH3 cells and HUVECs. In GH3 cells, we detected an additional band, which might be a glycosylated form of Tie-2 due to post-translational modifications in GH3 cells. ANG-2 is mainly stored in Weibel-Palade bodies in HUVECs (Saharinen *et al.* 2005). It can explain the faint signal of pTie-2 observed in these cells.

To further prove of our hypothesis that Ang-2 secreted by GH3 cells binds to Tie-2 localized on the membrane of the tumor cells, we checked the localization of both proteins. Since exogenously produced ANG-2 possessed a c-Myc tag, we used an anti c-Myc antibody for detecting ANG-2. IF showed that in many cells c-Myc and Tie-2 were co-localized on cell membrane (Figure 34).

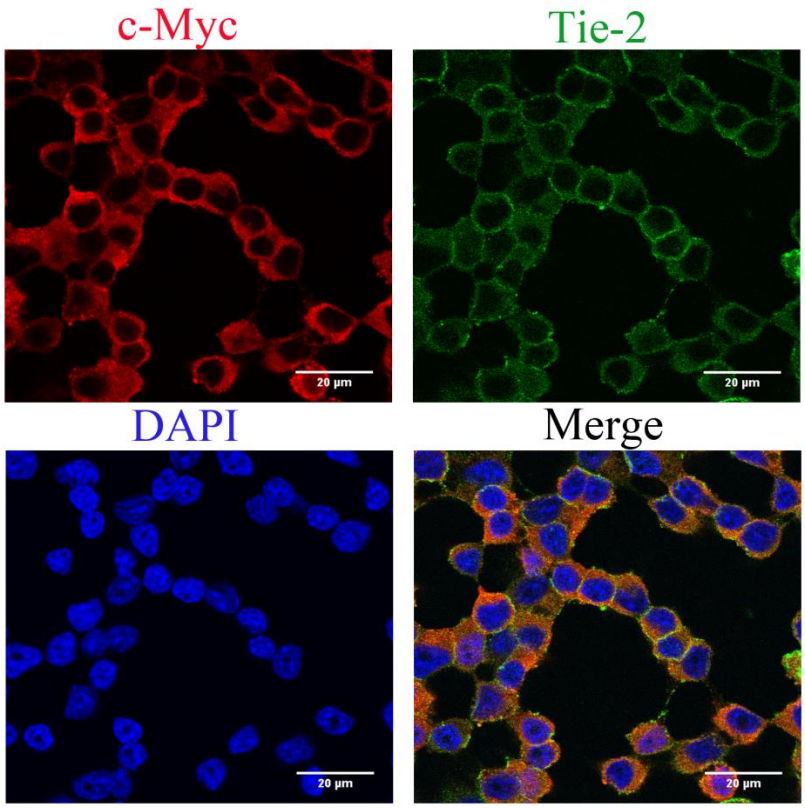

Figure 34: Co-immunofluorescence staining performed on K9OE cells. Antibodies against c-Myc (1:300) and Tie-2 (1:200) were used to assess localization of these two proteins. The experiment was performed with three technical replicates. Cell nuclei were counterstained with DAPI. Original magnification: 400x; scale bar: 20 µm.

In HUVECs, binding assays indicated that ANG-2 is not internalized with the receptor and is released again into culture medium within 5 min - 2h after binding (Bogdanovic *et al.* 2006).

To investigate the direct binding of Ang-2 to Tie-2 receptor in GH3 cells, we employed Co-IP. We used ANG-2 overexpressing K9OE cells treated with the cross-linker 3,3′-dithiobis to cross-link ligand to receptor.

K9OE cells were incubated for 3 days in serum free medium. After incubation with cross-linker, they were lysed and Tie2 was immunoprecipitated. Immunoblotting was conducted using an anti-Ang-2 antibody. We observed that exogenous Ang-2 was co-immunoprecipitated with Tie-2 (Figure 35).

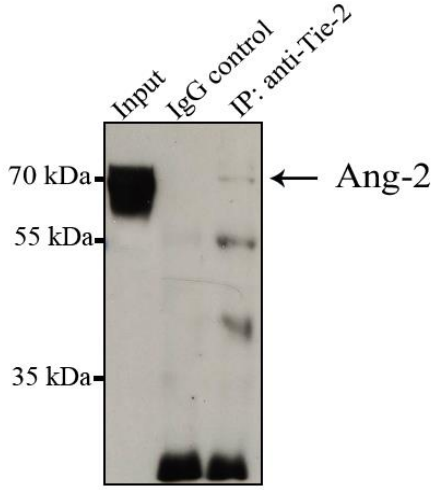

Figure 35: Exogenous Ang-2 is co-immunoprecipitated with Tie-2 in K9OE cells. Cells were lysed and the protein lysate was immunoprecipitated with an antibody against Tie-2. The resulting IP was analyzed by western blot and probed for Ang-2 (1:200).

We used the same lysate to immunoprecipitate Ang-2 using an anti-c-Myc antibody to investigate whether Tie-2 could co-immunoprecipitated with this protein (Figure 36).

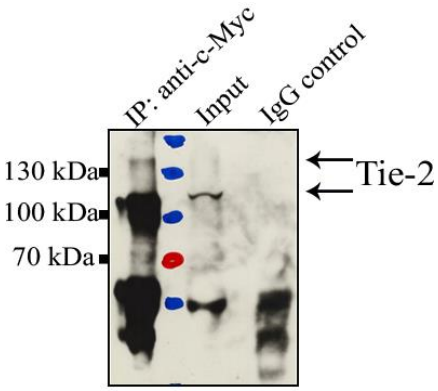

Figure 36: Co-immunoprecipitation of Tie-2 with exogenous Ang-2 in K9OE cells. Cell lysate from the experiment in Figure 35 was immunoprecipitated with anti-c-Myc antibody and immunoblotted with anti-Tie-2 antibody (1:500). Protein ruler is demonstrated in red and blue colors.

In GH3 cells, Tie-2 was found in the two previously reported isoforms (135 and 120kDa) (Yabkowitz *et al.* 1997) with the smaller one being the most abundant. This data showed that the exogenous ANG-2 is able to bind Tie-2 receptor in pituitary adenoma cells. We observed in previous experiments that Tie-2 can also be localized in the cytoplasm (Figure 31B & Figure 34). This can occur as a result of ANG-2/Tie-2 interaction, receptor activation and internalization. Excess of secreted ANG-2 in K9OE may lead to a constitutively active Tie-2

signaling and the cells try to compensate this effect and may explain why we could not detect increased levels of pAkt and pErk1/2 in these cells (Figure 29).

Then, we decided to use recombinant human ANG-2 protein to identify the downstream mediators of activated Ang-2/Tie-2 signaling in GH3 cells.

3.4.4 Ang-2 and Tie-2 interact in rat PA

We also investigated the interaction between Ang-2 and Tie-2 in rat PA tissues ex vivo using Proximity Ligation Assay (PLA). We detected a PLA signal using either antibodies against Ang-2 and Tie-2 or against Ang-2 and P-Tie-2 (Figure 37). No signal was present, when we used only the anti-Ang-2 antibody.

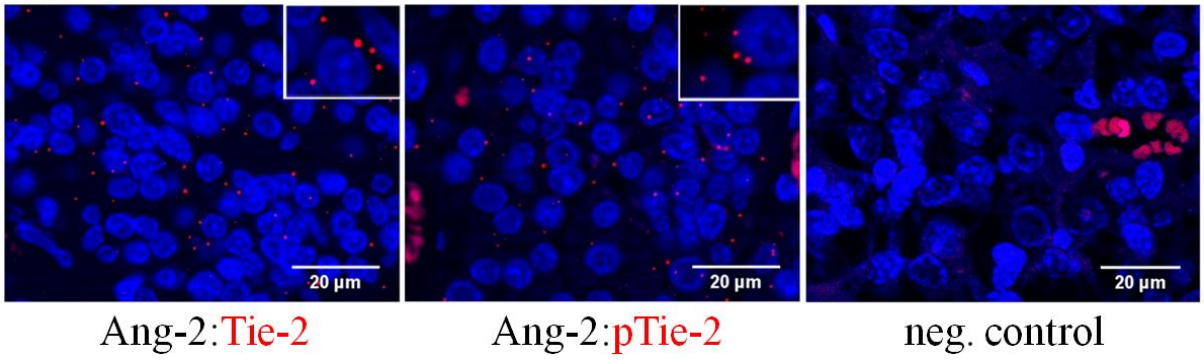

Figure 37: Proximity Ligation Assay (PLA) was performed on FFPE sections of rat PAs using antibodies against Ang-2, Tie-2 and P-Tie-2. Nuclei were counterstained with DAPI (blue). For negative control the experiment was performed using only anti-Ang-2 antibody. 400x; scale bar: 20 µm.

Thus, Tie-2 on the membrane of PA cells interacted with Ang-2 and was partially phosphorylated, thereby suggesting that endogenously-produced Ang-2 could initiate autocrine signaling in these cells.

3.4.5 Stimulation of GH3 cells with recombinant human ANG-2

It has been reported that incubation of HUVEC cells with rhANG-2 activates downstream signaling pathways in these cells (Kim *et al.* 2000c, Yuan *et al.* 2009). Treatment of HUVECs with rhANG-2 increases the amounts of pFak, pAkt, pP38 and pErk 1/2, known downstream signaling molecules of Ang-2/Tie-2 pathway (Harfouche and Hussain 2006b). Phosphorylation of Tie-2 at Tyr 1102 after binding of Ang-1 can activate PI3K and Grb7 and

these in turn are able to activate Fak at Tyr 397 (Kim *et al.* 2000a, Brindle *et al.* 2006, Han and Guan 1999), before other downstream effectors like Erk 1/2 are activated (Fukuhara *et al.* 2008). Therefore, we included Fak in our analysis. First, we investigated the activity of commercially provided rhANG-2 in HUVECs (Figure 38). HUVECs were incubated for 45 min or 24 h with 800 ng/ml rhANG-2. This concentration has been reported in the literature as the highest effective concentration able to activate the Tie-2 receptor (Hansen *et al.* 2010, Yuan *et al.* 2009, Kim *et al.* 2000c, Bogdanovic *et al.* 2006). Then, the cells were harvested and after protein extraction, lysates were examined by western blot.

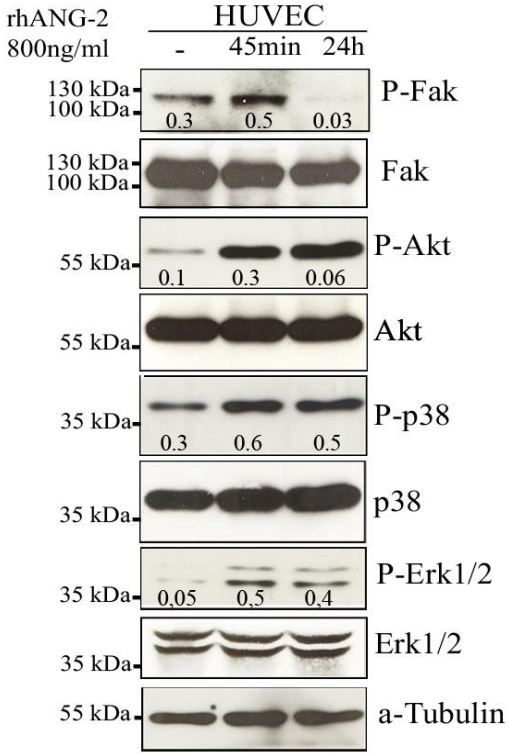

Figure 38: Effect of rhANG-2 on the phosphorylation of downstream signaling molecules in HUVECs. Cells were incubated for 24 h in serum-free medium before stimulation with rhANG-2. 800 ng/ml recombinant protein was added to the cells and incubated either for 45 min or 24 h in serum-free medium. Western blot was performed to evaluate the ability of commercially provided rhANG-2 to stimulate downstream signaling pathways. The membrane was probed with pFak (1:500) and reprobed with Fak (1:1000), anti-pAkt (Ser473) (1:500), Akt (1:1000), pP38 (1:1000), P38 (1:1000), pErk 1/2 (1:1000), Erk 1/2 (1:500) and α-Tubulin (1:1000). The numbers represent the ratio of phospho-/total-proteins.

These results showed that also in our hands these molecules could be activated upon stimulation with rhANG-2. In particular, Fak phosphorylation was detected after 45 min but was already gone at 24 h after treatment.

After confirming that rhANG-2 activates signaling pathways in ECs, we decided to assess the effect of rhANG-2 stimulation on GH3 cells and find a reliable readout for activation of signaling pathways downstream of Tie-2. We incubated cells serum-starved for (24 h) with 800 ng/ml rhANG-2 for different time intervals and then the total proteins were collected. We started with P38 molecule and observed that untreated GH3 cells possess variable levels of activated P38 and consequently their stimulation with rhANG-2 resulted in no clear changes. An example of the controversial results of stimulated GH3 is represented in Figure 39.

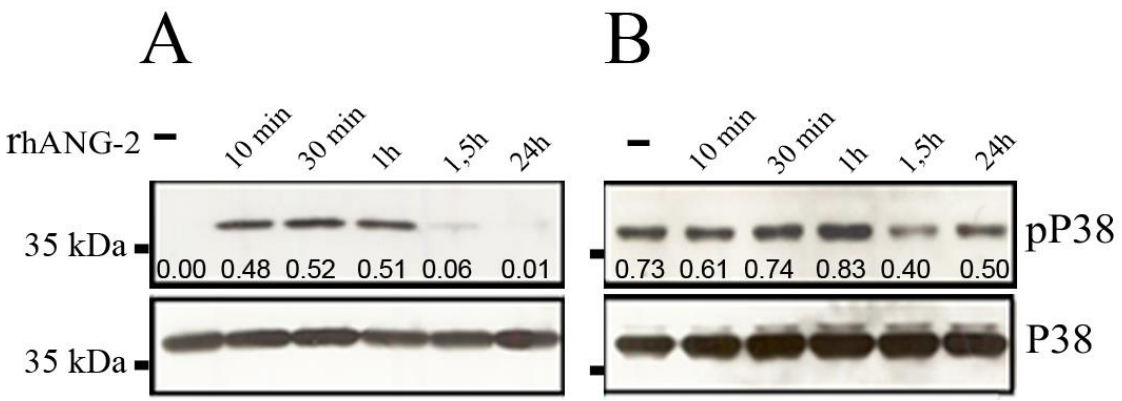

Figure 39: Effect of rhANG-2 on the phosphorylation of P38 in GH3 cells. Cells were incubated for 24 h in serum-free medium. After 24 h the cells were stimulated for various time points with 800 ng/ml rhANG-2 in serum-free condition. Western blot was performed to evaluate the ability of commercially provided rhANG-2 to stimulate downstream signaling pathways. The membrane was probed with anti-pP38 (1:1000) antibody and reprobed to detect total P38 (1:1000). The numbers represent the ratio of phospho-/total-proteins.

In part A of this Figure, which shows one of our experiments, pP38 was not detectable in unstimulated cells, but after 10 min P38 was activated. In part B, which was another independent experiment, pP38 was already present and saturated in basal condition. We speculate that as the cells were not synchronized they have different basal levels of endogenous Ang-2 and subsequently a different degree of activation of Tie-2. Therefore, we observed variable activation of downstream signaling molecules independent of stimulation with rhANG-2. Moreover, a competition between rat endogenous Ang-2 and rhANG-2 for binding to Tie-2 is conceivable. If at the starting point of the experiment the receptor is already activated by endogenous Ang-2, stimulation with rhANG-2 might have no additional impact on downstream signaling.

Furthermore, in contrast to HUVECs, where pAkt was increased after stimulation with the rhANG-2, we could not detect any pAkt in treated or untreated GH3 cells and, after 4 *in vitro* passages P38 could not be detected anymore (data not shown).

So, we decided to inhibit endogenous Ang-2 either with neutralizing peptibody, AMG386, or with a specific siRNA.

3.4.6 Stimulation of GH3 cells after blocking of endogenous Ang-2

3.4.6.1 rhANG-2 activates mitogen-activated protein kinase (MAPK) pathway in GH3 cells in a time-dependent manner

To overcome the problems caused by interference of endogenous Ang-2 with rhANG-2 while studying Ang-2/Tie-2 signaling, we changed our experimental design.

GH3 cells were grown in serum reduced medium (50%) for 24 h and then the medium was removed. Cells were washed and incubated for another 24 h in serum-free medium to which 0.01 mg/ml AMG386 was added. AMG 386 is a neutralizing peptide-Fc fusion protein (peptibody) against Ang-1 and Ang-2 (both secreted into culture medium). This peptibody binds to the ligands and inhibits their binding to the Tie-2 receptor and activation of signaling pathways downstream of this receptor (Herbst *et al.* 2009). Afterwards, the medium was changed and cells were stimulated with 800 ng/ml rhANG-2 in fresh serum-free medium. GH3 cells were harvested at various time points. Then, the cells lysates were analyzed by western blot (Figure 40).

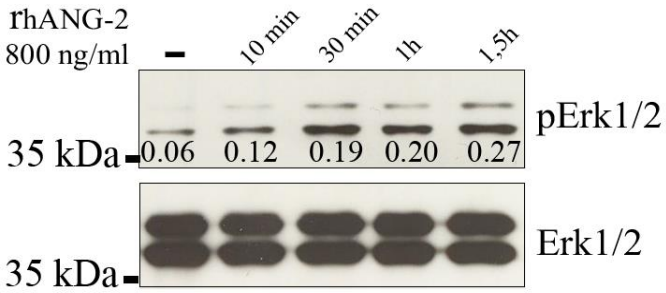

Figure 40: Upon rhANG-2 stimulation Erk1/2 is phosphorylated in GH3 cells in a time dependent manner. GH3 cells were stimulated with 800 ng/ml rhANG-2 for 10 min, 30 min, 1 h and 1.5 h in serum starved condition. The control group was not treated but the cells were incubated with fresh serum-free Medium for 1.5 h prior to harvesting. With the time progression, the amount of pErk1/2 (Thr202/Tyr204) is elevated. Figure 40 shows one experiment out of three independent experiments with similar results. The membrane was probed with anti-pErk1/2 (1:1000) antibody and reprobed to detect total Erk1/2 (1:500). The numbers represent the ratio of phospho-/total-proteins.

Our results showed that the MAPK signaling pathway was activated after stimulation of the GH3 cells with rhANG-2 in a time-dependent manner. Moreover, Erk1/2 was constantly expressed in GH3 cells. Thus, we consider this molecule an interesting control and potential readout to monitor Tie-2 dependent activation of MAPK pathway upon Ang-2 binding.

3.4.6.2 rhANG-2 activates mitogen-activated protein kinase (MAPK) pathway in GH3 cells in a concentration-dependent manner

Since Ang-1, the canonical agonist of Tie-2, was absent in GH3 cells and the treatment of these cells with 800 ng/ml of rhANG-2 was able to activate the MAPK pathway over time, we wondered if the stimulation of this signaling cascade by rhANG-2 was dose-dependent. Therefore, GH3 cells were plated as described in 3.4.5.1 and afterwards stimulated with increasing amounts of rhANG-2 for 30 Minutes (Figure 41).

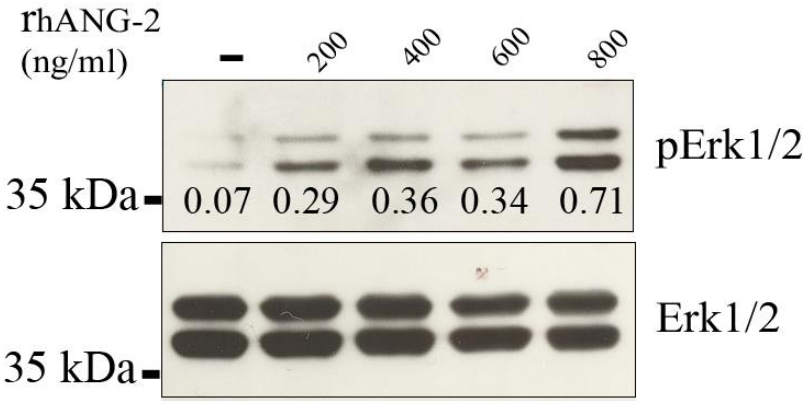

Figure 41: Upon rhANG-2 stimulation Erk1/2 is phosphorylated in GH3 cells in a concentration dependent manner. GH3 cells were stimulated with different concentrations of rhANG-2 for 30 min in serum starved condition. With the increasing concentration, the amount of pErk1/2 (Thr202/Tyr204) is elevated. If the cells were incubated with 600 ng/ml, we observed a slight drop of pErk1/2 amount. The control group was not treated but the cells were incubated with fresh serum-free Medium for 30 min prior to harvesting. Figure 41 shows one experiment out of three independent experiments with similar results. The membrane was probed with anti-pErk1/2 (1:1000) antibody and reprobed to detect total Erk1/2 (1:500). The numbers represent the ratio of phospho-/total-proteins.

Already, after stimulation of GH3 cells with 200 ng/ml rhANG-2, we observed an increase in pErk1/2 level. These data confirmed that Ang-2 could activate downstream signaling pathways in pituitary adenoma cells in a concentration-dependent manner.

3.4.6.3 rhANG-2 activates Tie-2 in a concentration-dependent manner

Subsequently, we also tried to assess the relationship between Tie-2 phosphorylation and the concentration of rhANG-2. GH3 cells were cultured as previously described (see 3.4.6.2) and incubated with various amounts of rhANG-2. 30 minutes after incubation with rhANG-2, the cells were washed carefully and protein was extracted using a special protocol to enrich in membrane proteins. The lysates were analyzed by western blot (Figure 42).

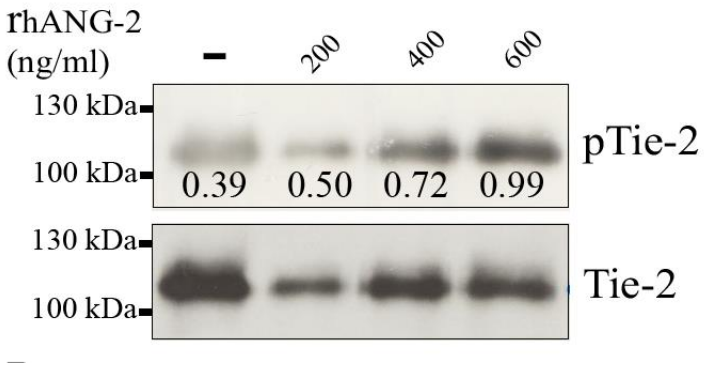

Figure 42: rhANG-2 activates Tie-2 in a concentration dependent manner. GH3 cells were stimulated with different concentrations of rhANG-2 for 30 min in serum starved condition. With the increasing concentration, the amount of pTie-2 (Tyr 1102/Tyr 1108) is elevated. Figure 42 shows one experiment out of two independent experiments with similar results. The membrane was probed with anti-pTie-2 (1:2000) antibody and reprobed to detect total Tie-2 (1:500). The numbers represent the ratio of phospho-/total-proteins.

We examined the phosphorylation of Tie-2 at tyrosine residues 1102/1108 in response to rhANG-2, since it is known to play an important role for the initiation of downstream signaling pathways. We observed that incubation of GH3 cells with rhANG-2 stimulated Tie-2 phosphorylation at Tyr1102/1108 in a concentration-dependent manner.

3.4.7 Downregulation of endogenous Ang-2 in GH3 cells

Since neutralization of endogenous Ang-2 in previous studies was not 100%, it (see Figure 40 & Figure 42, control lysate) may interfere with the stimulation of Tie-2 by rhANG-2. So, we decided to knock down Ang-2 expression in GH3 cells and then try to stimulate them with rhANG-2 to confirm our previous findings.

First, we transfected GH3 cells with 200 nM siRNA against *Ang-2* and collected them 24 h and 48 h later. Knockdown efficiency was assessed by qRT-PCR (Taqman) and western blot for Ang-2 (Figure 43). Non-targeting (scrambled) siRNA #3 was used as negative control.

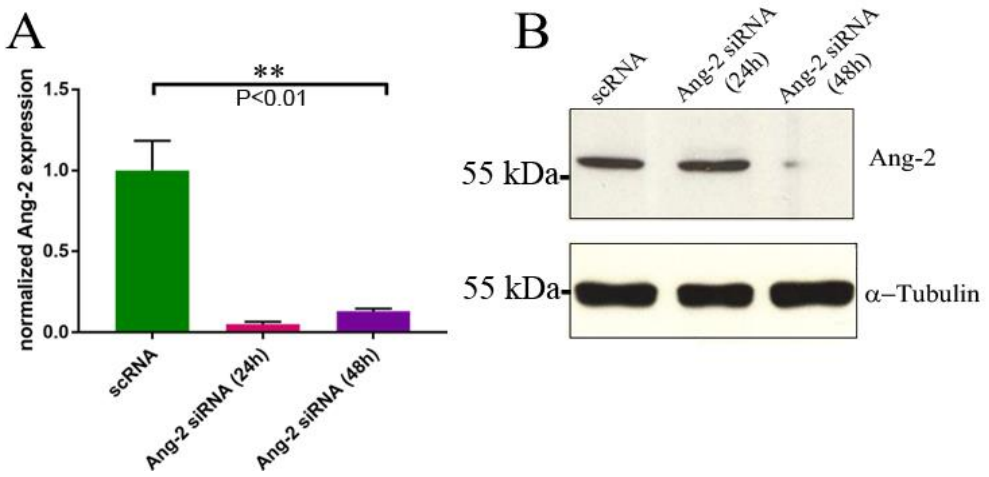

Figure 43: Validation of Ang-2 downregulation in GH3 cells. GH3 cells were transfected with scRNA or Ang-2 siRNA. 24 h and 48 h after transfection the cells were analyzed by Taqman and western blot. Cells transfected with scRNA harvested 48 h after transfection. (A) Total RNA was extracted and after reverse transcription, taqman, using specific primers and probes (Assay-on-Demand TM), was performed to assess the levels of *Ang-2* cDNA. *β2-microglobulin* served as endogenous control for normalization of RNA input. The *Ang-2* level in cells transfected with Ang-2 siRNA was normalized against Ang-2 expression level in scRNA-transfected cells, whose average was arbitrarily, set to 1. Data are analyzed independently with two biological and three technical replicates each and are expressed as the mean ± SEM. Statistical comparisons were performed using Mann Whitney test (**P<0.01). (B) The protein lysate was analyzed by western blot using specific anti-Ang-2 antibody (1:200). α-Tubulin (1:1000) was used as loading control.

At the mRNA level, *siAng-2*-transfected cells showed 95% reduction of *Ang-2* expression after 24 h, and 87% decrease after 48 h. In contrast, at the protein level, we observed downregulation of Ang-2 only after 48 h. Probably, Ang-2 is a stable protein and therefore, its reduction appeared first 48 h after transfection. So, we decided to perform our experiments at 48 h post-transfection.

3.4.7.1 Activation of Tie-2 signaling upon stimulation with rhANG-2 in the absence of endogenous Ang-2 is time- and concentration-dependent

We performed experiments similar to those mentioned in paragraph 3.4.5 to assess the effect of rhANG-2 on GH3 cells 48 h after downregulation of endogenous Ang-2 to confirm our previous findings regarding activation of Tie-2 by rhANG-2. Cells transfected with siRNA were grown to confluency. 24 h after transfection, the medium was changed and serum-free medium was added for an additional 24 h. Then, the cells were stimulated with rhANG-2 for

different time intervals. First, we checked the phosphorylation of Tie-2 at various time points after incubation with rhANG-2 (Figure 44).

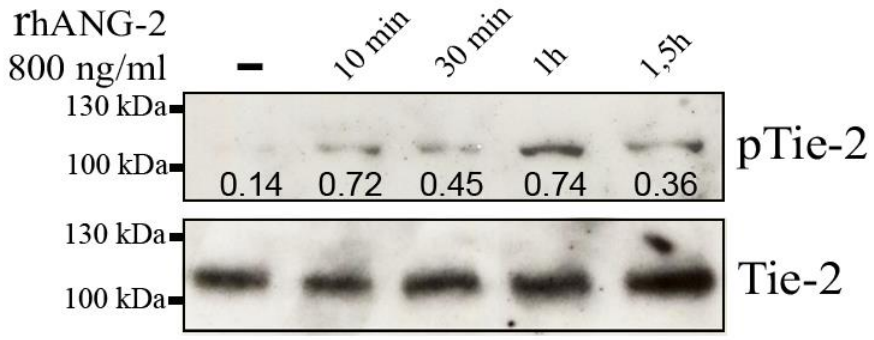

Figure 44: Tie-2 is activated in a time-dependent manner after stimulation with rhANG-2. GH3 cells were stimulated with 800 ng/ml rhANG-2 for 10 min, 30 min, 1 h and 1.5 h in serum starved condition. The control group was not treated but the cells were incubated with fresh serum-free Medium for 1.5 h prior to harvesting. The amounts of pTie-2 (Tyr 1102/1108) increases with the length of treatment. Figure 44 shows one experiment out of three independent experiments with similar results. The membrane was probed with anti-pTie-2 (1:2000) antibody and reprobed to detect total Tie-2 (1:500). The numbers represent the ratio of phospho-/total-proteins.

The pTie-2 amount increased within 10 min and after 1 h and dropped after 30 min and 1.5 h incubation with rhANG-2.

Then, we checked whether time dependent phosphorylation of Tie-2 correlates with the activation of downstream signaling molecules as already observed in previous experiments. As readout of the treatment, we chose an immediate interaction partner, Fak, and a downstream molecule, Erk 1/2 to optimize our studies regarding Tie-2 signaling in GH3 cells. Thus, GH3 cells transfected with *siAng-2* were stimulated with 800 ng/ml rhANG-2 for different time points. The amount of pFak and pErk1/2 was analyzed by western blot (Figure 45).

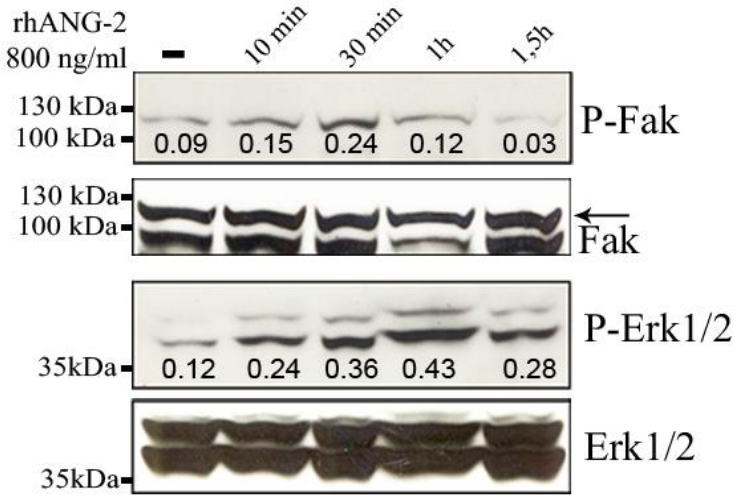

Figure 45: MAPK pathway is activated in a time dependent manner after stimulation with rhANG-2. GH3 cells were stimulated with 800 ng/ml rhANG-2 for 10 min, 30 min, 1 h and 1.5 h in serum starved condition. The control group was not treated but the cells were incubated with fresh serum-free Medium for 1.5 h prior to harvesting. The maximal activation of Fak appears 30 min after stimulation, whereas the amount of pErk1/2 (Thr202/Tyr204) increases with the length of treatment. Figure 45 shows one experiment out of three independent experiments with similar results. The membrane was probed with anti-pFak (1:500) and anti-pErk1/2 (1:1000) antibodies and reprobed to detect total Fak (1:1000) and Erk1/2 (1:500). The numbers represent the ratio of phospho-/total-proteins.

Our data suggest that in the absence of endogenous Ang-2, the incubation of GH3 cells with rhANG-2 can activate Tie-2 and subsequently Fak and the MAPK pathway in a time dependent manner. The amount of pFak increased between 10 and 30 min after treatment and then decreased again, but activation of Erk progressed with the incubation time and dropped after 1.5 h.

Additionally, we considered whether there is a correlation between the amounts of rhANG-2 and induced signaling response. Therefore, GH3 cells were transfected with siAng-2 and after 24 h, complete medium was replaced by serum-free medium. After an additional 24 h they were incubated with different amounts of rhANG-2 for 30 min. Then, the phosphorylation of Tie-2 was analyzed by western blot (Figure 46).

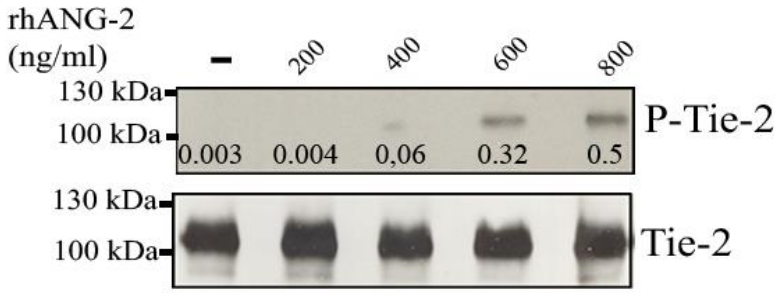

Figure 46: Tie-2 is activated in a concentration-dependent manner after stimulation with rhANG-2. GH3 cells were stimulated with different concentrations of rhANG-2 for 30 min in serum starved condition. The control group was not treated but the cells were incubated with fresh serum-free Medium for 30 min prior to harvesting. With the increasing concentration, the amount of pTie-2 (Tyr 1102/Tyr 1108) is elevated. Figure 466 shows one experiment out of two independent experiments with similar results. The membrane was probed with anti-pTie-2 (1:2000) antibody and reprobed to detect total Tie-2 (1:500). The numbers represent the ratio of phospho-/total-proteins.

We observed that Tie-2 is phosphorylated by rhANG-2 in a dose-dependent manner after 30 minutes.

Then, to investigate if the levels of phosphorylated Tie-2 correlate with the amounts of activated downstream molecules, the cells were transfected with Ang-2 siRNA and after 24 h complete culture medium was removed and serum-free medium was added to the cells. After additional 24 h cells were incubated with increasing concentrations of rhANG-2 for 30 minutes (Figure 47).

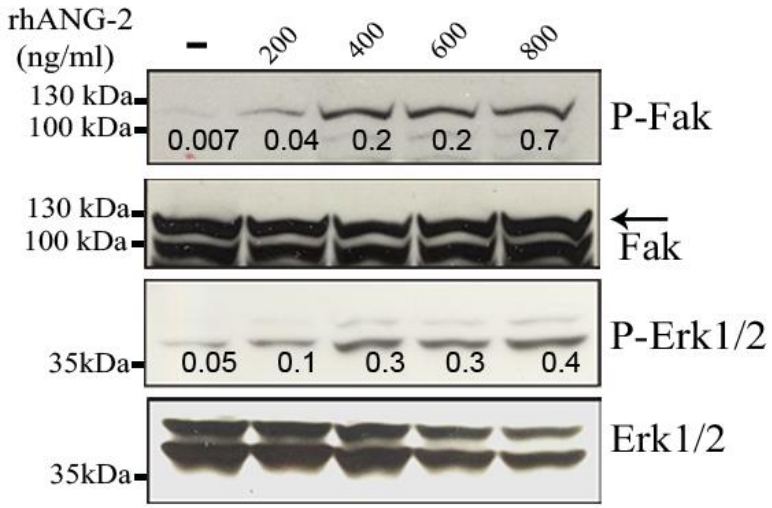

Figure 47: MAPK pathway is activated in a concentration dependent manner after stimulation with rhANG-2. GH3 cells were stimulated with different concentrations of rhANG-2 for 30 min in serum starved condition. The control group was not treated but the cells were incubated with fresh serum-free Medium for 30 min prior to harvesting. With increasing concentrations, the amount of pFak and pErk1/2 (Thr202/Tyr204) is elevated. Figure 47 shows one experiment out of at least three

independent experiments with similar results. The membrane was probed with anti-pFak (1:500) and anti-pErk1/2 (1:1000) antibody and reprobed to detect total Fak (1:1000) and Erk1/2 (1:500). The numbers represent the ratio of phospho-/total-proteins.

The western blots showed that in a given period of time (30 min), higher concentrations of rhANG-2 lead to increased phosphorylation of Tie-2, and consequently to a stronger activation of Fak and the MAPK pathway in GH3 cells.

3.4.8 The role of Ang-2 on cell viability and apoptosis

Stimulation of GH3 cells with rhANG-2 activates the MAPK pathway. Given that this pathway affects cell viability and apoptosis (Mebratu and Tesfaigzi 2009), we hypothesized that there may be a relationship between Ang-2 expression and these two processes. To challenge our hypothesis, we transfected GH3 cells with siRNA against Ang-2. As control, GH3 cells were transfected with scrambled RNA. 24 h after transfection the medium was changed and the cells were grown in serum-free conditions. 48 h later cell viability was measured using the WST-1 assay. The cell viability was significantly reduced (< 45%) in transfected cells (P<0.001) (Figure 48). This data indicated a pro-proliferative role of Ang-2 in GH3 cells.

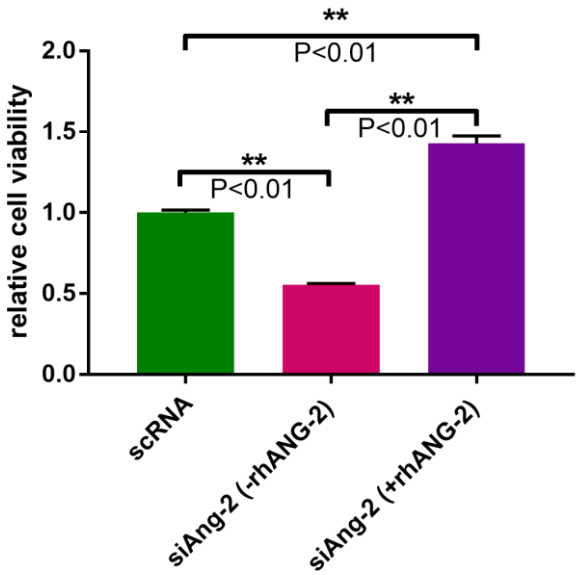

Figure 48: Downregulation of Ang-2 in GH3 cells decreases cell viability, which could be reversed by rhANG-2. GH3 cells were transfected with siAng-2 (siRNA against Ang-2) or scRNA. After 24 h the cells were incubated in serum-free medium and one group of transfected cells was treated additionally with 800 ng/ml rhANG-2. Cell viability was assessed 48 h after transfection. Cell viability of siAng-2-transfected cells was normalized against that of scRNA-transfected cells

arbitrarily, set to 1. The experiment is performed independently with six technical and three biological replicates. Results are expressed as mean ± SEM. Statistical comparisons were performed using Mann Whitney test (**P<0.01).

To see whether this effect is indeed due to Ang-2 knockdown, 24 h after transfection we additionally treated the siAng-2-transfected cells with 800 ng/ml rhANG-2 in serum-free medium. rhANG-2 could rescue this phenotype by significantly increasing the cell viability of siAng-2 transfected cells compared to control group (> 42%) (Figure 48).

Then, we wondered if the absence of Ang-2 could enhance apoptosis. To this aim, the activity of caspase 3/7 was measured in GH3 cells, which were transfected with siRNA against Ang-2 and compared with scRNA-transfected cells. 24 h after transfection the medium was changed and the cells were incubated in serum free medium. 24 h after serum deprivation the caspase 3/7 activity was measured using the Caspase-Glo® 3/7 Assay.

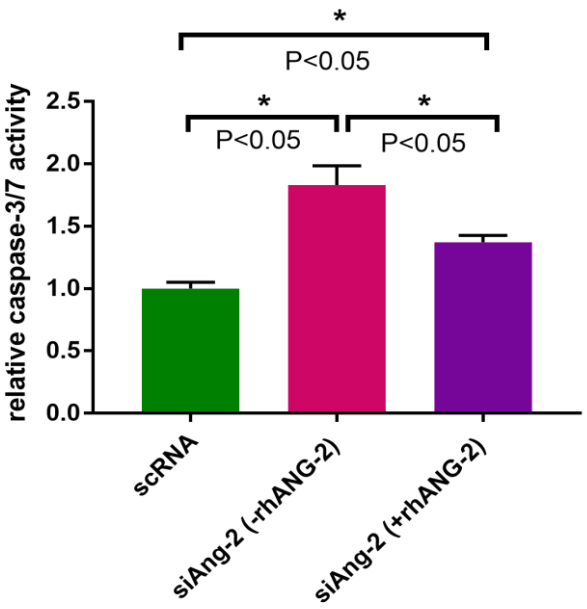

Figure 49: Downregulation of Ang-2 in GH3 cells induces apoptosis. GH3 cells were transfected with siAng-2 or scRNA. After 24 h, the cells were incubated in serum free medium and one group of transfected cells was treated additionally with 800 ng/ml rhANG-2. Apoptosis was measured 48 h after transfection. Activity of caspase-3/7 of siAng-2-transfected cells was normalized against the calculated value of scRNA-transfected cells and arbitrarily, set to 1. The experiment is performed independently with four technical and three biological replicates. Results are expressed as mean ± SEM. Statistical comparisons were performed using Mann Whitney test (*P<0.05).

Cells transfected with siAng-2 showed a significant increase in apoptosis compared to the cells transfected with scRNA (>83%). This data suggests that Ang-2 has an anti-apoptotic effect. This effect could be only partially rescued if the transfected cells were incubated with

800 ng/ml rhANG-2 as apoptosis remained higher than in scRNA-transfected cells (>37%) (Figure 49).

The results obtained from cell viability and apoptosis assays correlate with the activation of downstream signaling pathways after stimulation of GH3 cells with rhANG-2 and suggest an anti-apoptotic and pro-proliferative function of Ang-2 in these cells.

3.4.9 Treatment of GH3 cells with TKI

Next, we tried to down regulate Tie-2 receptor to investigate the specificity of activation of Tie-2 signaling by rhANG-2, but we were not able to downregulate the receptor using siRNA. Therefore, we used a small molecule to inhibit Tie-2 kinase activity (TKI). First, we treated GH3 cells with 10, 20 and 30 µM TKI for 2 h and 4 h and analyzed its effect on downstream signaling molecules by western blot (Figure 50).

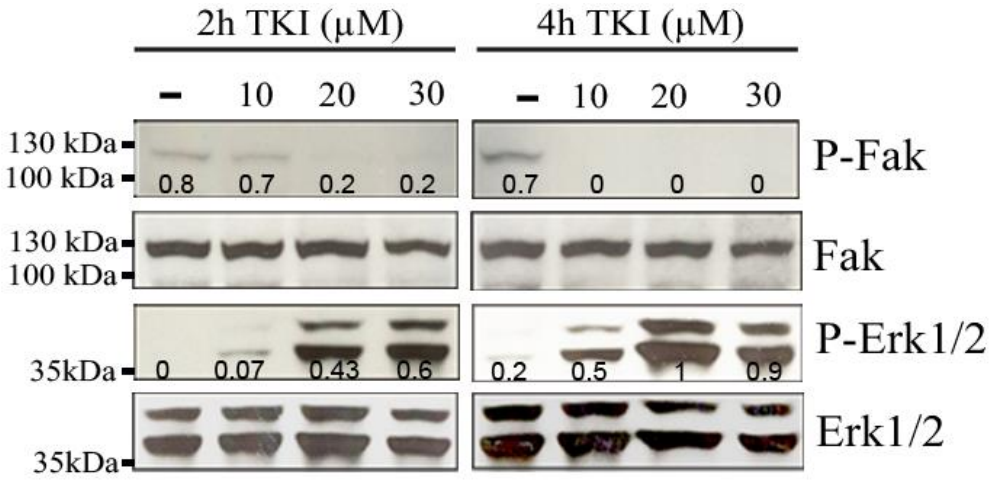

Figure 50: Effect of TKI on the phosphorylation of downstream signaling molecules activated by endogenous Ang-2 in GH3 cells. Cells were incubated for 2 h and 4 h in serum-free medium with different concentrations of TKI. Western blot was performed to evaluate the ability of TKI to inhibit the effect of cell driven Ang-2 on Fak and Erk1/2 activation. Figure 50 shows one experiment out of three independent experiments with similar results. The membrane was probed with pFak (1:500) and pErk 1/2 (1:1000) and reprobed with Fak (1:1000) and Erk1/2 (1:500). The numbers represent the ratio of phospho-/total-proteins.

2 h after incubation of the cells with TKI, pFak was reduced using both 20 and 30 µM concentrations and it almost disappeared after 4 h of incubation with all 3 concentrations. In contrast, Erk1/2 was activated upon treatment with TKI. Given that Erk1/2 is downstream of Fak, we hypothesized that its activation could be due to negative feedback loops.

For long-term treatment it was important to determine which TKI concentration could be tolerated by cells. To monitor the toxicity of TKI, GH3 cells were treated with 5, 10, 20 and 30 µM TKI for 24 h. The Incubation with 20 and 30 µM TKI for 24 h could not be tolerated by the cells since they detached from the plates. Therefore, we used the concentration of 5-10 µM for long-term treatments (Figure 51).

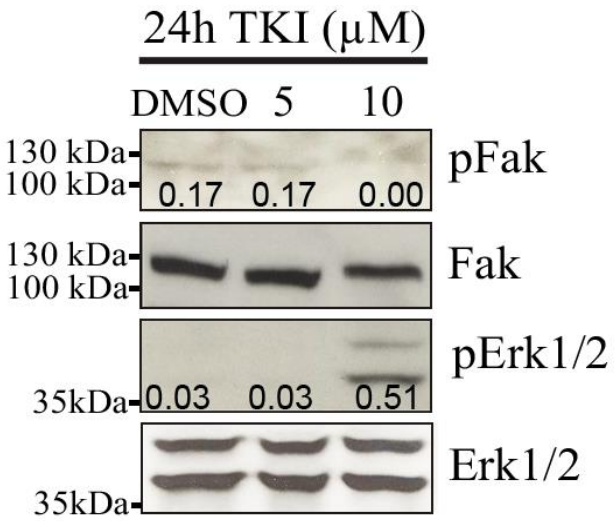

Figure 51: Effect of TKI on the phosphorylation of downstream signaling molecules and evaluation of its toxicity on GH3 cells. Cells were incubated for 24 h in serum-free medium with different concentrations of TKI. Western blot was performed to evaluate the ability of TKI to inhibit the effect of cell driven Ang-2 on Fak and Erk1/2 activation. Higher concentrations of TKI (20 and 30 µM) led to cell death. Figure 51 shows one experiment out of three independent experiments with similar results. The membrane was probed with pFak (1:500) and pErk 1/2 (1:1000) and reprobed with Fak (1:1000) and Erk1/2 (1:500). The numbers represent the ratio of phospho-/total-proteins.

Almost no signal was detected for pFak in the cells treated with 10 µM TKI. Activation of Erk1/2 was only observed upon treatment with 10µM TKI for 24 h.

Then, we wondered if TKI could block the effect of rhANG-2 in GH3 cells. Therefore, cells were treated for 3.5 h with increasing concentration of TKI (0-30µM) and then stimulated with 300ng/ml rhANG-2 or left untreated (control) (Figure 52).

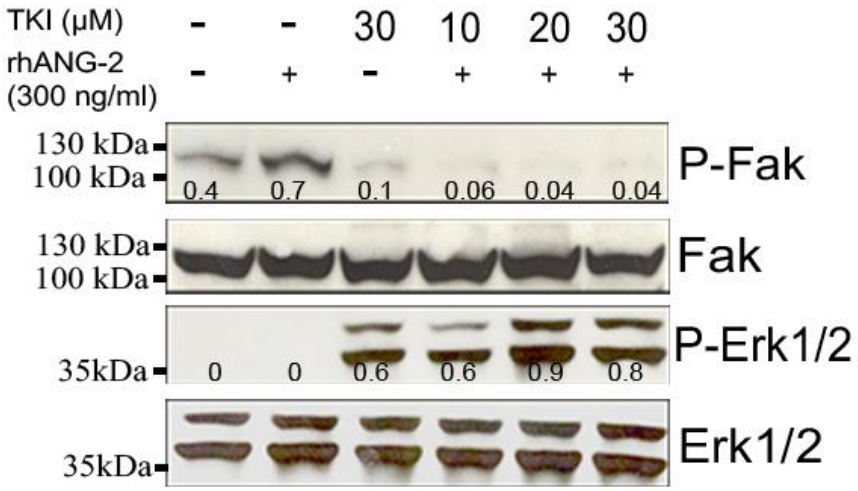

Figure 52: rhANG-2 could not activate Tie-2 signaling if kinase activity was blocked by TKI in GH3 cells. Cells were incubated for 3.5h in serum-free medium with different concentrations of TKI, and then stimulated with 300 ng/ml rhANG-2. Western blot was performed to evaluate the ability of rhANG-2 in activation of Tie-2 signaling if Tie-2 receptor was inhibited by TKI (10-30 µM). Figure 52 shows one experiment out of three independent experiments with similar results. The membrane was probed with pFak (1:500) and pErk 1/2 (1:1000) and reprobed with Fak (1:1000) and Erk1/2 (1:500). The numbers represent the ratio of phospho-/total-proteins.

The cells stimulated only with rhANG-2 showed elevated levels of pFak as expected. However, when rhANG-2 was present together with TKI, we observed reduction of pFak. Thus, pre-treatment with TKI suppressed the stimulatory effect of rhANG-2. In contrast, Erk1/2 activation following TKI treatment was independent from rhANG-2.

Altogether, these experiments demonstrate that the stimulation of Tie-2 with rhANG-2 has an impact on Fak activation and blocking of Tie-2 using TKI reduces the amount of pFak.

3.4.10 rhANG-2 phosphorylated Tie-2 receptor in Ang-2-silenced GH3 cells

Next, we generated Ang-2 silenced GH3 cells using shRNA to obtain an efficient downregulation of the gene. The efficiency of transduction was determined by Taqman and ELISA (Figure 53). We used three independent sh molecules cloned into a lentiviral vector named K1-K3 as listed in materials and methods, respectively.

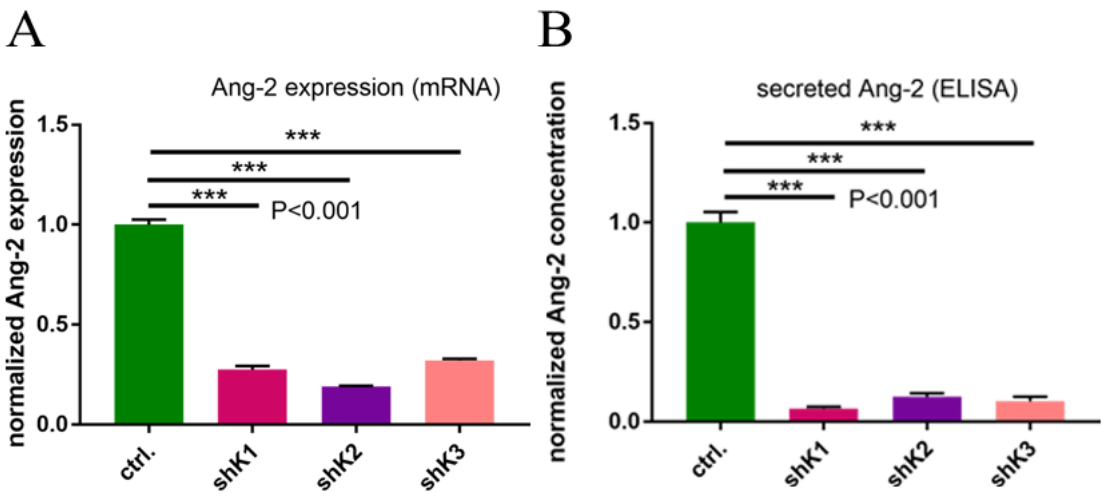

Figure 53: Validation of Ang-2 downregulation in GH3 cells by shRNA. GH3 cells were transduced with shRNAs against Ang-2 (K1-K3) or non-target shRNA (ctrl.). Two weeks after selection by puromycin, the cells were analyzed by Taqman and the amounts of released Ang-2 in supernatant was determined by ELISA (A) Total RNA was extracted and after reverse transcription, taqman, using specific primers and probes (Assay-on-Demand TM), was performed to assess the levels of *Ang-2* cDNA. *β2-microglobulin* served as endogenous control for normalization of RNA input. The *Ang-2* level in cells transduced with shAng-2 was normalized against Ang-2 expression level in mock-transduced cells, whose average was arbitrarily, set to 1. (B) The supernatant of each transduction condition (K1-K3 and ctrl.) was analyzed by an ELISA-Kit for Ang-2 detection. Data (A and B) are analyzed independently with two biological and three technical replicates each and are expressed as the mean ± SEM (***P<0.001). Statistical comparisons were performed using Mann Whitney test.

For the further experiments, we used GH3 cells transduced with shAng-2 construct 2 (shK2). The cells were grown on cover slips and after 24 h serum starvation were stimulated with 800 ng/ml rhANG-2 for 15 min (Figure 54).

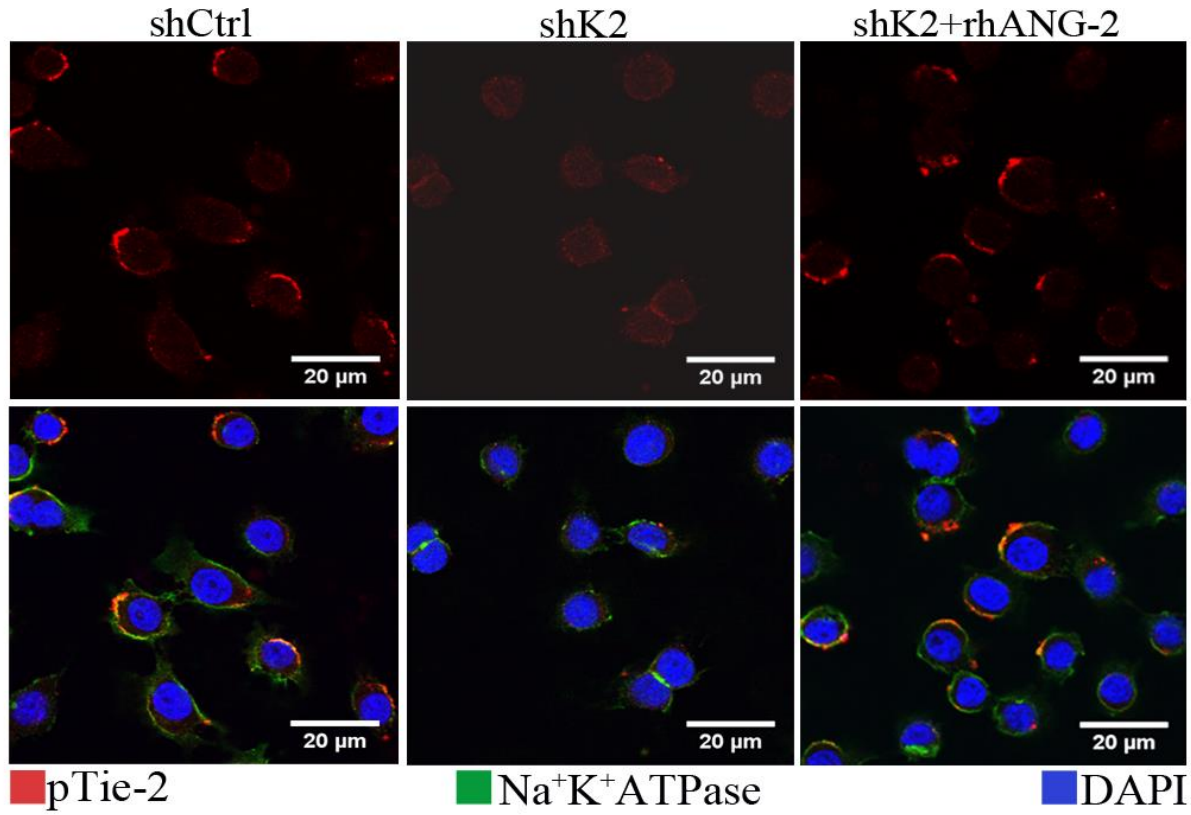

Figure 54: Activation of Tie-2 receptor by adding rhANG-2 in shK2 cells. Tie-2 receptor is activated after stimulation of Ang-2 silenced GH3 cells (shK2) by adding 800 ng/ml rhANG-2. IF was performed with anti-pTie-2 (1:400) and anti-Na^+K^+ ATPase (1:300) antibodies. Na^+K^+ ATPase served as membrane marker. Cell nuclei were counterstained with DAPI. For all cells/conditions the IF intensity of 30 cells was quantified using ImageJ, using the same threshold and are expressed as arbitrary units ±SEM. pTie-2 immunostaining intensity in shCrtl-transduced GH3 cells and in shK2 cells was as follow: 266.71±12.12 and 176.04±8.46, respectively (shCtrl vs. shK2; ***P<0.001, Mann Whitney test) pTie-2 immunostaining intensity in shK2 cells following incubation with rhANG-2 was 218.68±18.16 (shK2 vs. shK2+rhANG-2; ***P<0.001, Mann Whitney test). Original magnification: 400x; scale bar: 20 µm.

Interestingly, shK2 cells showed significantly reduced amount of pTie-2 when compared with cells transduced with unspecific shRNA control (shCtrl). However, Tie-2 phosphorylation in shK2 cells could be induced by rhANG-2 suggesting that they possess a functional receptor.

3.4.11 rhANG-1 activates Tie-2 receptor

Although GH3 cells do not express detectable levels of Ang-1 we also stimulated them with rhANG-1. GH3 cells were cultured for 24 h in serum-free medium containing AMG386 to block interference from endogenously-produced Ang-2. Cells were then washed and stimulated with 800 ng/ml rhANG-1 for 15 min (Figure 55).

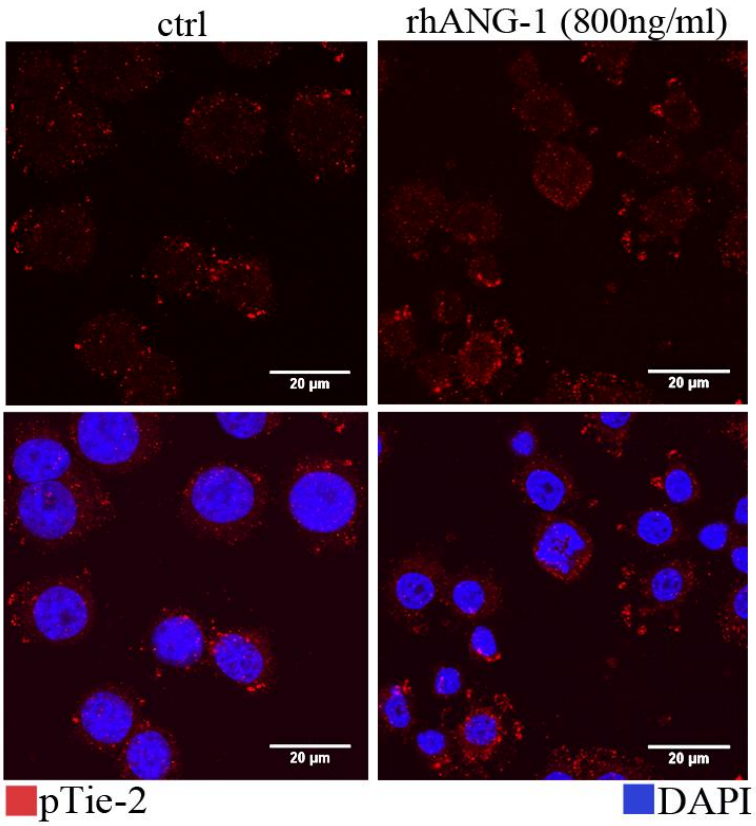

Figure 55: rhANG-1 activates Tie-2 on GH3 cells. GH3 cells were grown in serum-free medium for 24 h and then stimulated with 800 ng/ml rhANG-1 for 15 min to detect Tie-2 Phosphorylation. IF was performed for pTie-2 (Tyr 1102/1108). Nuclei were counterstained with DAPI. Pictures shown were taken with the same exposure time and are representative of three independent experiments. For all cells/conditions the IF intensity of 30 cells was quantified using ImageJ using the same threshold and are expressed as arbitrary units ± SEM. Parental GH3 cells: 217.34±7.65; GH3+rhANG-1 800 ng/ml: 239.49±7.38 (*P<0.05, Mann Whitney test). Original magnification: 400x; scale bar: 20 µm.

We observed an increase in Tie-2 phosphorylation thereby showing that Tie-2 on adenoma cells can respond to its canonical ligand.

3.4.12 Characterization of rat pituitary adenoma primary cells

3.4.12.1 MENX rats primary cells

Our IHC and IF stainings of MENX rat PAs revealed that the tumors express Ang-2 and Tie-2. Surprisingly, the receptor was activated by Ang-2 in these tissues and we could detect pTie-2 in tumor areas. Using MENX rat pituitaries, we were able to establish tumor primary cell cultures. To perform further experiments we characterized the rat primary cells for their

ability to retain the expression of Ang-2 and Tie-2 in cell culture. The cells were grown on cover slips and after 48 h the expression of these two proteins was assessed by IF (Figure 56).

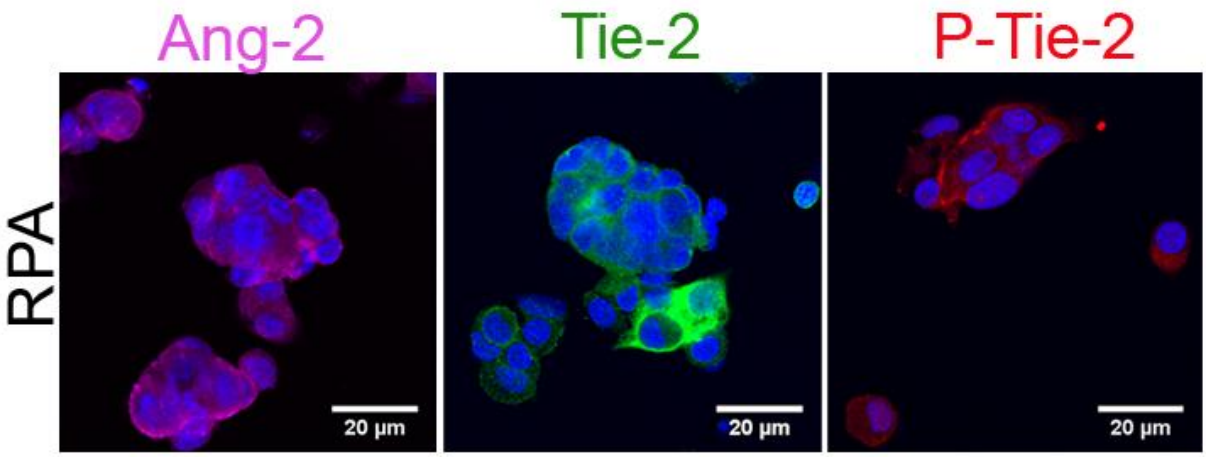

Figure 56: Immunofluorescence detection of Ang-2, Tie-2 and pTie-2 in MENX rat pituitary adenoma (RPA) primary cell culture. Expression of Ang-2 (1:400), Tie-2 (1:200) and pTie-2 (1:2000) was evaluated in RPA cells. Ang-2 is detected in cytoplasm whereas Tie-2 and pTie-2 are detected in cytoplasm and cell membrane. Cell nuclei were counterstained with DAPI. Original magnification: 400x; scale bar: 20 µm.

The primary cells were found to express Ang-2, Tie-2 and the receptor was also phosphorylated. Then, we wondered whether Ang-2 is also secreted by the rat primary tumor cells (RPA) into the culture medium. Therefore, the supernatant was analyzed by western blot (Figure 57) and ELISA (Table 22).

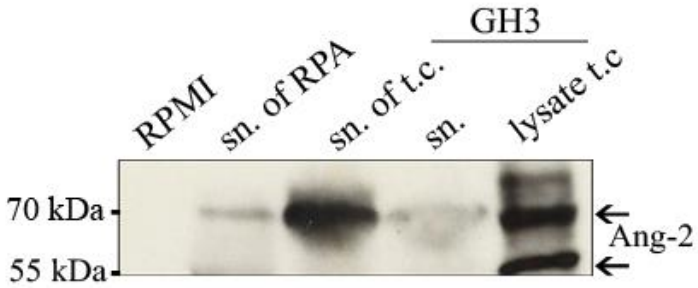

Figure 57: RPA cells release Ang-2 into the culture medium. The western blot shows RPMI culture medium as negative control. Ang-2 is detected in supernatant (sn.) of RPA cells (70kDa). As positive control, the following samples were loaded: supernatant of transfected GH3 cells named K9OE (sn. Of t.c.), supernatant of untransfected GH3 cells (sn.) and cell lysate of K9OE cells. In transfected GH3 cell lysate both glycosylated (70kDa) and non-glycosylated (56kDa) forms could be detected by western blot. In the supernatant (sn.) of RPA and GH3 cells, only the glycosylated form of Ang-2 was observed. Specific anti-Ang-2 (1:200) antibody was used to detect Ang-2 in RPA and GH3 cells.

Table 22: Ang-2 level in the concentrated supernatant of RPA cells (three biological and 2 technical replicates) measured by ELISA.

	RPA
Cell number	9×10^5
ng/ml±SD	49.64±1.85

We were able to detect Ang-2 in the supernatant of RPA primary cultures by western blot and ELISA.

3.4.12.2 Separation of rat pituitary ECs from adenoma cells

Rat primary cells retained their ability to express Ang-2 and to secrete it into the cell culture medium. We wondered whether EC or pituitary adenoma cells were the main source of the Ang-2 secreted from these cultures. Therefore, after the pituitary cells were disassociated, the ECs were separated from the rest of the cells by taking advantage of the expression of the CD31 antigen on their surface as described in material and methods.

After 72 h, CD31+ cells exhibited the specific EC morphology, whereas the CD31 negative cells showed a spherical form typical of pituitary adenoma cells (Figure 58).

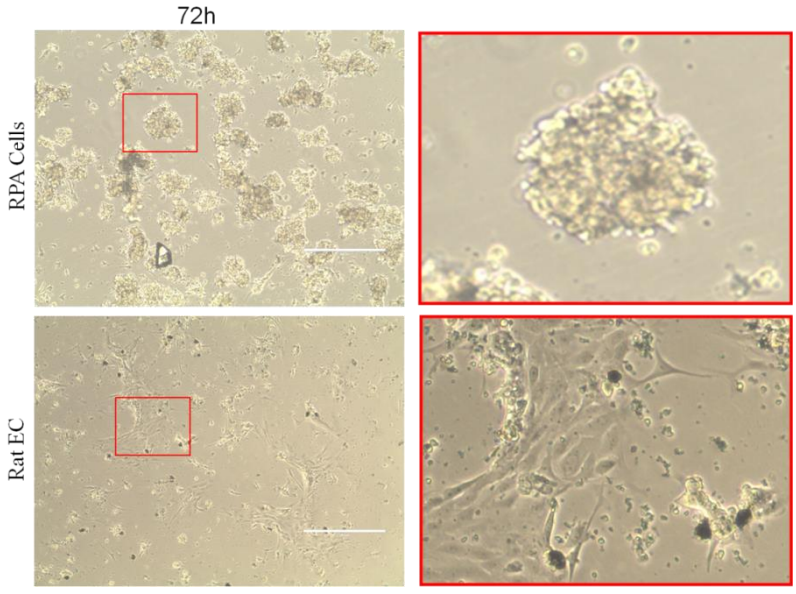

Figure 58: Separation of EC from RPA cells. EC were separated from RPA cells using biotin conjugated CD31 antibody and streptavidin coated magnetic beads. After 72 h EC shows the known morphology of these cells. Original magnification of left panels: 200x; scale bar: 400 µm.

After 72 h the supernatant of both cell populations was collected, concentrated and the levels of secreted Ang-2 were measured by ELISA (Table 23).

Table 23: Ang-2 level in the concentrated supernatant of EC and RPA cells measured by ELISA (two biological and two technical replicates).

	EC	RPA
Cell number	$1{,}5\times10^6$	$1{,}5\times10^6$
ng/ml±SD	11.65±0.32	23.45±0.71

The ELISA measurement revealed that pituitary adenoma cells expressed and released in average more Ang-2 compared to EC (an equal number of cells were cultured in each well). Then, we wondered whether Ang-2 binds to Tie-2 in these cells and whether this interaction could eventually be detected by co-immunoprecipitation. In both rat ECs and RPA cells Ang-2 was co-immunoprecipitated with pTie-2 (Figure 59).

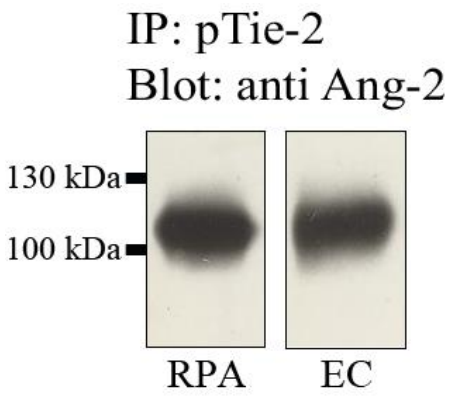

Figure 59: Endogenous Ang-2 is co-immunoprecipitated with pTie-2 in RPA and rat EC cells. 72 h after separation of rat ECs from RPA cells, both cell populations were lysed and protein lysate was immunoprecipitated with an antibody against pTie-2 (Tyr 1102/1108). The resulting IP was analyzed by western blot and probed for Ang-2 (1:200).

Immunoprecipitation using separated EC and RPA could perform once because the cell number obtained from other RPAs was not enough to repeat the experiment. A negative control could also not be included because of the same reason.

Then, we investigated the effect of ECs supernatant on RPA cells and vice versa, since they contained Ang-2. RPA cells were incubated for 48 h in serum free medium containing 10 µl of concentrated rat EC supernatant (Ang-2= 0.166 ng/ml, final concentration in medium). The same condition was applied for rat ECs (Ang-2= 0.335 ng/ml, final concentration in medium).

In both cell populations the cell viability was elevated after incubation with the conditioned medium (c.m.) from the other population (Figure 60).

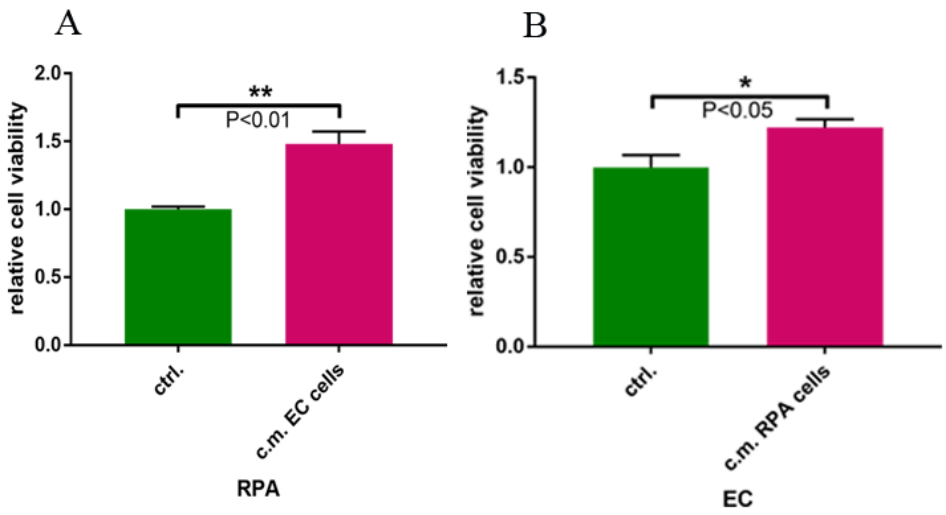

Figure 60: Incubation with conditioned medium increases cell viability in RPA cells and ECs. Both RPA (A) cells and ECs (B) were incubated for 48 h in serum free medium containing 10µl c.m. . Then the cell viability was measured and normalized against the values of control cells treated with concentrated serum free culture medium arbitrarily, set to 1. The experiment was performed independently with six technical and two biological replicates. Results are expressed as mean ± SEM (*P<0.05;**P<0.01). Statistical comparisons were performed using Mann Whitney test.

The supernatant of pituitary adenoma cells was then used to treat GH3 cells silenced for the expression of endogenous Ang-2. In parallel, we treated these transfected cells also with rhANG-2 as positive control and investigated the role of c.m. and rhANG-2 on cell viability and apoptosis. GH3 cells transfected with scRNA served as control (Figure 61).

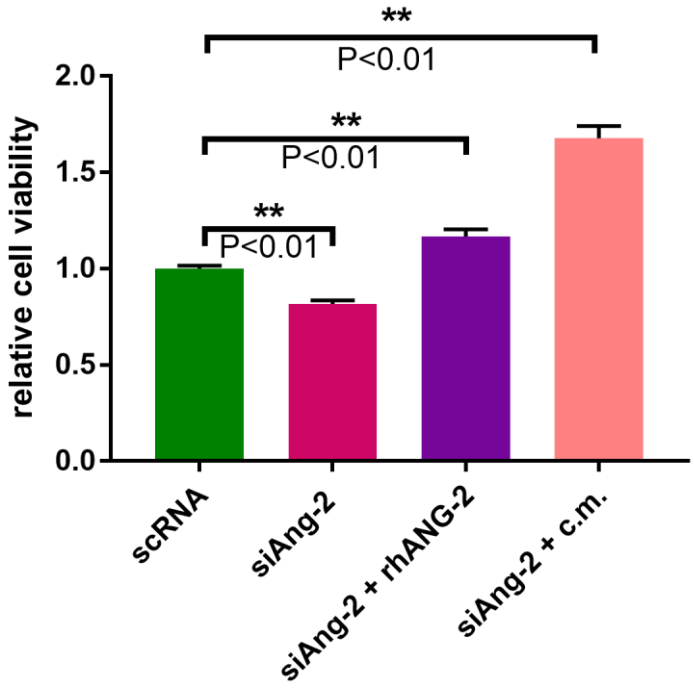

Figure 61: Conditioned medium increases cell viability in GH3 cells. GH3 cells were transfected with siAng-2 or scRNA. After 24 h, cells were switched to serum free medium or supplemented with 800 ng/ml rhANG-2 (siAng-2+rhANG-2) or a medium containing 10µl concentrated RPA c.m (siAng-2+c.m). Cell viability was assessed 48 h after transfection. Cell viability was measured and normalized against the values of cells, transfected with scRNA, arbitrarily, set to 1. The experiment was performed independently with six technical and three biological replicates. Results are expressed as mean ± SEM (**P<0.01). Statistical comparisons were performed using Mann Whitney test.

As previously shown, Ang-2 knockdown decreased the viability of GH3 cells (Figure 48). The incubation of rhANG-2 rescued this phenotype by increasing cell viability. Interestingly, incubation of siAng-2 transfected cells with RPA c.m. promoted cell viability to an even greater extent than rhANG-2.

We could also show that the increased apoptosis of *Ang-2*-downregulated GH3 cells could be rescued if the cells were incubated with 800 ng/ml rhANG-2. Moreover, we could demonstrate a similar effect if cells were grown in a medium containing 10 µl concentrated RPA c.m (Figure 62).

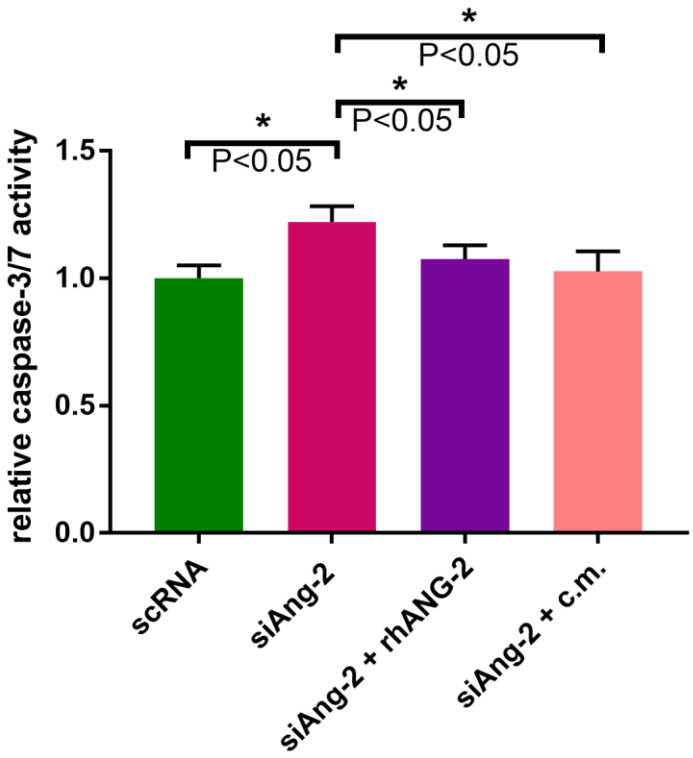

Figure 62: Conditioned medium decreases apoptosis in GH3 cells. GH3 cells were transfected with siAng-2 or scRNA. After 24 h, the cells were incubated in serum free medium with 800 ng/ml rhANG-2 or a medium containing 10µl concentrated RPA c.m. Activity of caspase-3/7 was assessed 48 h after transfection and normalized against the values of the cells transfected with scRNA, arbitrarily, set to 1. The experiment was performed independently with six technical and three biological replicates. Results are expressed as mean ± SEM (*P<0.05). Statistical comparisons were performed using Mann Whitney test.

Conditioned medium contains various growth factors secreted from rat PA cells but only Angiopoietins are known to be able to activate Tie-2 receptor (Figure 63). Therefore, Ang-2-silenced cells, shK2, were grown in serum free medium for 24 h. Then, they were stimulated in serum-free medium with 10 µl of concentrated RPA c.m for 15 min at 37°C. Afterwards, the receptor activation was analyzed by IF. Incubation of shK2 cells with primary PA cell-derived c.m led stimulated Tie-2 phosphorylation, suggesting that the receptor may be activated by Ang-2, which was secreted by RPA cells in the culture supernatant (Figure 63).

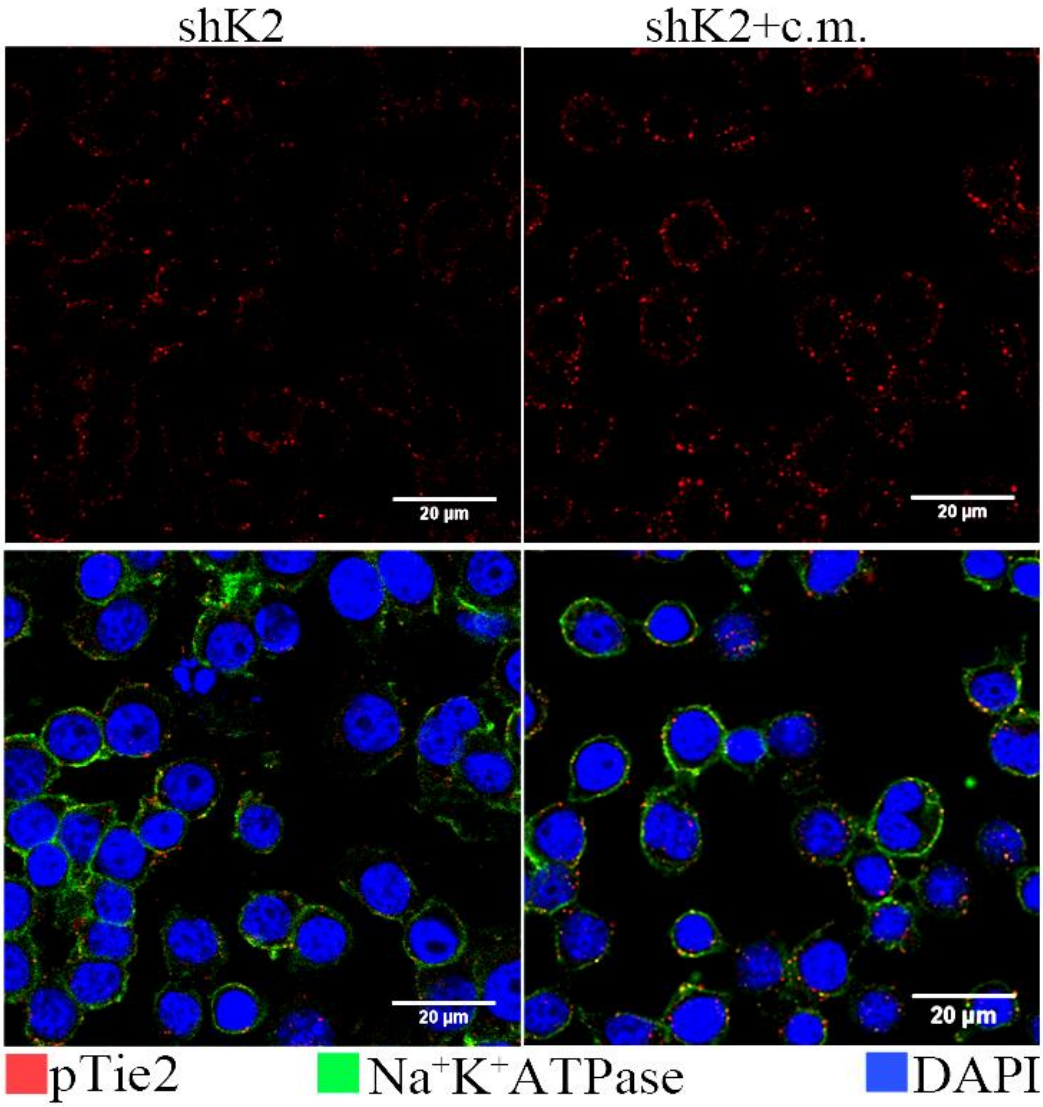

Figure 63: Activation of Tie-2 receptor by adding rat PA c.m. in shK2 cells. Tie-2 receptor is activated after stimulation of Ang-2 silenced GH3 cells by adding c.m. IF was performed with anti-pTie-2 (1:400) and anti-Na^+K^+ ATPase (1:300) antibodies. Na^+K^+ ATPase served as membrane marker. Cell nuclei were counterstained with DAPI. For all cells/conditions the IF intensity of 30 cells was quantified using ImageJ, using the same threshold and are expressed as arbitrary units ± SEM. pTie-2 immunostaining intensity in shK2 GH3 cells and in shK2+c.m was as follow: 143.62±5.98 and 217.48±11.35, respectively (shK2 vs. shK2+c.m.;***P<0.001, Mann Whitney test). Original magnification: 400x; scale bar: 20 µm.

The cells incubated with c.m. showed an increased level of phosphorylated Tie-2 compared to the cells, which were incubated with concentrated serum-free Medium. This observation confirmed the bioactivity of released rat Ang-2 in culture medium.

3.4.13 *in vitro* evaluation of anti-angiogenic drugs

3.4.13.1 AMG386 (Trebananib) and TKI

ANG-2 is a secretory growth factor and we could detect this protein in the supernatant of GH3 and MENX rat primary cell cultures by western blot or ELISA. Moreover, the stimulation of Ang-2 silenced GH3 cells with rhANG-2 enhanced cell viability and reduced apoptosis.

To investigate the potential para- or autocrine function of secreted endogenous Ang-2, we performed additional experiments using a neutralizing peptibody, AMG386, against Ang-1 and -2, which binds these ligands and thus inhibits their binding to Tie-2. Drugs targeting the Ang-Tie2 axis in advanced solid tumors have been reported to be well tolerated and have shown promising antitumor activity (Mita *et al.* 2010). We tested AMG386 and TKI on GH3, RPA and human NFPA primary cells to investigate the effect Ang-2-Tie-2 inhibition in these cells.

GH3 and AMG386

GH3 cells were cultured in serum-free condition with 5 µg/ml AMG386. Cell viability was assessed 48 h later using the WST-1 assay. Vehicle-treated cells in serum-free condition were used as control. We observed reduced cell viability (-37%) in AMG386 treated cells (Figure 64).

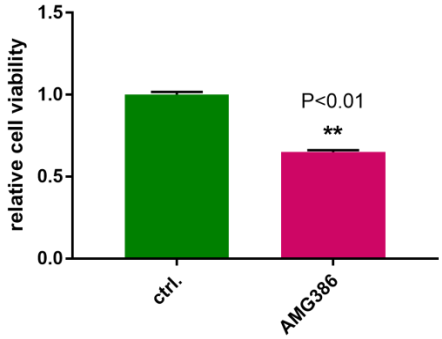

Figure 64: AMG386 reduces cell viability in GH3 cells. GH3 cells were treated with 5 µg/ml AMG386 in serum free condition. Cell viability was assessed 48 h after treatment. Cell viability of treated cells was normalized against the cell viability of untreated control cells (ctrl.) arbitrarily, set to 1. The experiment is performed independently with six technical and three biological replicates. Results are expressed as mean ± SEM (**P<0.01). Statistical comparisons were performed using Mann Whitney test.

GH3 cells were also treated with TKI. They were cultured in serum-free condition with 5 µM TKI. Cell viability was assessed 48 h later using the WST-1 assay. Vehicle-treated cells in serum-free condition were used as control. We observed reduced cell viability (-33%) in TKI treated cells (Figure 65).

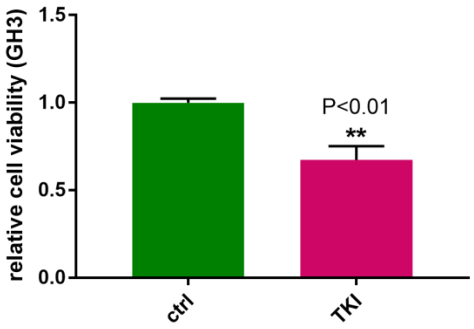

Figure 65: TKI reduces cell viability in GH3 cells. GH3 cells were treated with 5 µM TKI in serum-free conditions or left untreated (ctrl). Cell viability was assessed 48 h after treatment. Cell viability of treated cells was normalized against the cell viability of untreated control cells arbitrarily, set to 1. The experiment is performed independently with six technical and three biological replicates. Results are expressed as mean ± SEM (**P<0.01). Statistical comparisons were performed using Mann Whitney test.

This finding supported our hypothesis that the binding of Ang-2 to Tie-2 is required for cell viability and that inhibition of this binding using AMG386 or TKI neutralizes the pro-proliferative effect of secreted Ang-2 as a growth factor in GH3 cells.

Treatment of rat pituitary adenoma primary cells with AMG or TKI

Primary cultures were established from the PA of 7 MENX rats. 24 h later, they were treated with AMG386 (5 µg/ml) and the cell viability was determined 48 h after treatment. Two of these cultures showed no response to the treatment with AMG386 but the cell viability of the remaining 5 samples was significantly reduced compaired to untreated cells of the same animals (Figure 66).

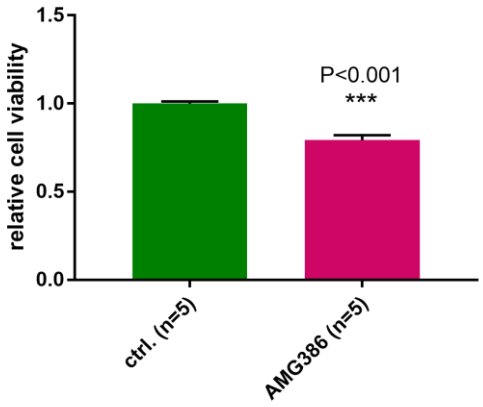

Figure 66: AMG386 reduces cell viability in RPA cells. RPA cells were treated with 5 µg/ml AMG386 in serum-free condition. Cell viability was assessed 48 h after treatment. Cell viability of treated cells was normalized against the cell viability of untreated control cells arbitrarily, set to 1. The experiment was performed independently with six technical and five biological replicates. Results are expressed as mean ± SEM (***P<0.001). Statistical comparisons were performed using Mann Whitney test.

Additionally, different concentrations of AMG386 were examined to determine the most effective dose, which was able to efficiently reduce downstream signaling activities in RPA (Figure 67 represents two of these cultures, rat 1 and rat 2). 6 out of 8 treated cell cultures exhibit a reduction of activated signaling molecules downstream of Tie-2, but this reduction occurred at various time points after treatment (24 h, 48 h and 72 h were tested).

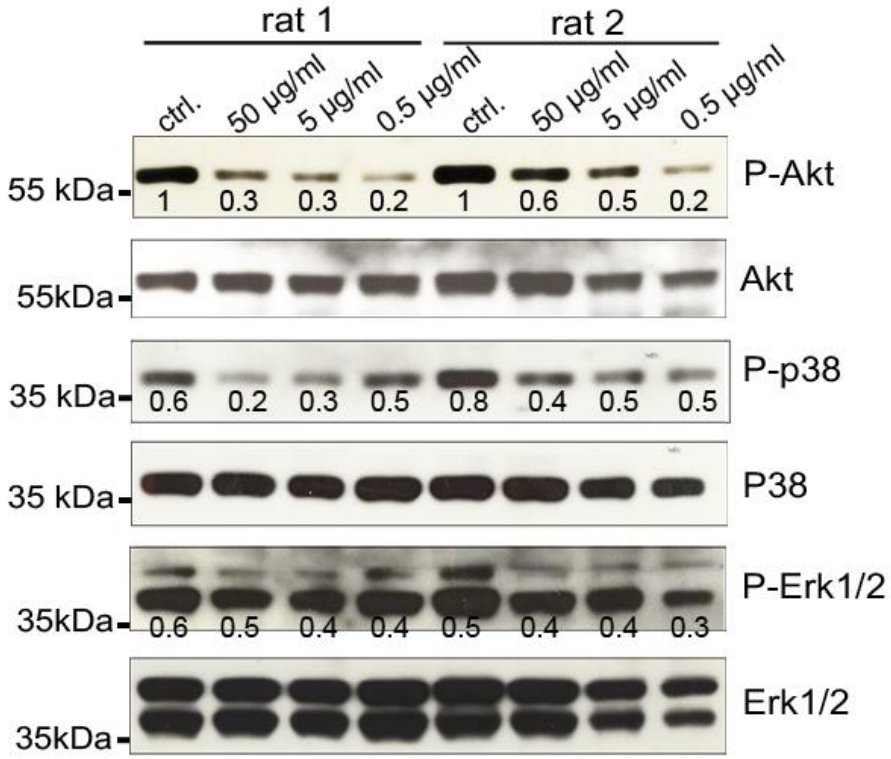

Figure 67: RPA cell treatment with AMG386. RPA cells were treated with 50, 5 and 0.5 µg/ml AMG386 for 48 h. The effect of Ang-2 neutralization on downstream signaling pathways was assessed using antibodies against activated and total Akt, P38 and Erk1/2. Figure 67 shows two experiments out of at least six independent experiments with similar results. Same membrane was used to detect pAkt (1:500), Akt (1:1000), pP38 (1:1000), P38 (1:1000), pErk1/2 (1:1000) and Erk1/2 (1:500) with specific antibodies. The numbers represent the ratio of phospho-/total-proteins.

Previous studies indicated that stimulation of HUVECs with rhANG-1 and rhANG-2 was able to activate TIE-2 signaling and downstream pathways like PI3K and MAPK having an impact on survival and proliferation (Kim *et al.* 2000c, Nguyen *et al.* 2007, Harfouche and Hussain 2006a). Therefore, after treatment of RPA primary cells with AMG386, we assessed the effect of ligand/receptor binding inhibition on PI3K and MAPK pathway. We studied Akt, P38 and Erk1/2 (Figure 67). The activated forms of all three signaling molecules were reduced after 48 h incubation of RPA cells with AMG386 if compared with not treated control group. Since these pathways are involved in survival and proliferation, this result could also explain the reduction of cell viability after AMG386 treatment in RPA cells. Reduction of pAkt correlated with AMG386 concentration. So, we used this molecule as treatment readout for further experiments.

Then, we studied the effect of Tie-2 kinase inhibition on downstream signaling pathways and on cell viability. Primary cell cultures (n=4) were established as above and 24 h later treated with TKI (5000 nM) for 48 h. Cells were then used either for protein extraction or measurement of cell viability.

After Tie-2 kinase inhibition we found that the viability of all RPA primary cells was reduced after treatment with TKI (Figure 68).

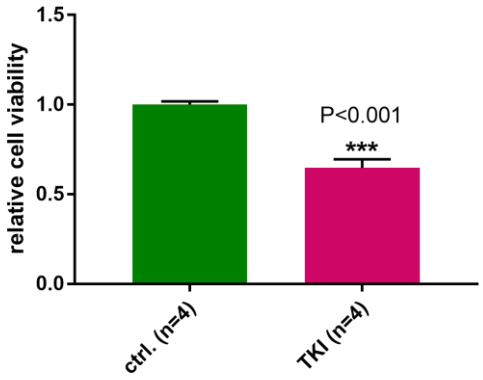

Figure 68: TKI reduces cell viability in RPA cells. RPA cells were treated with 5000 nM TKI in serum free condition. Cell viability was assessed 48 h after treatment. Cell viability of treated cells was normalized against the cell viability of untreated control cells arbitrarily, set to 1. The experiment was performed independently with six technical and four biological replicates. Results are expressed as mean ± SEM (***P<0.001). Statistical comparisons were performed using Mann Whitney test.

48 h after incubation of RPA cells with TKI, we observed reduction of activated Akt (Figure 69).

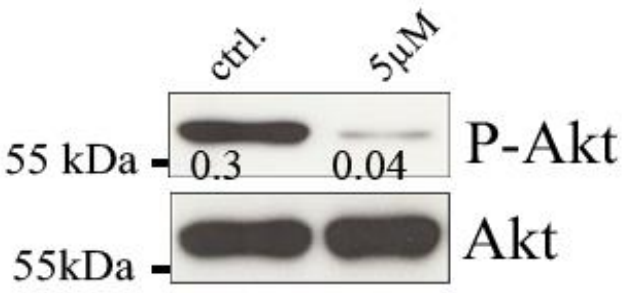

Figure 69: RPA cell treatment with TKI. RPA cells were treated with 5000nM TKI for 48 h. The effect of kinase inhibitor on downstream signaling pathways was assessed using antibodies against activated Akt (1:500) and total Akt (1:1000). Figure 69 shows one experiment out of at least three independent experiments with similar results. The numbers represent the ratio of phospho-/total-proteins.

Our observations indicate that blocking Ang-2/Tie-2 signaling at either the ligand or the receptor level could have an impact on cell viability of PA cells.

Treatment of human NFPA primary cells with AMG386

Human NFPA primary cells were obtained from 16 PA patients operated at the Tübingen neurosurgical clinic. 48 h after being in culture, cells were treated individually with AMG386 (5 µg/ml). The cell viability was determined 48 h after treatment (Figure 70). For 11 samples we observed a >20% reduction in cell viability after treatment when compared to untreated control cell group. For all drug treatments a >20% reduction in cell proliferation *versus* vehicle-treated controls was considered indicative of response to the drug. In each experiment, the values obtained from untreated culture were set to 1.

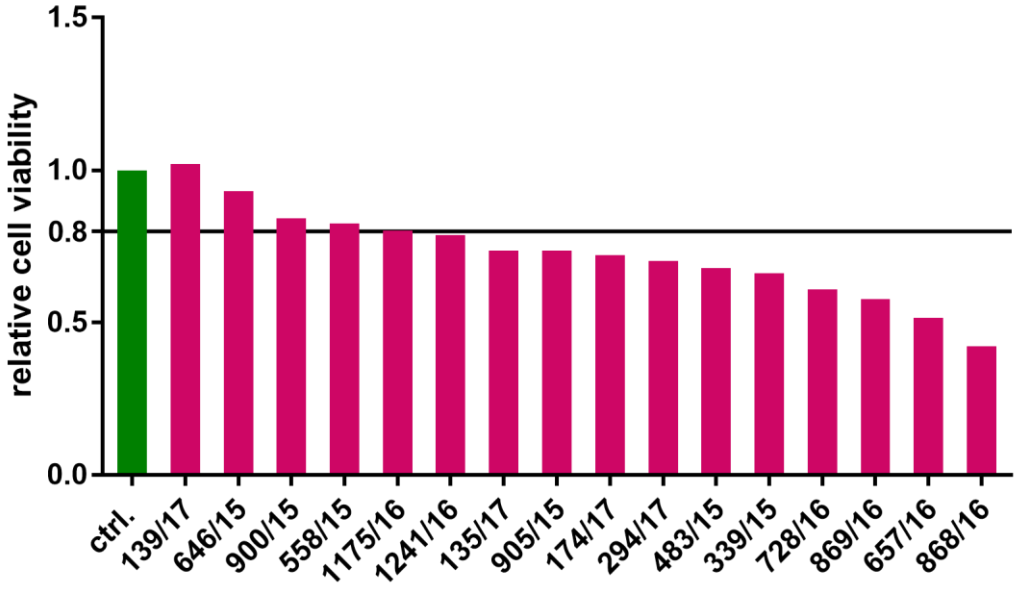

Figure 70: AMG386 reduces cell viability in some human NFPA cells. Human PA cells were treated with 5 µg/ml AMG386 for 48 h and cell viability was assessed using the WST-1 assay kit. Cell viability of treated cells was normalized against the cell viability of untreated control cells from the same patient arbitrarily, set to 1. The experiment was performed independently with six technical and 16 biological replicates.

From 12 NFPAs we could obtain enough cells to treat them with TKI. The cell cultures were treated for 48 h. In 9 of them the reduction of cell viability was > 20% (Figure 71) indicated that they responded to the inhibitor. Two NFPA cell cultures had no response to the treatment with either agent.

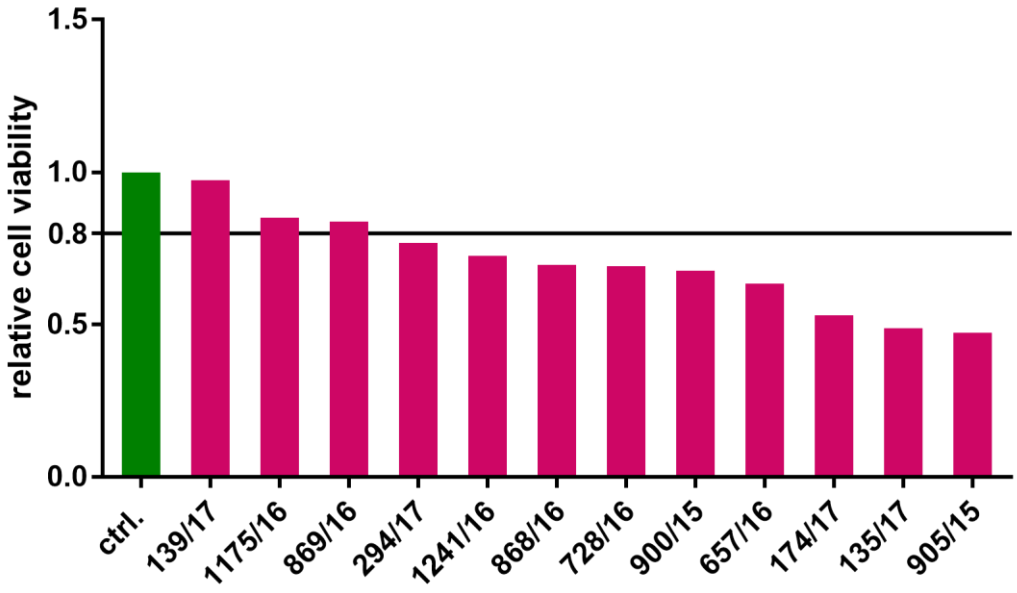

Figure 71: TKI reduces cell viability in some human NFPA cells. Human PA cells were treated with 5000 nM TKI for 48 h and cell viability was assessed using the WST-1 assay kit. Cell viability of treated cells was normalized against the cell viability of untreated control cells from the same patient arbitrarily, set to 1. The experiment was performed independently with six technical and 12 biological replicates.

From six human NFPA primary cells treated with AMG386 and from 2 treated with TKI we could collect enough cells for protein extraction. Thus, we could study the effect of signaling blockage on the PI3K pathway (Figure 72).

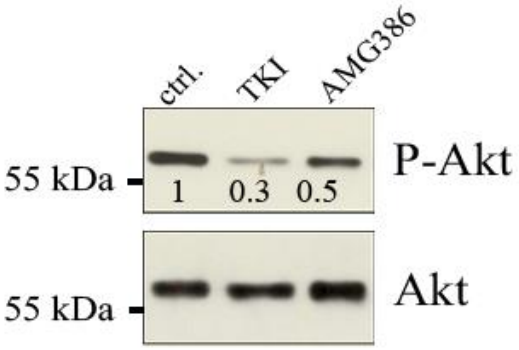

Figure 72: Human NFPA cell treatment with TKI. Human PA cells were treated with 5000 nM TKI for 48 h. The effect of kinase inhibitor on downstream signaling pathways was assessed using antibodies against activated pAkt (1:500) and total Akt (1:1000). Figure 72 shows one experiment out of at least five independent experiments using AMG386 and two using TKI with similar results. The numbers represent the ratio of phospho-/total-proteins.

In 5 out of 6 treated samples with AMG386 we observed reduction of pAkt compared to the untreated group and this effect occurred either 48 h or 72 h after treatment. Both of human NFPA primary cultures showed response to the treatment with TKI. Figure 72 represents one of the treatments with AMG and TKI.

All together, our *in vitro* data showed that blocking Ang-2/Tie-2 signaling inhibits the viability of human NFPAs.

3.5 *in vivo* experiments- evaluation of AMG386 in MENX rat

Our *in vitro* results suggest an anti-apoptotic and pro-proliferative function for Ang-2 in PAs making Ang-2/Tie-2 signaling an interesting therapeutic target.

We then studied the effect of Ang-2/Tie-2 pathway inhibition by AMG386 in MENX rats *in vivo*. To monitor if the drug is well tolerated and is able to reach the pituitary gland, two mutant rats were injected with 2 mg AMG386 per kg (mg/kgbw) intraperitoneally each day for 3 days. Two control rats were injected with placebo. The levels of Tie-2/pTie-2 in the rat pituitary tumors, as determined by immunofluorescence, were used as treatment readout (Figure 73).

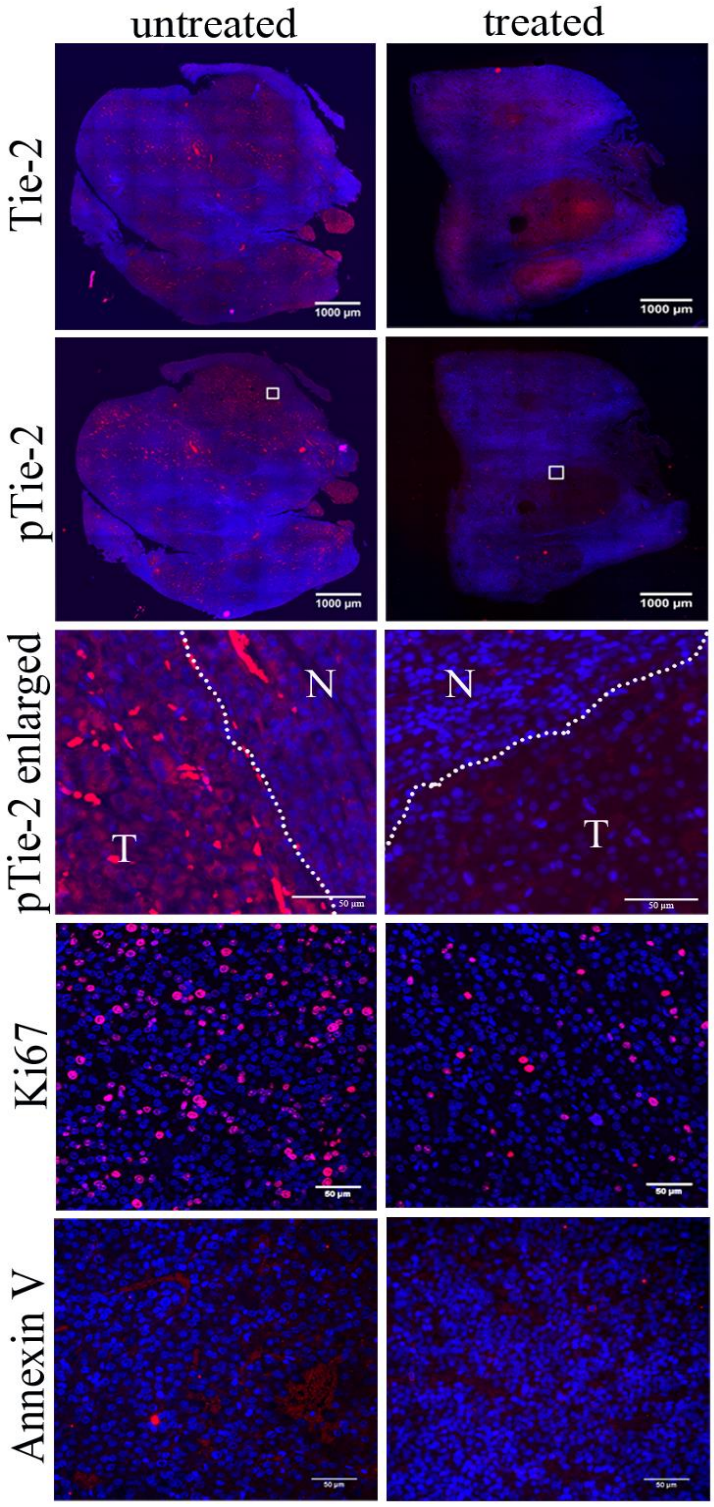

Figure 73: Treatment of MENX rat with AMG386 reduced the phosphorylation of Tie-2 after three days. The expression of Tie-2 (1:300), pTie-2 (1:2000), Ki67 (1:250) and Annexin V (1:200) was assessed using specific antibodies. The whole pituitary of treated and untreated animals was scanned to get an overall overview about the expression of Tie-2 and activated state of this receptor. N, normal area; T, tumor area in digitally enlarged sections. Original magnification: 200x; scale bar: 1000 µm. To investigate the potential apoptotic effect of Ang-2/Tie-2 signaling inhibition the

expression of Ki67 (marker of proliferation) and Annexin V (marker of apoptosis) was also considered. Cell nuclei were counterstained with DAPI. Original magnification: 200x; scale bar: 50 µm.

Treated animals did not show any side effects due to treatment and the AMG386 was well tolerated. Necropsy of treated animals indicated no pathological changes at of internal organs. Tie-2 receptor was expressed in the PAs of both treated and untreated MENX rats but Tie-2 phosphorylation was considerably reduced in the pituitary of treated rats, which indicated that AMG386 was able to inhibit the biding of Ang-2 to Tie-2 also *in vivo*. Annexin V expression, a marker of apoptosis, revealed no changes in treated rats vs. untreated, which might be due to the short-term treatment. Ki67 positivity seemed to decrease in the treated rats.

Next, we treated the MENX rats for a longer period (2 weeks and 5 applications) following the scheme illustrated in Figure 10 (n=10 treated; n=5 untreated).

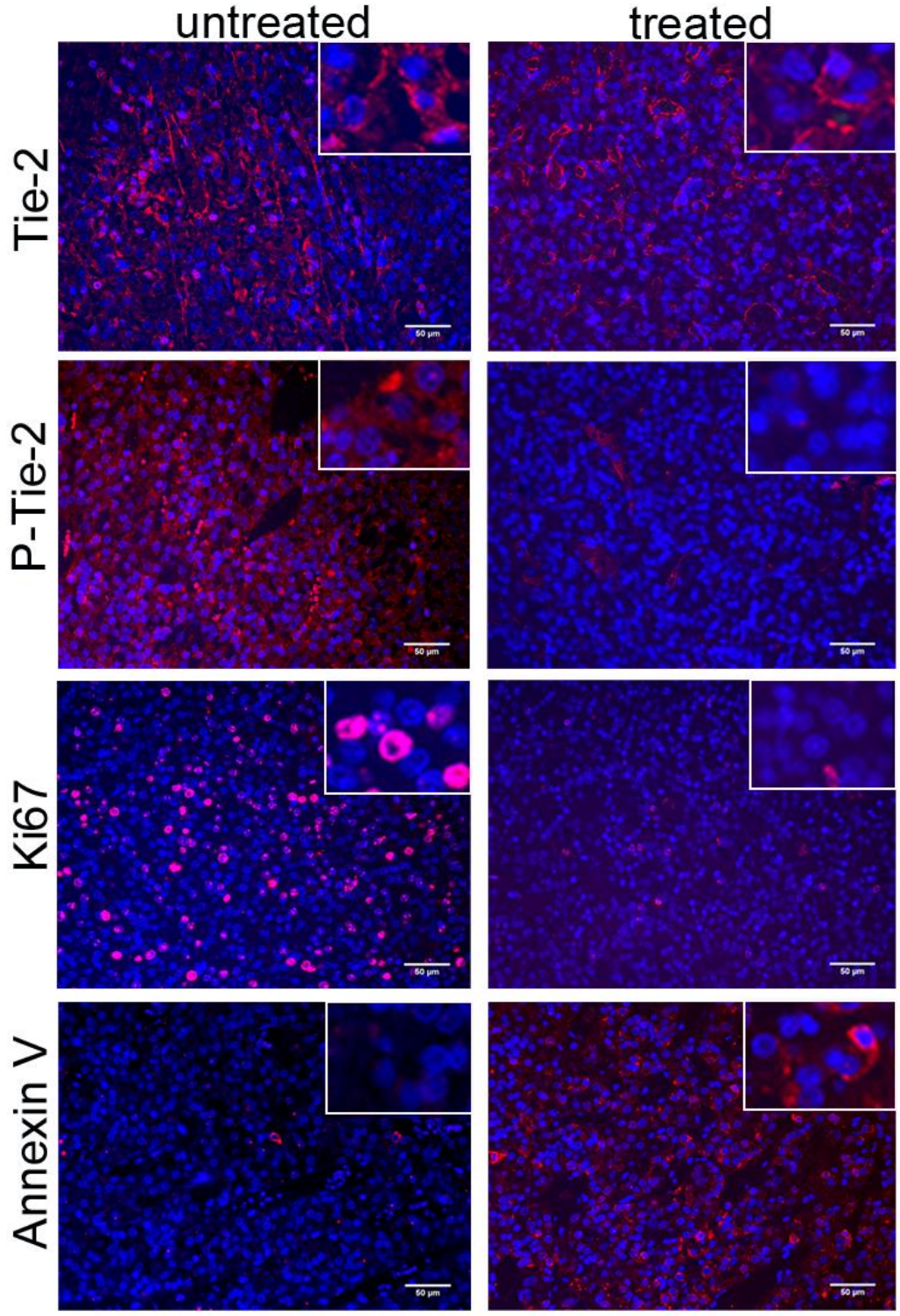

Figure 74: Treatment of MENX rat with AMG386 reduced cell proliferation and enhanced apoptosis. The expression of Tie-2 (1:300), pTie-2 (1:2000), Ki67 (1:250) and Annexin V (1:200) was assessed using specific antibodies. To investigate the potential apoptotic effect of Ang-2/Tie-2 signaling inhibition the expression of Annexin V was also considered. Cell nuclei were counterstained with DAPI. Original magnification: 200x; scale bar: 50 µm.

When the animals were treated for a longer period of time, Tie-2 phosphorylation was inhibited. The Ki67 labelling index was significantly reduced in drug-treated *versus* placebo-treated adenomas (7.5±0.81% *versus* 24.53±3.24%, respectively; ***P<0.001, Mann Whitney test), whereas Annexin V expression was enhanced. Therefore, inhibition of Ang/Tie-2 signaling enhanced apoptosis and decries proliferation of PA cells *in vivo* (Figure 74).

4 Discussion

Gonadotroph adenomas are clinically nonfunctioning and comprise about 80% of NFPAs. In the case of invasive NFPAs, a complete surgical removal is not always achieved thereby leading to tumor recurrence. Because of the lack of pharmacological therapy, radiotherapy is the main post-operative choice for recurrent NFPAs, which reduces further tumor progression although it is not curative (Pereira and Biermasz 2012, Ferrante *et al.* 2006). Therefore, understanding the molecular mechanisms leading to development and progression of NFPAs may help developing novel therapeutic approaches preventing tumor growth and tumor recurrence.

Previous studies in our group indicated that pituitary tumors developed in MENX rats closely represent their human counterparts. These animals bear a germline frameshift mutation in *Cdkn1b* and develop multifocal gonadotroph NFPAs with 100% penetrance (Pellegata *et al.* 2006, Fritz *et al.* 2002). Transcriptome analysis of rat pituitary tumors identified many genes deregulated in these lesions, when compared with the pituitary of wild-type rats (Lee *et al.* 2013). Among them were angiogenesis promoting genes. Especially, genes encoding Ang-2 and Ang-1 were up- or downregulated, respectively, in rat PAs. We have studied the role of angiopoietins in NFPA, since these molecules have not been reported in the development and progression of PAs so far. Tumor cells must be supplied with oxygen and nutrient and this is achieved by promoting neo-vascularization. Thus, inhibition of pathways involved in this process may also inhibit tumor growth. In this study, we could demonstrate that highly expressed Ang-2/ANG-2 in rat and human PAs was able to bind to Tie-2/TIE-2 receptor expressed in these cells and even activate the receptor and affect PA cell proliferation and survival. Moreover, inhibition of Ang-2/Tie-2 signaling with either siRNA or AMG386 confirmed anti-apoptotic and pro-proliferative effect of Ang-2 in PA cells *in vitro* and *in vivo.*

We observed that *Ang-2* was significantly elevated at mRNA level in the PAs of MENX rats whereas *Ang-1* was significantly downregulated when compared with wild-type rat pituitaries. IHC staining for Ang-1 and Ang-2 demonstrate that mRNA expression correlates with the amounts of the corresponding protein. We could see no expression of Ang-1 in rat pituitary tumors whereas the adjacent non-tumorous tissues were positive for Ang-1. In contrast, Ang-2 expression was found to be increased only in tumor tissues. Similar to Ang-2, IHC staining for Tie-2 receptor was positive only in MENX rat PAs. Interestingly, these cells kept their

ability to express Ang-2 and secrete it into the culture medium when grown as primary cultures.

Then, we investigated the expression of *ANG-1* and *ANG-2* in 14 human NFPA samples. The expression level was compared with two samples of healthy pituitary. In agreement with the array data, we found that the expression of *ANG-1* was downregulated in the adenomas compared to normal pituitaries. Except for one (case 296) the expression of *ANG-1* was more than two fold reduced compared to the human healthy controls. *ANG-2* expression was elevated (> 2 fold) in 6 out of 14 pituitary adenomas compared with normal pituitaries.

As mentioned previously, a shifted ratio of ANG-2/ANG-1 toward ANG-2 at the protein and mRNA level triggers tumor angiogenesis. We compared the expression of *ANG-2* with *ANG-1* in each sample; we found indeed that this ratio was changed in favor of *ANG-2* in 13 out of 14 pituitary adenoma samples but not in the human healthy controls. Thereafter, we performed IHC staining to investigate if there was correlation between the high amount of *ANG-2* mRNA and the translated protein in human NFPAs. All 37 samples studied expressed ANG-2 in the tumor cells, with more than half of them showing moderate to strong expression. In contrast, the majority of the samples showed no or weak ANG-1 expression in the adenoma cells (total samples=15). Both of these proteins are mainly expressed in the cytoplasm of the tumor cells, which is in agreement with the observations of other researchers in some tumor types. Only some tumor-associated blood vessels were expressing prominent amounts of ANG-1. In healthy human controls, ANG-1 was highly expressed in the pituitary gland (all cell lineages) and ANG-2 expression was found mostly in somatotroph cells. These studies assessed for the first time the expression profile of ANG-1 and ANG-2 in human NFPAs. As seen for primary cultures of rat PAs, the human NFPA cells also secrete ANG-2 *in vitro*.

Consistent with our findings in PAs, it has been reported that Tie-2 is expressed not only in ECs but also in gastric carcinoma cells (Moon *et al.* 2006, Hacker *et al.* 2016). In addition to Ang-2/ANG-2, we observed membranous and cytoplasmic expression of Tie-2/TIE-2, the receptor for ANG-1/-2, in NFPA cells and in some tumor-associated ECs. ELISA and WB confirmed the release of Ang-2/ANG-2 into the culture medium of rat and human PA primary cells. This observation, together with the expression of Tie-2 receptor on the membrane of these cells, suggests a possible Ang-2/ANG-2 mediated autocrine/paracrine signaling in PA cells supporting Ang-2 function as a growth factor in the tumor cells (Figure 75).

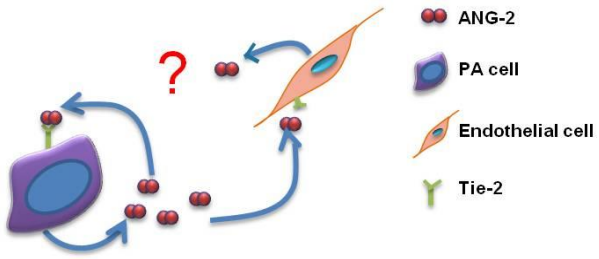

Figure 75: Schematic representation of potential function of ANG-2 in NFPAs. ANG-2 may bind to Tie-2 receptor on PA cells and activate this signaling pathway in pituitary adenoma cells. Secreted ANG-2 from PA cells may also bind to Tie-2 on EC or vice versa. Ang-2/Tie-2 signaling plays a pro-proliferative and anti-apoptotic role in PA cells.

Findings regarding VEGF, the main player in angiogenesis are controversial in PAs. Some groups reported higher expression of VEGF in functioning PAs versus NFPAs, while others reported the opposite results (Lloyd *et al.* 1999, McCabe *et al.* 2002).
In specific PAs, *ANG-2* expression was elevated compared to *ANG-1*. Since angiogenesis is activated in the presence of higher amounts of VEGF during tumorigenesis (Maisonpierre *et al.* 1997), and *VEGF* was not significantly increased in our samples, our findings suggest another still unknown function for increased *ANG-2* besides being an angiogenesis promoting ligand in ECs. Indeed, Ang-2 has an anti-apoptotic and pro-survival function in PA cells.

Moreover, it has been reported that in human glioma cell lines expressing Tie-2, but not in Tie-2-negative glioma cells, ANG-2 inhibited VEGF-A expression at both mRNA and protein levels by decreasing (HIF)-1α expression and HIF-DNA-binding activity. When Tie-2 was silenced by siRNA, Ang2-mediated downregulation of VEGF could be rescued, which shows the importance of Tie-2 for expression of VEGF in glioma cells (Lee *et al.* 2008). Since PAs exhibit a prominent ANG-2 and TIE-2 expression, this may explain why NFPAs do not express a remarkable high amounts of VEGF and why they do not possess enhanced microvascular density (MVD) compared to many other solid tumors because co-expression of ANG-2 and its receptor may inhibit VEGF expression as reported in glioma cells, and even though the expression of ANG-2 is enhanced in PAs, an enhanced angiogenesis is not reported during PA development (Jugenburg *et al.* 1995, Turner *et al.* 2000a).

ANG-2 was reported to be elevated at protein level either in serum/plasma of patients suffering from a range of human tumors including ovarian cancer (Sallinen *et al.* 2010) and hepatocellular carcinoma (Scholz *et al.* 2007) or in cultured tumor cells like bladder cancer

(Oka *et al.* 2005) and colon cancer (Ahmad *et al.* 2001). Increased expression of *ANG-2* mRNA level is also detected in the tumor vessels of non-small cell lung cancer (Wong *et al.* 2000). Ang-2 is also elevated in serum of NET patients (Detjen *et al.* 2010). Upregulated Ang-2 is correlated with tumor progression and poor prognosis in these cancer types.

We could demonstrate that Ang-2/ANG-2 is secreted by rat and human primary PA cells into the culture medium. Thus, we assumed that this protein might be detectable in the circulating blood of NFPA patients. The levels of circulating ANG-2 were measured in the pre-operative plasma of 60 NFPA patients and compared with those of age- and gender-matched healthy controls. ANG-2 levels were significantly elevated in patients. We could not find any correlation between tumor size, age, gender, invasiveness and ANG-2 secretion in NFPA patients. Our data showed that the adenoma cells could secrete a wide range of ANG-2 independent of tumor size. There was, however, a trend with increased proliferation. This indicates that increased ANG-2 expression can occur at any age and stage of the disease, thereby making of this molecule a valuable therapy target to inhibit tumor growth, but not necessarily an early diagnostic marker for NFPAs.

Previously, it was reported that depending on in which tissue Ang-2 is expressed, and if Ang-1 is present or not, Ang-2 can act as agonist or antagonist of Tie-2 (Yuan *et al.* 2009, Harfouche and Hussain 2006a, Kim *et al.* 2000c). To better understand the role of elevated ANG-2 expression and the presence of its receptor, TIE-2, in tumor cells, we overexpressed ANG-2 in GH3 rat PA cells. Here we observed no effect on cell viability or downstream signaling pathways although the exogenous protein was detected by western blot and ELISA. Moreover, IF staining done in ANG-2-overexpressing cells showed internalization of the Tie-2 receptor compared to not transfected GH3 cells, which indicates the activation of Tie-2 by exogenous ANG-2. Probably, the cells were able to compensate the effects of permanent excess of ANG-2.

Therefore, we used commercially available rhANG-2, which was able to induce downstream signaling pathways in HUVECs (Bogdanovic *et al.* 2006, Yuan *et al.* 2009) to study the role of this protein in PA cells. In GH3 cells, we noticed inconstant results when we tried to stimulate these cells with rhANG-2. Due to our observations in GH3 cells, we suspected that secreted endogenous Ang-2 could activate Tie-2 in a paracrine or autocrine manner. If the receptor is already activated by endogenous Ang-2, rhANG-2 may not cause any additional

effects. Therefore, we first tried to neutralize endogenously-produced Ang-2 using AMG386 and we then stimulated the cells with rhANG-2. In this experimental setting our data showed, that Tie-2 receptor was activated in a time- and concentration-dependent manner by rhANG-2. Accordingly, downstream signaling molecules (Erk1/2) were activated in a time- and concentration-dependent fashion suggesting that tumor cell-associated Tie-2 can be stimulated by ANG-2 and further activate signaling pathways. This is in agreement with previous observations in HUVECs that ANG-2 at high concentrations is able to activate Tie-2 and associated downstream signaling pathways (Kim *et al.* 2000c, Yuan *et al.* 2009).

Then, we downregulated endogenous Ang-2 in GH3 cells using siRNA to confirm and prove our hypothesis. We could show that in Ang-2-silenced GH3 cells rhANG-2 was also able to activate Tie-2, Fak (on Y397), an immediate signaling molecule, and MAPK pathway in a concentration- and time- dependent manner although the induction of downstream target, Erk1/2 was weaker than upon treatment with rhANG-1. It has been reported that ANG-2 is able to activate Erk1/2 effectively in HUVECs, if VEGF is absent (Harfouche and Hussain 2006b), which correlates with our results.

To investigate, if the activation of downstream signaling molecules is triggered by rhANG-2, we treated GH3 cells with different concentrations of TKI, which reversibly and selectively binds to the ATP-binding pocket of the kinase and inhibits its catalytic activity (Hasenstein *et al.* 2012, Semones *et al.* 2007), and then rhANG-2 was given to the cells. In all conditions, where TKI was present with rhANG-2 the phosphorylation of Fak was inhibited, whereas rhANG-2 alone was able to activate Fak. This observation confirmed that rhANG-2 was responsible for Tie-2 phosphorylation und subsequently Fak activation. Unlike Fak, Erk1/2 was activated in cells treated with TKI. Therefore, the cells were treated only with different concentrations of TKI without rhANG-2 and the effect of this kinase inhibitor was monitored over two different time points. Notably, Fak was completely inactivated after 2h with 20 and 30 µM TKI, and after 4h all 3 concentrations (10, 20 and 30 µM) were able to inactivate Fak. In contrast, we observed a TKI concentration-dependent activation of Erk1/2, which may be activated as a result of a negative feedback loop, since Erk1/2 is a signaling molecule downstream of Fak and activation/inhibition of other pathways may cause changes in MAPK pathway.

Previous studies in HUVECs indicated that upon stimulation of these cells with rhANG-2 Fak is phosphorylated at S910, but not at Y397. S910 activation leads subsequently to EC destabilization and migration (Thomas *et al.* 2010). In GH3 cells, after adding rhANG-2, Fak was phosphorylated at Y397 in a time- and concentration dependent manner. Moreover, stimulation of Ang-2-silenced GH3 cells with rhANG-2 increased significantly the phosphorylation of Y1102 and Y1108 on Tie-2 receptor, residues responsible for the activation of downstream signaling pathways.

GH3 cells which were transfected with siAng-2 showed significantly decreased cell viability, which could be reversed by adding rhANG-2. Additionally, downregulation of Ang-2 in GH3 cells also enhanced apoptosis, a phenotype that was rescued by adding rhANG-2. All observations in GH3 cells indicate that Ang-2-dependent activation of Tie-2 has an impact on cell survival and viability. These findings are in agreement with observations in serum-deprived EC cells, in which adding rhANG-2 supports cell survival and exhibits anti-apoptotic effect (Kim *et al.* 2000c, Yuan *et al.* 2009).

We could also measure the released Ang-2 in the supernatant of rat PA primary cells after separation of CD31+ EC population. Incubation of siAng-2 transfected GH3 cells with concentrated supernatant of isolated RPA cells could also increase cell viability and reduce apoptosis. Interestingly, incubation of GH3 cells with CM obtained from rat PA cells could activate Tie-2 receptor, which confirmed the presence of Ang-2 in the supernatant and its bioactivity.

Recent studies reported putative biological role of Ang-2 in the tumorigenic process by modulating its cellular levels in the corresponding target cells. In agreement with our data, it has been shown that silencing endogenous ANG-2 expression decreases the proliferation of colorectal (Kim *et al.* 2017), lung (Dong *et al.* 2018) and estrogen receptor-positive breast cancer cells (Han *et al.* 2016), the migration and invasion of colorectal cancer (Kim *et al.* 2017).

Expression of Ang-2 and Tie-2 in PA cells and their role in supporting cell survival make them attractive targets for therapy. Since these proteins have been heavily involved in tumor angiogenesis, there are currently several inhibitors available that block Ang-2/Tie-2 signaling. AMG386, a peptide-Fc fusion protein, was the first well-studied peptibody, which inhibits the

binding of angiopoietins to Tie-2 receptor. AMG386 was evaluated in patients with solid tumors (Herbst *et al.* 2009). This ANG-1/ANG-2 neutralizing peptibody was used in our *in vitro* and *in vivo* experiments. Incubation of GH3 cells with AMG386 was able to reduce cell viability after 48 h. No data is currently available on the inhibition of Tie-2 activity by AMG386 in *in vitro* experiments. However, in one of the first reports studing AMG386 effects, this peptibody exhibited no effect on the viability of A431 human epidermoid tumor cells (Oliner *et al.* 2004). Notably, they indicated the applicated concentrations in molar unit without indicating the molecular weight of AMG386. Moreover, authors did not report, if this cell line expresses Tie-2. Xenografts made with A431 cells showed a reduction of tumor mass when treated with AMG386. This reduction was ascribed to anti-angiogenic effects of the drug. Treatment of GH3 cells as well as rat and human primary PA cells with AMG386 reduced cell viability after 48 h in the responders group. In rat and human PAs, the known downstream pathways activated by Tie-2 (Harfouche and Hussain 2006b) were also affected after AMG386 treatment, which resulted in a reduction of activated signaling molecules at the protein level. Additionally, we also tried to target the activity of the Tie-2 receptor by TKI. Similar to AMG386, treatment with TKI reduced cell viability and activity of downstream signaling molecules in rat and human primary PA cells. These observations correlated with previous findings in ECs indicating that endogenous Ang-2 is responsible for the basal activity of Tie-2 in an autocrine manner and this in turn supports cell survival by activating the PI3K pathway (Yuan *et al.* 2009). Our results suggest that Ang-2/ANG-2 works as a pro-proliferative and anti-apoptotic growth factor in PA cells.

To further confirm this role of Ang-2, MENX rats were treated with AMG386 for 3 or 14 days. Following daily administration of AMG386 for 3 days, we could already observe an inhibition of Ang-2 signaling in the rat PAs. We first detected a reduction in the phosphorylation of Tie-2, but we could not detect any apoptosis. Interestingly, after 2 weeks of treatment Tie-2 remained unphosphorylated in tumors of treated MENX rats and we also observed decreased cell proliferation and increased apoptosis. This data confirmed our *in vitro* findings indicating the important role of Ang-2 for the maintenance of PA cell viability in an autocrine and paracrine manner. Our findings show that NFPAs might respond to agents inhibiting the Ang/Tie-2 pathway, thereby providing the rationale for the clinical implementation of these drugs to treat recurrent PAs currently lacking effective therapy.

5 Conclusion

In the current study, we confirmed the higher expression of Ang-2 at the mRNA and protein levels in rat and human PA cells with the ability of being secreted into blood or culture medium. This protein was significantly more highly secreted in patients with NFPA compared to human healthy controls without correlating with age, gender, adenoma size and disease progression. In GH3 cells, rhANG-2 was able to activate Tie-2 and downstream signaling molecules of the MAPK pathway in a time- and concentration-dependent manner. Moreover, if endogenous Ang-2 was downregulated in these cells the cell viability was decreased, whereas apoptosis was increased, which supported the pro-proliferative and anti-apoptotic role of Ang-2 in pituitary adenoma cells. This observation could be reversed by adding rhANG-2. In rat and human PA cells, blocking of Tie-2 signaling by AMG386 or TKI affected mainly PI3K pathway and consequently decreased cell viability. *in vivo* studies demonstrated that tumor-associated Ang-2 promotes angiogenesis and plays an important role in PA cell proliferation and survival.

This work showed a novel role for Ang-2 in PA cells that extends its function beyond being an angiogenesis promoting factor. This protein acts also as a growth factor in a para- and autocrine manner in PA cells. Altogether, Ang-2/Tie-2 signaling can be considered as a therapeutic target for inoperable or invasive human NFPAs.

6 References

Adams, R. H. & K. Alitalo (2007) Molecular regulation of angiogenesis and lymphangiogenesis. *Nat Rev Mol Cell Biol,* 8**,** 464-78.

Agarwal, S. K., C. M. Mateo & S. J. Marx (2009) Rare germline mutations in cyclin-dependent kinase inhibitor genes in multiple endocrine neoplasia type 1 and related states. *J Clin Endocrinol Metab,* 94**,** 1826-34.

Ahmad, S. A., W. Liu, Y. D. Jung, F. Fan, N. Reinmuth, C. D. Bucana & L. M. Ellis (2001) Differential expression of angiopoietin-1 and angiopoietin-2 in colon carcinoma. A possible mechanism for the initiation of angiogenesis. *Cancer,* 92**,** 1138-43.

Al-Brahim, N. Y. & S. L. Asa (2006) My approach to pathology of the pituitary gland. *J Clin Pathol,* 59**,** 1245-53.

Alrezk, R., F. Hannah-Shmouni & C. A. Stratakis (2017) MEN4 and CDKN1B mutations: the latest of the MEN syndromes. *Endocr Relat Cancer,* 24**,** T195-T208.

Amar, A. P. & M. H. Weiss (2003) Pituitary anatomy and physiology. *Neurosurgery Clinics of North America,* 14**,** 11-+.

Asa, S. L., A. M. Bamberger, B. Cao, M. Wong, K. L. Parker & S. Ezzat (1996) The transcription activator steroidogenic factor-1 is preferentially expressed in the human pituitary gonadotroph. *J Clin Endocrinol Metab,* 81**,** 2165-70.

Asa, S. L. & S. Ezzat (1998) The cytogenesis and pathogenesis of pituitary adenomas. *Endocr Rev,* 19**,** 798-827.

Asa, S. L. & S. Ezzat (2002) The pathogenesis of pituitary tumours. *Nat Rev Cancer,* 2**,** 836-49.

Bevan, J. S., J. Webster, C. W. Burke & M. F. Scanlon (1992) Dopamine agonists and pituitary tumor shrinkage. *Endocr Rev,* 13**,** 220-40.

Bogdanovic, E., V. P. K. H. Nguyen & D. J. Dumont (2006) Activation of Tie2 by angiopoietin-1 and angiopoietin-2 results in their release and receptor internalization. *Journal of Cell Science,* 119**,** 3551-3560.

Brindle, N. P., P. Saharinen & K. Alitalo (2006) Signaling and functions of angiopoietin-1 in vascular protection. *Circ Res,* 98**,** 1014-23.

Brochier, S., F. Galland, M. Kujas, F. Parker, S. Gaillard, C. Raftopoulos, J. Young, O. Alexopoulou, D. Maiter & P. Chanson (2010) Factors predicting relapse of nonfunctioning pituitary macroadenomas after neurosurgery: a study of 142 patients. *Eur J Endocrinol,* 163**,** 193-200.

Cardone, M. H., N. Roy, H. R. Stennicke, G. S. Salvesen, T. F. Franke, E. Stanbridge, S. Frisch & J. C. Reed (1998) Regulation of cell death protease caspase-9 by phosphorylation. *Science,* 282**,** 1318-21.

Carmeliet, P. (2003) Angiogenesis in health and disease. *Nat Med,* 9**,** 653-60.

Carmeliet, P., V. Ferreira, G. Breier, S. Pollefeyt, L. Kieckens, M. Gertsenstein, M. Fahrig, A. Vandenhoeck, K. Harpal, C. Eberhardt, C. Declercq, J. Pawling, L. Moons, D. Collen, W. Risau & A. Nagy (1996) Abnormal blood vessel development and lethality in embryos lacking a single VEGF allele. *Nature,* 380**,** 435-9.

Carroll, R. W. (2013) Multiple endocrine neoplasia type 1 (MEN1). *Asia Pac J Clin Oncol,* 9**,** 297-309.

Cascone, I., L. Napione, F. Maniero, G. Serini & F. Bussolino (2005) Stable interaction between alpha 5 beta 1 integrin and Tie2 tyrosine kinase receptor regulates endothelial cell response to Ang-1. *Journal of Cell Biology,* 170**,** 993-1004.

Chanson, P., G. Raverot, F. Castinetti, C. Cortet-Rudelli, F. Galland, S. Salenave & w.-g. French Endocrinology Society non-functioning pituitary adenoma (2015) Management of clinically non-functioning pituitary adenoma. *Ann Endocrinol (Paris),* 76**,** 239-47.

Chen, J. X. & B. Meyrick (2004) Hypoxia increases Hsp90 binding to eNOS via PI3K-Akt in porcine coronary artery endothelium. *Laboratory Investigation,* 84**,** 182-190.

Cheung, A. H., R. J. Stewart & P. A. Marsden (1998) Endothelial Tie2/Tek ligands angiopoietin-1 (ANGPT1) and angiopoietin-2 (ANGPT2): regional localization of the human genes to 8q22.3-q23 and 8p23. *Genomics,* 48**,** 389-91.

Chiloiro, S., A. Bianchi, F. Doglietto, C. de Waure, A. Giampietro, A. Fusco, D. Iacovazzo, L. Tartaglione, F. Di Nardo, F. Signorelli, L. Lauriola, C. Anile, G. Rindi, G. Maira, A. Pontecorvi & L. De Marinis (2014) Radically resected pituitary adenomas: prognostic role of Ki 67 labeling index in a monocentric retrospective series and literature review. *Pituitary,* 17**,** 267-76.

Chu, I. M., L. Hengst & J. M. Slingerland (2008) The Cdk inhibitor p27 in human cancer: prognostic potential and relevance to anticancer therapy. *Nat Rev Cancer,* 8**,** 253-67.

Cleaver, O. & P. A. Krieg (1998) VEGF mediates angioblast migration during development of the dorsal aorta in Xenopus. *Development,* 125**,** 3905-14.

Colao, A., G. Cerbone, P. Cappabianca, D. Ferone, A. Alfieri, F. Di Salle, A. Faggiano, B. Merola, E. de Divitiis & G. Lombardi (1998) Effect of surgery and radiotherapy on visual and endocrine function in nonfunctioning pituitary adenomas. *J Endocrinol Invest,* 21**,** 284-90.

Dales, J. P., S. Garcia, S. Carpentier, L. Andrac, O. Ramuz, M. N. Lavaut, C. Allasia, P. Bonnier & C. Charpin (2004) Long-term prognostic significance of neoangiogenesis in breast carcinomas: Comparison of Tie-2/Tek, CD105, and CD31 immunocytochemical expression. *Human Pathology,* 35**,** 176-183.

Daly, A. F., M. A. Tichomirow & A. Beckers (2009) Update on Familial Pituitary Tumors: from Multiple Endocrine Neoplasia Type 1 to Familial Isolated Pituitary Adenoma. *Hormone Research,* 71**,** 105-111.

Daly, C., V. Wong, E. Burova, Y. Wei, S. Zabski, J. Griffiths, K. M. Lai, H. C. Lin, E. Ioffe, G. D. Yancopoulos & J. S. Rudge (2004) Angiopoietin-1 modulates endothelial cell function and gene expression via the transcription factor FKHR (FOXO1). *Genes Dev,* 18**,** 1060-71.

Davis, S., T. H. Aldrich, P. F. Jones, A. Acheson, D. L. Compton, V. Jain, T. E. Ryan, J. Bruno, C. Radziejewski, P. C. Maisonpierre & G. D. Yancopoulos (1996) Isolation of Angiopoietin-1, a ligand for the TIE2 receptor, by secretion-trap expression cloning. *Cell,* 87**,** 1161-1169.

Davis, S., N. Papadopoulos, T. H. Aldrich, P. C. Maisonpierre, T. Huang, L. Kovac, A. Xu, R. Leidich, E. Radziejewska, A. Rafique, J. Goldberg, V. Jain, K. Bailey, M. Karow, J. Fandl, S. J. Samuelsson, E. Ioffe, J. S. Rudge, T. J. Daly, C. Radziejewski & G. D. Yancopoulos (2003) Angiopoietins have distinct modular domains essential for receptor binding, dimerization and superclustering. *Nat Struct Biol,* 10**,** 38-44.

de Bruin, T. W., D. J. Kwekkeboom, J. W. Van't Verlaat, J. C. Reubi, E. P. Krenning, S. W. Lamberts & R. J. Croughs (1992) Clinically nonfunctioning pituitary adenoma and octreotide response to long term high dose treatment, and studies in vitro. *J Clin Endocrinol Metab,* 75**,** 1310-7.

Dellinger, M., R. Hunter, M. Bernas, N. Gale, G. Yancopoulos, R. Erickson & M. Witte (2008) Defective remodeling and maturation of the lymphatic vasculature in Angiopoietin-2 deficient mice. *Dev Biol,* 319**,** 309-20.

Detjen, K. M., S. Rieke, A. Deters, P. Schulz, A. Rexin, S. Vollmer, P. Hauff, B. Wiedenmann, M. Pavel & A. Scholz (2010) Angiopoietin-2 Promotes Disease Progression of Neuroendocrine Tumors. *Clinical Cancer Research,* 16**,** 420-429.

Dong, Z., J. Chen, X. Yang, W. Zheng, L. Wang, M. Fang, M. Wu, M. Yao & D. Yao (2018) Ang-2 promotes lung cancer metastasis by increasing epithelial-mesenchymal transition. *Oncotarget,* 9**,** 12705-12717.

Dumont, D. J., G. Gradwohl, G. H. Fong, M. C. Puri, M. Gertsenstein, A. Auerbach & M. L. Breitman (1994) Dominant-negative and targeted null mutations in the endothelial receptor tyrosine kinase, tek, reveal a critical role in vasculogenesis of the embryo. *Genes Dev,* 8**,** 1897-909.

Dumont, D. J., T. P. Yamaguchi, R. A. Conlon, J. Rossant & M. L. Breitman (1992) Tek, a novel tyrosine kinase gene located on mouse chromosome 4, is expressed in endothelial cells and their presumptive precursors. *Oncogene,* 7**,** 1471-80.

Ebersold, M. J., L. M. Quast, E. R. Laws, Jr., B. Scheithauer & R. V. Randall (1986) Long-term results in transsphenoidal removal of nonfunctioning pituitary adenomas. *J Neurosurg,* 64**,** 713-9.

Evans, C. O., C. S. Moreno, X. Q. Zhan, M. T. McCabe, P. M. Vertino, D. M. Desiderio & N. M. Oyesiku (2008) Molecular pathogenesis of human prolactinomas identified by gene expression profiling, RT-qPCR, and proteomic analyses. *Pituitary,* 11**,** 231-245.

Ferrante, E., M. Ferraroni, T. Castrignano, L. Menicatti, M. Anagni, G. Reimondo, P. Del Monte, D. Bernasconi, P. Loli, M. Faustini-Fustini, G. Borretta, M. Terzolo, M. Losa, A. Morabito, A. Spada, P. Beck-Peccoz & A. G. Lania (2006) Non-functioning pituitary adenoma database: a useful resource to improve the clinical management of pituitary tumors. *Eur J Endocrinol,* 155**,** 823-9.

Ferrara, N., K. Carver-Moore, H. Chen, M. Dowd, L. Lu, K. S. O'Shea, L. Powell-Braxton, K. J. Hillan & M. W. Moore (1996) Heterozygous embryonic lethality induced by targeted inactivation of the VEGF gene. *Nature,* 380**,** 439-42.

Ferrara, N. & T. Davis-Smyth (1997) The biology of vascular endothelial growth factor. *Endocr Rev,* 18**,** 4-25.

Ferrara, N., H. P. Gerber & J. LeCouter (2003) The biology of VEGF and its receptors. *Nat Med,* 9**,** 669-76.

Fiedler, U., M. Scharpfenecker, S. Koidl, A. Hegen, V. Grunow, J. M. Schmidt, W. Kriz, G. Thurston & H. G. Augustin (2004) The Tie-2 ligand angiopoietin-2 is stored in and rapidly released upon stimulation from endothelial cell Weibel-Paladebodies. *Blood,* 103**,** 4150-4156.

Folkman, J. (1995) Angiogenesis in cancer, vascular, rheumatoid and other disease. *Nat Med,* 1**,** 27-31.

Fritz, A., A. Walch, K. Piotrowska, M. Rosemann, E. Schaffer, K. Weber, A. Timper, G. Wildner, J. Graw, H. Hofler & M. J. Atkinson (2002) Recessive transmission of a multiple endocrine neoplasia syndrome in the rat. *Cancer Res,* 62**,** 3048-51.

Fukuhara, S., K. Sako, T. Minami, K. Noda, H. Z. Kim, T. Kodama, M. Shibuya, N. Takakura, G. Y. Koh & N. Mochizuki (2008) Differential function of Tie2 at cell-cell contacts and cell-substratum contacts regulated by angiopoietin-1. *Nat Cell Biol,* 10**,** 513-26.

Gale, N. W., G. Thurston, S. F. Hackett, R. Renard, Q. Wang, J. McClain, C. Martin, C. Witte, M. H. Witte, D. Jackson, C. Suri, P. A. Campochiaro, S. J. Wiegand & G. D. Yancopoulos (2002) Angiopoietin-2 is required for postnatal angiogenesis and lymphatic patterning, and only the latter role is rescued by Angiopoietin-1. *Dev Cell,* 3**,** 411-23.

Georgitsi, M., A. Raitila, A. Karhu, R. B. van der Luijt, C. M. Aalfs, T. Sane, O. Vierimaa, M. J. Makinen, K. Tuppurainen, R. Paschke, O. Gimm, C. A. Koch, S. Gundogdu, A. Lucassen, M. Tischkowitz, L. Izatt, S. Aylwin, G. Bano, S. Hodgson, E. De Menis, V. Launonen, P. Vahteristo & L. A. Aaltonen (2007) Germline CDKN1B/p27Kip1 mutation in multiple endocrine neoplasia. *J Clin Endocrinol Metab,* 92**,** 3321-5.

Gerald, D., S. Chintharlapalli, H. G. Augustin & L. E. Benjamin (2013) Angiopoietin-2: an attractive target for improved antiangiogenic tumor therapy. *Cancer Res,* 73**,** 1649-57.

Gerhardt, H. & C. Betsholtz (2003) Endothelial-pericyte interactions in angiogenesis. *Cell Tissue Res,* 314**,** 15-23.

Greenman, Y. & S. Melmed (1996) Diagnosis and management of nonfunctioning pituitary tumors. *Annu Rev Med,* 47**,** 95-106.

Greenman, Y., G. Ouaknine, I. Veshchev, G. Reider, II, Y. Segev & N. Stern (2003) Postoperative surveillance of clinically nonfunctioning pituitary macroadenomas: markers of tumour quiescence and regrowth. *Clin Endocrinol (Oxf),* 58**,** 763-9.

Guru, S. C., P. K. Goldsmith, A. L. Burns, S. J. Marx, A. M. Spiegel, F. S. Collins & S. C. Chandrasekharappa (1998) Menin, the product of the MEN1 gene, is a nuclear protein. *Proc Natl Acad Sci U S A,* 95**,** 1630-4.

Hacker, U. T., L. Escalona-Espinosa, N. Consalvo, V. Goede, L. Schiffmann, S. J. Scherer, P. Hedge, E. Van Cutsem, O. Coutelle & H. Buning (2016) Evaluation of Angiopoietin-2 as a biomarker in gastric cancer: results from the randomised phase III AVAGAST trial. *Br J Cancer,* 114**,** 855-62.

Hackett, S. F., H. Ozaki, R. W. Strauss, K. Wahlin, C. Suri, P. Maisonpierre, G. Yancopoulos & P. A. Campochiaro (2000) Angiopoietin 2 expression in the retina: Upregulation during physiologic and pathologic neovascularization. *Journal of Cellular Physiology,* 184**,** 275-284.

Hackett, S. F., S. Wiegand, G. Yancopoulos & P. A. Campochiaro (2002) Angiopoietin-2 plays an important role in retinal angiogenesis. *J Cell Physiol,* 192**,** 182-7.

Hammes, H. P., J. Lin, P. Wagner, Y. Feng, F. Vom Hagen, T. Krzizok, O. Renner, G. Breier, M. Brownlee & U. Deutsch (2004) Angiopoietin-2 causes pericyte dropout in the normal retina: evidence for involvement in diabetic retinopathy. *Diabetes,* 53**,** 1104-10.

Han, D. C. & J. L. Guan (1999) Association of focal adhesion kinase with Grb7 and its role in cell migration. *J Biol Chem,* 274**,** 24425-30.

Han, H. H., B. G. Kim, J. H. Lee, S. Kang, J. E. Kim & N. H. Cho (2016) Angiopoietin-2 promotes ER+ breast cancer cell survival in bone marrow niche. *Endocr Relat Cancer,* 23**,** 609-23.

Hansen, L. K. & M. E. Molitch (1998) Postoperative radiotherapy for clinically nonfunctioning pituitary adenomas. *Endocrinologist,* 8**,** 71-78.

Hansen, T. M., H. Singh, T. A. Tahir & N. P. Brindle (2010) Effects of angiopoietins-1 and -2 on the receptor tyrosine kinase Tie2 are differentially regulated at the endothelial cell surface. *Cell Signal,* 22**,** 527-32.

Harfouche, R. & S. N. Hussain (2006a) Signaling and regulation of endothelial cell survival by angiopoietin-2. *Am J Physiol Heart Circ Physiol,* 291**,** H1635-45.

Harfouche, R. & S. N. A. Hussain (2006b) Signaling and regulation of endothelial cell survival by angiopoietin-2. *American Journal of Physiology-Heart and Circulatory Physiology,* 291**,** H1635-H1645.

Harshman, L. C. & S. Srinivas (2010) The bevacizumab experience in advanced renal cell carcinoma. *Oncotargets and Therapy,* 3**,** 179-189.

Hasenstein, J. R., K. Kasmerchak, D. Buehler, G. R. Hafez, K. Cleary, J. S. Moody & K. R. Kozak (2012) Efficacy of Tie2 Receptor Antagonism in Angiosarcoma. *Neoplasia,* 14**,** 131-U62.

Hayes, A. J., W. Q. Huang, J. Yu, P. C. Maisonpierre, A. Liu, F. G. Kern, M. E. Lippman, S. W. McLeskey & L. Y. Li (2000) Expression and function of angiopoietin-1 in breast cancer. *British Journal of Cancer,* 83**,** 1154-1160.

Helfrich, I., L. Edler, A. Sucker, M. Thomas, S. Christian, D. Schadendorf & H. G. Augustin (2009) Angiopoietin-2 levels are associated with disease progression in metastatic malignant melanoma. *Clin Cancer Res,* 15**,** 1384-92.

Hellstrom, M., M. Kalen, P. Lindahl, A. Abramsson & C. Betsholtz (1999) Role of PDGF-B and PDGFR-beta in recruitment of vascular smooth muscle cells and pericytes during embryonic blood vessel formation in the mouse. *Development,* 126**,** 3047-55.

Herbst, R. S., D. Hong, L. Chap, R. Kurzrock, E. Jackson, J. M. Silverman, E. Rasmussen, Y. N. Sun, D. Zhong, Y. C. Hwang, J. L. Evelhoch, J. D. Oliner, N. Le & L. S. Rosen (2009) Safety, pharmacokinetics, and antitumor activity of AMG 386, a selective angiopoietin inhibitor, in adult patients with advanced solid tumors. *J Clin Oncol,* 27**,** 3557-65.

Holash, J., P. C. Maisonpierre, D. Compton, P. Boland, C. R. Alexander, D. Zagzag, G. D. Yancopoulos & S. J. Wiegand (1999) Vessel cooption, regression, and growth in tumors mediated by angiopoietins and VEGF. *Science,* 284**,** 1994-8.

Holopainen, T., H. L. Huang, C. P. Chen, K. E. Kim, L. Q. Zhang, F. Zhou, W. C. Han, C. J. Li, J. Yu, J. Wu, G. Y. Koh, K. Alitalo & Y. L. He (2009) Angiopoietin-1 overexpression modulates vascular endothelium to facilitate tumor cell dissemination and metastasis establishment (vol 69, pg 4656, 2009). *Cancer Research,* 69**,** 5618-5618.

Hu, B., M. J. Jarzynka, P. Guo, Y. Imanishi, D. D. Schlaepfer & S. Y. Cheng (2006) Angiopoietin 2 induces glioma cell invasion by stimulating matrix metalloprotease 2 expression through the alpha(v)beta(1) integrin and focal adhesion kinase signaling pathway. *Cancer Research,* 66**,** 775-783.

Huang, C. W. Turck, P. Rao & K. G. Peters (1995) GRB2 and SH-PTP2: potentially important endothelial signaling molecules downstream of the TEK/TIE2 receptor tyrosine kinase. *Oncogene,* 11**,** 2097-103.

Huang, Y. Q., J. J. Li & S. Karpatkin (2000) Identification of a family of alternatively spliced mRNA species of angiopoietin-1. *Blood,* 95**,** 1993-9.

Hurwitz, H., L. Fehrenbacher, W. Novotny, T. Cartwright, J. Hainsworth, W. Heim, J. Berlin, A. Baron, S. Griffing, E. Holmgren, N. Ferrara, G. Fyfe, B. Rogers, R. Ross & F. Kabbinavar (2004) Bevacizumab plus irinotecan, fluorouracil, and leucovorin for metastatic colorectal cancer. *N Engl J Med,* 350**,** 2335-42.

Inoshita, N. & H. Nishioka (2018) The 2017 WHO classification of pituitary adenoma: overview and comments. *Brain Tumor Pathol,* 35**,** 51-56.

Inoue, K., E. F. Couch, K. Takano & S. Ogawa (1999) The structure and function of folliculo-stellate cells in the anterior pituitary gland. *Arch Histol Cytol,* 62**,** 205-18.

Jeon, B. H., F. Khanday, S. Deshpande, A. Haile, M. Ozaki & K. Irani (2003) Tie-ing the antiinflammatory effect of angiopoietin-1 to inhibition of NF-kappaB. *Circ Res,* 92**,** 586-8.

Jones, N. & D. J. Dumont (1998) The Tek/Tie2 receptor signals through a novel Dok-related docking protein, Dok-R. *Oncogene,* 17**,** 1097-108.

Jugenburg, M., K. Kovacs, L. Stefaneanu & B. W. Scheithauer (1995) Vasculature in Nontumorous Hypophyses, Pituitary Adenomas, and Carcinomas: A Quantitative Morphologic Study. *Endocr Pathol,* 6**,** 115-124.

Kelberman, D., K. Rizzoti, R. Lovell-Badge, I. C. Robinson & M. T. Dattani (2009) Genetic regulation of pituitary gland development in human and mouse. *Endocr Rev,* 30**,** 790-829.

Kim, H., T. S. Ahn, C. J. Kim, S. B. Bae, H. J. Kim, C. S. Lee, T. H. Kim, J. Im, S. H. Lee, M. W. Son, M. S. Lee, M. J. Baek & D. Jeong (2017) Oncogenic function of angiopoietin-2 in vitro and its modulation of tumor progression in colorectal carcinoma. *Oncol Lett,* 14**,** 553-560.

Kim, I., H. G. Kim, S. O. Moon, S. W. Chae, J. N. So, K. N. Koh, B. C. Ahn & G. Y. Koh (2000a) Angiopoietin-1 induces endothelial cell sprouting through the activation of focal adhesion kinase and plasmin secretion. *Circ Res,* 86**,** 952-9.

Kim, I., H. G. Kim, J. N. So, J. H. Kim, H. J. Kwak & G. Y. Koh (2000b) Angiopoietin-1 regulates endothelial cell survival through the phosphatidylinositol 3'-kinase/Akt signal transduction pathway. *Circulation Research,* 86**,** 24-29.

Kim, I., J. H. Kim, S. O. Moon, H. J. Kwak, N. G. Kim & G. Y. Koh (2000c) Angiopoietin-2 at high concentration can enhance endothelial cell survival through the phosphatidylinositol 3 '-kinase/Akt signal transduction pathway. *Oncogene,* 19**,** 4549-4552.

Kim, I., J. H. Kim, Y. S. Ryu, S. H. Jung, J. J. Nah & G. Y. Koh (2000d) Characterization and expression of a novel alternatively spliced human angiopoietin-2. *J Biol Chem,* 275**,** 18550-6.

Kim, I., S. O. Moon, S. H. Kim, H. J. Kim, Y. S. Koh & G. Y. Koh (2001) Vascular endothelial growth factor expression of intercellular adhesion molecule 1 (ICAM-1), vascular cell adhesion molecule 1 (VCAM-1), and E-selectin through nuclear factor-kappa B activation in endothelial cells. *J Biol Chem,* 276**,** 7614-20.

Kim, I., Y. S. Ryu, H. J. Kwak, S. Y. Ahn, J. L. Oh, G. D. Yancopoulos, N. W. Gale & G. Y. Koh (2002) EphB ligand, ephrinB2, suppresses the VEGF- and angiopoietin 1-induced Ras/mitogen-activated protein kinase pathway in venous endothelial cells. *FASEB J,* 16**,** 1126-8.

Kim, K. J., B. Li, J. Winer, M. Armanini, N. Gillett, H. S. Phillips & N. Ferrara (1993) Inhibition of vascular endothelial growth factor-induced angiogenesis suppresses tumour growth in vivo. *Nature,* 362**,** 841-4.

Kim, K. T., H. H. Choi, M. O. Steinmetz, B. Maco, R. A. Kammerer, S. Y. Ahn, H. Z. Kim, G. M. Lee & G. Y. Koh (2005) Oligomerization and multimerization are critical for angiopoietin-1 to bind and phosphorylate Tie2. *J Biol Chem,* 280**,** 20126-31.

Koga, K., T. Todaka, M. Morioka, J. Hamada, Y. Kai, S. Yano, A. Okamura, N. Takakura, T. Suda & Y. Ushio (2001) Expression of angiopoietin-2 in human glioma cells and its role for angiogenesis. *Cancer Res,* 61**,** 6248-54.

Kontos, C. D., T. P. Stauffer, W. P. Yang, J. D. York, L. Huang, M. A. Blanar, T. Meyer & K. G. Peters (1998) Tyrosine 1101 of Tie2 is the major site of association of p85 and is required for activation of phosphatidylinositol 3-kinase and Akt. *Mol Cell Biol,* 18**,** 4131-40.

Kosty, M. P., J. R. Brahmer, M. Jahanzeb, P. Kumar, R. Robles, A. J. Wozniak, L. Leon, E. D. Flick, D. Dalal & T. J. Lynch (2011) Use of Bevacizumab (BV) After Induction Therapy is Associated With Survival Benefit in Patients (pts) With Non-small Cell Lung Cancer (NSCLC) in the ARIES Observational Cohort Study (OCS). *European Journal of Cancer,* 47**,** S598-S598.

Lauro, S., C. E. Onesti, R. Righini & P. Marchetti (2014) The Use of Bevacizumab in Non-Small Cell Lung Cancer: An Update. *Anticancer Research,* 34**,** 1537-1545.

Lee & N. S. Pellegata. 2013. Multiple Endocrine Neoplasia Type 4. In *Endocrine Tumor Syndromes and Their Genetics,* ed. C. A. Stratakis, 63-78. Basel: Karger.

Lee, M., I. Marinoni, M. Irmler, T. Psaras, J. B. Honegger, R. Beschorner, N. Anastasov, J. Beckers, M. Theodoropoulou, F. Roncaroli & N. S. Pellegata (2013) Transcriptome analysis of MENX-associated rat pituitary adenomas identifies novel molecular mechanisms involved in the pathogenesis of human pituitary gonadotroph adenomas. *Acta Neuropathologica,* 126**,** 137-150.

Lee, O. H., J. Xu, J. Fueyo, M. M. Alonso, D. Liu, V. Martin, H. Jiang, Y. Piao, T. J. Liu & C. Gomez-Manzano (2008) Angiopoietin-2 decreases vascular endothelial growth factor expression by modulating HIF-1 alpha levels in gliomas. *Oncogene,* 27**,** 1310-1314.

Li, X., M. Stankovic, C. S. Bonder, C. N. Hahn, M. Parsons, S. M. Pitson, P. Xia, R. L. Proia, M. A. Vadas & J. R. Gamble (2008) Basal and angiopoietin-1-mediated endothelial permeability is regulated by sphingosine kinase-1. *Blood,* 111**,** 3489-97.

Liontos, M., M. Lykka, M. A. Dimopoulos & A. Bamias (2014) Profile of trebananib (AMG386) and its potential in the treatment of ovarian cancer. *Onco Targets Ther,* 7**,** 1837-45.

Lloyd, R. V., R. Y. Osamura, G. Klöppel, J. Rosai, F. T. Bosman, E. S. Jaffe, S. R. Lakhani, H. Ohgaki, World Health Organization. & International Agency for Research on Cancer. 2017. *WHO classification of tumours of endocrine organs*. Lyon: International Agency for Research on Cancer.

Lloyd, R. V., B. W. Scheithauer, T. Kuroki, S. Vidal, K. Kovacs & L. Stefaneanu (1999) Vascular endothelial growth factor (VEGF) expression in human pituitary adenomas and carcinomas. *Endocrine Pathology,* 10**,** 229-235.

Lobov, I. B., P. C. Brooks & R. A. Lang (2002) Angiopoietin-2 displays VEGF-dependent modulation of capillary structure and endothelial cell survival in vivo. *Proc Natl Acad Sci U S A,* 99**,** 11205-10.

Maisonpierre, P. C., C. Suri, P. F. Jones, S. Bartunkova, S. Wiegand, C. Radziejewski, D. Compton, J. McClain, T. H. Aldrich, N. Papadopoulos, T. J. Daly, S. Davis, T. N. Sato & G. D. Yancopoulos (1997) Angiopoietin-2, a natural antagonist for Tie2 that disrupts in vivo angiogenesis. *Science,* 277**,** 55-60.

Mandriota, S. J., G. Seghezzi, J. D. Vassalli, N. Ferrara, S. Wasi, R. Mazzieri, P. Mignatti & M. S. Pepper (1995) Vascular endothelial growth factor increases urokinase receptor expression in vascular endothelial cells. *J Biol Chem,* 270**,** 9709-16.

Manojlovic-Gacic, E., B. E. Engstrom & O. Casar-Borota (2018) Histopathological classification of non-functioning pituitary neuroendocrine tumors. *Pituitary,* 21**,** 119-129.

Marini, F., A. Falchetti, F. Del Monte, S. Carbonell Sala, I. Tognarini, E. Luzi & M. L. Brandi (2006) Multiple endocrine neoplasia type 2. *Orphanet J Rare Dis,* 1**,** 45.

Marinoni, I., M. Lee, S. Mountford, A. Perren, I. Bravi, L. Jennen, A. Feuchtinger, J. Drouin, F. Roncaroli & N. S. Pellegata (2013) Characterization of MENX-associated pituitary tumours. *Neuropathology and Applied Neurobiology,* 39**,** 256-269.

McCabe, C. J., K. Boelaert, L. A. Tannahill, A. P. Heaney, A. L. Stratford, J. S. Khaira, S. Hussain, M. C. Sheppard, J. A. Franklyn & N. J. L. Gittoes (2002) Vascular endothelial growth factor, its receptor

KDR/Flk-1, and pituitary tumor transforming gene in pituitary tumors. *Journal of Clinical Endocrinology & Metabolism,* 87**,** 4238-4244.

Mebratu, Y. & Y. Tesfaigzi (2009) How ERK1/2 activation controls cell proliferation and cell death is subcellular localization the answer? *Cell Cycle,* 8**,** 1168-1175.

Mete, O. & S. L. Asa (2012) Clinicopathological correlations in pituitary adenomas. *Brain Pathol,* 22**,** 443-53.

Mete, O. & M. B. Lopes (2017) Overview of the 2017 WHO Classification of Pituitary Tumors. *Endocr Pathol,* 28**,** 228-243.

Mezquita, J., B. Mezquita, M. Pau & C. Mezquita (1999) Characterization of a novel form of angiopoietin-2 (Ang-2B) and expression of VEGF and angiopoietin-2 during chicken testicular development and regression. *Biochem Biophys Res Commun,* 260**,** 492-8.

Micko, A. S., A. Wohrer, S. Wolfsberger & E. Knosp (2015) Invasion of the cavernous sinus space in pituitary adenomas: endoscopic verification and its correlation with an MRI-based classification. *J Neurosurg,* 122**,** 803-11.

Mita, A. C., C. H. Takimoto, M. Mita, A. Tolcher, K. Sankhala, J. Sarantopoulos, M. Valdivieso, L. Wood, E. Rasmussen, Y. N. Sun, Z. D. Zhong, M. B. Bass, N. Le & P. LoRusso (2010) Phase 1 study of AMG 386, a selective angiopoietin 1/2-neutralizing peptibody, in combination with chemotherapy in adults with advanced solid tumors. *Clin Cancer Res,* 16**,** 3044-56.

Molatore, S., E. Kiermaier, C. B. Jung, M. Lee, E. Pulz, H. Hofler, M. J. Atkinson & N. S. Pellegata (2010) Characterization of a naturally-occurring p27 mutation predisposing to multiple endocrine tumors. *Mol Cancer,* 9**,** 116.

Molatore, S., A. Kugler, M. Irmler, T. Wiedemann, F. Neff, A. Feuchtinger, J. Beckers, M. Robledo, F. Roncaroli & N. S. Pellegata (2018) Characterization of neuroendocrine tumors in heterozygous mutant MENX rats: a novel model of invasive medullary thyroid carcinoma. *Endocr Relat Cancer,* 25**,** 145-162.

Monk, B. J., A. Poveda, I. Vergote, F. Raspagliesi, K. Fujiwara, D. S. Bae, A. Oaknin, I. Ray-Coquard, D. M. Provencher, B. Y. Karlan, C. Lhomme, G. Richardson, D. G. Rincon, R. L. Coleman, T. J. Herzog, C. Marth, A. Brize, M. Fabbro, A. Redondo, A. Bamias, M. Tassoudji, L. Navale, D. J. Warner & A. M. Oza (2014) Anti-angiopoietin therapy with trebananib for recurrent ovarian cancer (TRINOVA-1): a randomised, multicentre, double-blind, placebo-controlled phase 3 trial. *Lancet Oncol,* 15**,** 799-808.

Monk, B. J., A. Poveda, I. Vergote, F. Raspagliesi, K. Fujiwara, D. S. Bae, A. Oaknin, I. Ray-Coquard, D. M. Provencher, B. Y. Karlan, C. Lhomme, G. Richardson, D. G. Rincon, R. L. Coleman, C. Marth, A. Brize, M. Fabbro, A. Redondo, A. Bamias, H. Ma, F. D. Vogl, B. A. Bach & A. M. Oza (2016) Final results of a phase 3 study of trebananib plus weekly paclitaxel in recurrent ovarian cancer (TRINOVA-1): Long-term survival, impact of ascites, and progression-free survival-2. *Gynecol Oncol,* 143**,** 27-34.

Moon, W. S., H. S. Park, K. H. Yu, K. Y. Jang, M. J. Kang, H. Park & A. S. Tarnawski (2006) Expression of angiopoietin 1, 2 and their common receptor Tie2 in human gastric carcinoma: implication for angiogenesis. *J Korean Med Sci,* 21**,** 272-8.

Moreno, C. S., C. O. Evans, X. Q. Zhan, M. Okor, D. M. Desiderio & N. M. Oyesiku (2005) Novel molecular signaling and classification of human clinically nonfunctional pituitary adenomas identified by gene expression profiling and proteomic analyses. *Cancer Research,* 65**,** 10214-10222.

Mulligan, L. M., J. B. Kwok, C. S. Healey, M. J. Elsdon, C. Eng, E. Gardner, D. R. Love, S. E. Mole, J. K. Moore, L. Papi & et al. (1993) Germ-line mutations of the RET proto-oncogene in multiple endocrine neoplasia type 2A. *Nature,* 363**,** 458-60.

Namihira, H., M. Sato, S. Matsubara, H. Ohye, M. M. R. Bhuiyan, K. Murao & J. Takahara (1999) No evidence of germline mutation or somatic deletion of the MEN1 gene in a case of familial multiple endocrine neoplasia type 1 (MEN1). *Endocrine Journal,* 46**,** 811-816.

Nguyen, V. P. K. H., S. H. Chen, J. Trinh, H. Kim, B. L. Coomber & D. J. Dumont (2007) Differential response of lymphatic, venous and arterial endothelial cells to angiopoietin-1 and angiopoietin-2. *Bmc Cell Biology,* 8.

Nishioka, H. & N. Inoshita (2018) New WHO classification of pituitary adenomas (4th edition): assessment of pituitary transcription factors and the prognostic histological factors. *Brain Tumor Pathol,* 35**,** 57-61.

Nishishita, T. & P. C. Lin (2004) Angiopoietin 1, PDGF-B, and TGF-beta gene regulation in endothelial cell and smooth muscle cell interaction. *J Cell Biochem,* 91**,** 584-93.

Oka, N., Y. Yamamoto, M. Takahashi, M. Nishitani, H. O. Kanayama & S. Kagawa (2005) Expression of angiopoietin-1 and -2, and its clinical significance in human bladder cancer. *BJU Int,* 95**,** 660-3.

Oki, Y. (2014) Medical management of functioning pituitary adenoma: an update. *Neurol Med Chir (Tokyo),* 54**,** 958-65.

Oliner, J., H. Min, J. Leal, D. Yu, S. Rao, E. You, X. Tang, H. Kim, S. Meyer, S. J. Han, N. Hawkins, R. Rosenfeld, E. Davy, K. Graham, F. Jacobsen, S. Stevenson, J. Ho, Q. Chen, T. Hartmann, M. Michaels, M. Kelley, L. Li, K. Sitney, F. Martin, J. R. Sun, N. Zhang, J. Lu, J. Estrada, R. Kumar, A. Coxon, S. Kaufman, J. Pretorius, S. Scully, R. Cattley, M. Payton, S. Coats, L. Nguyen, B. Desilva, A. Ndifor, I. Hayward, R. Radinsky, T. Boone & R. Kendall (2004) Suppression of angiogenesis and tumor growth by selective inhibition of angiopoietin-2. *Cancer Cell,* 6**,** 507-16.

Onofri, C., M. Theodoropoulou, M. Losa, E. Uhl, M. Lange, E. Arzt, G. K. Stalla & U. Renner (2006) Localization of vascular endothelial growth factor (VEGF) receptors in normal and adenomatous pituitaries: detection of a non-endothelial function of VEGF in pituitary tumours. *J Endocrinol,* 191**,** 249-61.

Ooi, G. T., N. Tawadros & R. M. Escalona (2004) Pituitary cell lines and their endocrine applications. *Molecular and Cellular Endocrinology,* 228**,** 1-21.

Ortiz, L. D., L. V. Syro, B. W. Scheithauer, A. Ersen, H. Uribe, C. E. Fadul, F. Rotondo, E. Horvath & K. Kovacs (2012) Anti-VEGF therapy in pituitary carcinoma. *Pituitary,* 15**,** 445-9.

Palmer, D. H. (2008) TKI Sorafenib in advanced hepatocellular carcinoma. *N Engl J Med,* 359**,** 2498; author reply 2498-9.

Papapetropoulos, A., D. Fulton, K. Mahboubi, R. G. Kalb, D. S. O'Connor, F. Li, D. C. Altieri & W. C. Sessa (2000) Angiopoietin-1 inhibits endothelial cell apoptosis via the Akt/survivin pathway. *J Biol Chem,* 275**,** 9102-5.

Papetti, M. & I. M. Herman (2002) Mechanisms of normal and tumor-derived angiogenesis. *Am J Physiol Cell Physiol,* 282**,** C947-70.

Park, J. E., G. A. Keller & N. Ferrara (1993) The vascular endothelial growth factor (VEGF) isoforms: differential deposition into the subepithelial extracellular matrix and bioactivity of extracellular matrix-bound VEGF. *Mol Biol Cell,* 4**,** 1317-26.

Park, J. H., K. J. Park, Y. S. Kim, S. S. Sheen, K. S. Lee, H. N. Lee, Y. J. Oh & S. C. Hwang (2007) Serum angiopoietin-2 as a clinical marker for lung cancer. *Chest,* 132**,** 200-6.

Partanen, J., E. Armstrong, T. P. Makela, J. Korhonen, M. Sandberg, R. Renkonen, S. Knuutila, K. Huebner & K. Alitalo (1992) A novel endothelial-cell surface-receptor tyrosine kinase with extracellular epidermal growth-factor homology domains. *Molecular and Cellular Biology,* 12**,** 1698-1707.

Pellegata, N. S., L. Quintanilla-Martinez, H. Siggelkow, E. Samson, K. Bink, H. Hofler, F. Fend, J. Graw & M. J. Atkinson (2006) Germ-line mutations in p27(Kip1) cause a multiple endocrine neoplasia syndrome in rats and humans. *Proceedings of the National Academy of Sciences of the United States of America,* 103**,** 15558-15563.

Pepper, M. S. (1997) Transforming growth factor-beta: vasculogenesis, angiogenesis, and vessel wall integrity. *Cytokine Growth Factor Rev,* 8**,** 21-43.

Pepper, M. S., N. Ferrara, L. Orci & R. Montesano (1991) Vascular endothelial growth factor (VEGF) induces plasminogen activators and plasminogen activator inhibitor-1 in microvascular endothelial cells. *Biochem Biophys Res Commun,* 181**,** 902-6.

Pereira, A. M. & N. R. Biermasz (2012) Treatment of nonfunctioning pituitary adenomas: what were the contributions of the last 10 years? A critical view. *Ann Endocrinol (Paris),* 73**,** 111-6.

Prewett, M., J. Huber, Y. Li, A. Santiago, W. O'Connor, K. King, J. Overholser, A. Hooper, B. Pytowski, L. Witte, P. Bohlen & D. J. Hicklin (1999) VEGFR Antivascular endothelial growth factor receptor (fetal liver kinase 1) monoclonal antibody inhibits tumor angiogenesis and growth of several mouse and human tumors. *Cancer Res,* 59**,** 5209-18.

Procopio, W. N., P. I. Pelavin, W. M. F. Lee & N. M. Yeilding (1999) Angiopoietin-1 and-2 coiled coil domains mediate distinct homo-oligomerization patterns, but fibrinogen-like domains mediate ligand activity. *Journal of Biological Chemistry,* 274**,** 30196-30201.

Puri, M. C., J. Partanen, J. Rossant & A. Bernstein (1999) Interaction of the TEK and TIE receptor tyrosine kinases during cardiovascular development. *Development,* 126**,** 4569-80.

Puri, M. C., J. Rossant, K. Alitalo, A. Bernstein & J. Partanen (1995) The receptor tyrosine kinase TIE is required for integrity and survival of vascular endothelial cells. *EMBO J,* 14**,** 5884-91.

Raue, F., K. Frank-Raue & A. Grauer (1994) Multiple endocrine neoplasia type 2. Clinical features and screening. *Endocrinol Metab Clin North Am,* 23**,** 137-56.

Risau, W. (1997) Mechanisms of angiogenesis. *Nature,* 386**,** 671-4.

Saharinen, P., L. Eklund, J. Miettinen, R. Wirkkala, A. Anisimov, M. Winderlich, A. Nottebaum, D. Vestweber, U. Deutsch, G. Y. Koh, B. R. Olsen & K. Alitalo (2008) Angiopoietins assemble distinct Tie2 signalling complexes in endothelial cell-cell and cell-matrix contacts. *Nat Cell Biol,* 10**,** 527-37.

Saharinen, P., K. Kerkela, N. Ekman, M. Marron, N. Brindle, G. M. Lee, H. Augustin, G. Y. Koh & K. Alitalo (2005) Multiple angiopoietin recombinant proteins activate the Tie1 receptor tyrosine kinase and promote its interaction with Tie2. *J Cell Biol,* 169**,** 239-43.

Sallinen, H., T. Heikura, S. Laidinen, V. M. Kosma, S. Heinonen, S. Yla-Herttuala & M. Anttila (2010) Preoperative angiopoietin-2 serum levels: a marker of malignant potential in ovarian neoplasms and poor prognosis in epithelial ovarian cancer. *Int J Gynecol Cancer,* 20**,** 1498-505.

Sato, T. N., Y. Tozawa, U. Deutsch, K. Wolburgbuchholz, Y. Fujiwara, M. Gendronmaguire, T. Gridley, H. Wolburg, W. Risau & Y. Qin (1995) Distinct roles of the receptor tyrosine kinases Tie-1 and Tie-2 in blood-vessel formation. *Nature,* 376**,** 70-74.

Schnurch, H. & W. Risau (1993) Expression of tie-2, a member of a novel family of receptor tyrosine kinases, in the endothelial cell lineage. *Development,* 119**,** 957-68.

Scholz, A., V. A. Rehm, S. Rieke, K. Derkow, P. Schulz, K. Neumann, I. Koch, M. Pascu, B. Wiedenmann, T. Berg & E. Schott (2007) Angiopoietin-2 serum levels are elevated in patients with liver cirrhosis and hepatocellular carcinoma. *Am J Gastroenterol,* 102**,** 2471-81.

Semones, M., Y. Feng, N. Johnson, J. L. Adams, J. Winkler & M. Hansbury (2007) Pyridinylimidazole inhibitors of Tie2 kinase. *Bioorg Med Chem Lett,* 17**,** 4756-60.

Shimoda, H., M. J. Bernas, M. H. Witte, N. W. Gale, G. D. Yancopoulos & S. Kato (2007) Abnormal recruitment of periendothelial cells to lymphatic capillaries in digestive organs of angiopoietin-2-deficient mice. *Cell Tissue Res,* 328**,** 329-37.

Sievert, W., S. Tapio, S. Breuninger, U. Gaipl, N. Andratschke, K. R. Trott & G. Multhoff (2014) Adhesion molecule expression and function of primary endothelial cells in benign and malignant tissues correlates with proliferation. *PLoS One,* 9**,** e91808.

Steiner, A. L., A. D. Goodman & S. R. Powers (1968) Study of a kindred with pheochromocytoma, medullary thyroid carcinoma, hyperparathyroidism and Cushing's disease: multiple endocrine neoplasia, type 2. *Medicine (Baltimore),* 47**,** 371-409.

Sturk, C. & D. J. Dumont (2010) Tyrosine phosphorylation of Grb14 by Tie2. *Cell Commun Signal,* 8**,** 30.

Suri, C., P. F. Jones, S. Patan, S. Bartunkova, P. C. Maisonpierre, S. Davis, T. N. Sato & G. D. Yancopoulos (1996) Requisite role of angiopoietin-1, a ligand for the TIE2 receptor, during embryonic angiogenesis. *Cell,* 87**,** 1171-80.

Suri, C., J. McClain, G. Thurston, D. M. McDonald, H. Zhou, E. H. Oldmixon, T. N. Sato & G. D. Yancopoulos (1998) Increased vascularization in mice overexpressing angiopoietin-1. *Science,* 282**,** 468-71.

Tadros, A., D. P. Hughes, B. J. Dunmore & N. P. Brindle (2003) ABIN-2 protects endothelial cells from death and has a role in the antiapoptotic effect of angiopoietin-1. *Blood,* 102**,** 4407-9.

Tait, C. R. & P. F. Jones (2004) Angiopoietins in tumours: the angiogenic switch. *J Pathol,* 204**,** 1-10.

Takagi, H., G. L. King, G. S. Robinson, N. Ferrara & L. P. Aiello (1996) Adenosine mediates hypoxic induction of vascular endothelial growth factor in retinal pericytes and endothelial cells. *Invest Ophthalmol Vis Sci,* 37**,** 2165-76.

Takanami, I. (2004) Overexpression of Ang-2 mRNA in non-small cell lung cancer: association with angiogenesis and poor prognosis. *Oncol Rep,* 12**,** 849-53.

Terpos, E., K. Anargyrou, E. Katodritou, E. Kastritis, A. Papatheodorou, D. Christoulas, A. Pouli, E. Michalis, S. Delimpasi, M. Gkotzamanidou, N. Nikitas, V. Koumoustiotis, D. Margaritis, K. Tsionos, E. Stefanoudaki, J. Meletis, K. Zervas, M. A. Dimopoulos & G. Greek Myeloma Study (2012) Circulating angiopoietin-1 to angiopoietin-2 ratio is an independent prognostic factor for survival in newly diagnosed patients with multiple myeloma who received therapy with novel antimyeloma agents. *International Journal of Cancer,* 130**,** 735-742.

Thakker, R. V., P. Bouloux, C. Wooding, K. Chotai, P. M. Broad, N. K. Spurr, G. M. Besser & J. L. O'Riordan (1989) Association of parathyroid tumors in multiple endocrine neoplasia type 1 with loss of alleles on chromosome 11. *N Engl J Med,* 321**,** 218-24.

Thomas, M., M. Felcht, K. Kruse, S. Kretschmer, C. Deppermann, A. Biesdorf, K. Rohr, A. V. Benest, U. Fiedler & H. G. Augustin (2010) Angiopoietin-2 stimulation of endothelial cells induces alphavbeta3 integrin internalization and degradation. *J Biol Chem,* 285**,** 23842-9.

Trouillas, J., P. Roy, N. Sturm, E. Dantony, C. Cortet-Rudelli, G. Viennet, J. F. Bonneville, R. Assaker, C. Auger, T. Brue, A. Cornelius, H. Dufour, E. Jouanneau, P. Francois, F. Galland, F. Mougel, F. Chapuis, L. Villeneuve, C. A. Maurage, D. Figarella-Branger, G. Raverot, H. members of, A. Barlier, M. Bernier, F. Bonnet, F. Borson-Chazot, G. Brassier, S. Caulet-Maugendre, O. Chabre, P. Chanson, J. F. Cottier, B. Delemer, E. Delgrange, L. Di Tommaso, S. Eimer, S. Gaillard, M. Jan, J. J. Girard, V. Lapras, H. Loiseau, J. G. Passagia, M. Patey, A. Penfornis, J. Y. Poirier, G. Perrin & A. Tabarin (2013)

A new prognostic clinicopathological classification of pituitary adenomas: a multicentric case-control study of 410 patients with 8 years post-operative follow-up. *Acta Neuropathol,* 126**,** 123-35.

Turner, H. E., Z. Nagy, K. C. Gatter, M. M. Esiri, A. L. Harris & J. A. H. Wass (2000a) Angiogenesis in pituitary adenomas - relationship to endocrine function, treatment and outcome. *Journal of Endocrinology,* 165**,** 475-481.

Turner, H. E., Z. Nagy, K. C. Gatter, M. M. Esiri, A. L. Harris & J. A. H. Wass (2000b) Angiogenesis in pituitary adenomas and the normal pituitary gland. *Journal of Clinical Endocrinology & Metabolism,* 85**,** 1159-1162.

Unemori, E. N., N. Ferrara, E. A. Bauer & E. P. Amento (1992) Vascular endothelial growth factor induces interstitial collagenase expression in human endothelial cells. *J Cell Physiol,* 153**,** 557-62.

Valenzuela, D. M., J. A. Griffiths, J. Rojas, T. H. Aldrich, P. F. Jones, H. Zhou, J. McClain, N. G. Copeland, D. J. Gilbert, N. A. Jenkins, T. Huang, N. Papadopoulos, P. C. Maisonpierre, S. Davis & G. D. Yancopoulos (1999) Angiopoietins 3 and 4: diverging gene counterparts in mice and humans. *Proc Natl Acad Sci U S A,* 96**,** 1904-9.

Wermer, P. (1954) Genetic aspects of adenomatosis of endocrine glands. *American Journal of Medicine,* 16**,** 363-371.

Wong, M. P., S. Y. Chan, K. H. Fu, S. Y. Leung, N. Cheung, S. T. Yuen & L. P. Chung (2000) The angiopoietins, tie2 and vascular endothelial growth factor are differentially expressed in the transformation of normal lung to non-small cell lung carcinomas. *Lung Cancer,* 29**,** 11-22.

Yabkowitz, R., S. Meyer, D. Yanagihara, D. Brankow, T. Staley, G. Elliott, S. Hu & B. Ratzkin (1997) Regulation of tie receptor expression on human endothelial cells by protein kinase C-mediated release of soluble tie. *Blood,* 90**,** 706-15.

Yuan, H. T., E. V. Khankin, S. A. Karumanchi & S. M. Parikh (2009) Angiopoietin 2 Is a Partial Agonist/Antagonist of Tie2 Signaling in the Endothelium. *Molecular and Cellular Biology,* 29**,** 2011-2022.

Yuan, H. T., S. Venkatesha, B. Chan, U. Deutsch, T. Mammoto, V. P. Sukhatme, A. S. Woolf & S. A. Karumanchi (2007) Activation of the orphan endothelial receptor Tie1 modifies Tie2-mediated intracellular signaling and cell survival. *Faseb Journal,* 21**,** 3171-3183.

Zagzag, D., A. Hooper, D. R. Friedlander, W. Chan, J. Holash, S. J. Wiegand, G. D. Yancopoulos & M. Grumet (1999) In situ expression of angiopoietins in astrocytomas identifies angiopoietin-2 as an early marker of tumor angiogenesis. *Experimental Neurology,* 159**,** 391-400.

7 List of Figures

8 List of Tables

9 Acknowledgements

I would first like to thank Prof. Natalia Pellegata, my project supervisor, for giving me the opportunity to work in her group and on this interesting project, for her scientific and experimental support and helpful discussions and last but not least, sharing her valuable experience. I will forever be grateful for all the experiences that I gained while working under her supervision.

I am grateful to other members of thesis advisory committee, Prof. Michael Atkinson and Prof. Jochen Graw for their valuable advices, great ideas and interesting discussions during Thesis Committee Meetings.

I would like to express my deepest gratitude to Dr. Misu Lee with whom I have worked with many times and learnt much from her great scientific experience and expertise and for her precious suggestions.

I am very thankful to Dr. Hermine Mohr for her scientific discussions. Moreover, I am grateful to Eva Bogner, Sebastian Gulde, Swapna Satam and Tobias Wiedemann and other lab members for important discussions and being nice and helpful bench-workers. Special thanks to Elke Pulz for her help and support.

Additionally, I want to thank Lea and Elham for the fun we had during our coffee breaks and nice chats.

A big “Thank you!” to my great parents and family for supporting and helping me wherever they could and never let me feel being alone.